GENERAL METHODS FOR ANALYZING HIGGS POTENTIALS

Thesis by

Jai Sam Kim

In Partial Fulfillment of the Requirements

for the Degree of

Doctor of Philosophy

California Institute of Technology

Pasadena, California

1982

(Submitted May 4, 1982)

TO MY WIFE, HYUN JEAN, and TO MY PARENTS

ACKNOWLEDGEMENTS

ABSTRACT

This thesis is based on several papers published by the author and some more work to be published. We explain the technical problem of minimizing Higgs potentials using group theoretical concepts. Three mathematical results which belong to distinct areas are used to analyze the Higgs potential in an abstract way. The problem reduces to one of finding "contours" of directional minima and thus our method is geometrical. It is explained in detail and demonstrated for some simple cases. We show that the Michel-Radicati conjecture and the Gell-Mann-Slansky conjecture have geometrical significance besides predicting the most likely symmetry groups of the absolute minimum of the potential. We also apply the method to a non-monotonic potential.

TABLE OF CONTENTS

LIST OF FIGURES AND TABLES

CHAPTER I

I.1 INTRODUCTION

After the discovery of the Higgs mechanism [1], it has been employed almost exclusively in the gauge symmetry breaking problem because it breaks a local gauge symmetry without damaging the renormalizability [2]. Though it is not the only known mechanism to do such a job [3,4], certainly it is the only tractable one. Partly due to its tractability it drew considerable attention of theoretical physicists despite some ugly features. There is a consensus that though it may not be a fundamental mechanism it would describe the effective phenomena arising from some unknown fundamental interactions. It was applied to the unification of electromagnetic and weak interactions [5] with great success and subsequently to fancier grand unification theories [6]. Here some major difficulties arose, namely the gauge hierarchy problem [7] and proliferation of Higgs parameters etc. As the spontaneous symmetry breaking mechanism was devised by Landau [8] to explain the second order phase transition in type II superconductors, the mechanism has been widely employed in condensed matter physics [9,10]. The importance of the Higgs problem in the contemporary theoretical physics is indicated by the existence of several extensive review articles [11].

The technical problem of minimizing the Higgs potential and finding the symmetry of the vacuum actually was overlooked by most model builders. It is not the least aspect of model building because the representation content of scalar particles is not the only ingredient in determining the vacuum symmetry; the actual structure of the potential also comes in to play a major role. Sometimes the surviving symmetry group turns out to be smaller than we expected

from branching rules of the Higgs representation.

It seems a bit in reverse order to review historical developments of the theory before presenting some explanations of the terminology. We urge the reader unfamiliar with the subject to skip the following paragraph for a moment until he finishes reading the whole of chapter I.

There are three major mathematical results one needs to solve the Higgs problem:

1) invariant polynomials specify orbit;

2) there is a basic set of invariant polynomials;

3) the structure of the orbit space.

The first result which is the most important for our purpose was clearly perceived by Aronhold [12] in 1863. The second result is due to Hilbert [13]. As Weyl stated in his book [14], "Hilbert founded the proof of the invariant theoretical main theorems on a general proposition concerning polynomial ideals that is one of the simplest and most important in the whole of algebra". Relatively recently much work was done [15] on the orbit space structure of a single irreducible representation. These results lay in the backyard until very recently. Brout [16] first noticed the importance of the orbit structure and of the conjugacy classes of subgroups. Michel and Radicati [17,18] took further steps in this direction and in addition studied the geometrical structure (in the field component space) of orbits. They defined the orbit parameters and explicitly constructed the orbit space. Based on a theorem by Michel [17] concerning the critical orbits, they conjectured that a fourth degree Higgs potential preserves the maximal symmetries possible. Later Li [19] simplified a set of Higgs fields by group transformations, which was equivalent to parametrizing orbits succinctly. But his method of minimizing the Higgs potentials was a conventional one. Recently Ruegg et al. [20,21] looked for the minimizing directions

while keeping the magnitudes of the Higgs fields constant instead of extremizing the whole potential with respect to field components, which was partly in conformity with Michel's method but was a first step towards new methods of minimization. Subsequently Gell-Mann and Slansky [22] attempted to generalize Michel's conjecture for one irreducible representation to two irreducible representations. Most recently Abud and Sartori [23] fully utilized the above results in their work and treated each invariant as a coordinate in a hyper-space where an orbit is represented by a point. They further unveiled some geometrical aspects of the hyper-space.

The geometrical method that is going to be reviewed in this thesis, is based on a collection of papers [24,25,26,27] published by the author plus work presently in progress [28]. Although this method was inspired by Prof. Gell-Mann's remark in his lecture concerning the existence of some parameter specifying the orbit of SU_3 adjoint representation, it carries the foregoing works further and elucidates the rich geometrical nature of the extremization problem. It is based on the observation that the orbits and the conjugacy classes of subgroups are the relevant quantities to describe the minimum of the Higgs potential which is invariant under a linear transformation of a compact Lie group on the scalar fields. Hilbert proved that there is a basic set of invariants such that all the other invariants are expressed in terms of them and provided a systematic method to find all the basic invariants. It has been known that invariants specify orbits, i.e., one can view an orbit as a point in a $(l+1)$-dimensional vector space. How can we describe a direction in such a space? Indeed there is a set of parameters that can be used for such purpose. We define dimensionless ratios of invariant polynomials as orbit parameters. These parameters can be considered as some set of generalized angles specifying a direction in the representation space. Their ranges being bounded they occupy a localized

region (called the orbit space) in the orbit parameter space, which can be regarded as a l-dimensional vector space.

Since the scalar potential is a group invariant function it can be expressed in terms of the basic invariants. But a classical scalar potential is restricted to be a fourth degree polynomial of the scalar fields due to renormalizability*. Because of this restriction it is normal that a subset of all the basic invariants appear linearly in the Higgs potential. The potential can be written in terms of the norm of the field and a few orbit parameters. For a given set of orbit parameters we can survey the behavior, particularly extrema, of the potential along the corresponding direction in the vector space. By varying the orbit parameters we can survey the whole space in search of the absolute minimum where the vacuum resides. Because of the linearity the absolute minimum of the potential occurs on the boundary of the orbit space, which is a projection of the complete orbit space.

The potential can be minimized abstractly for a general representation of a general compact group. The difficult part of extremizing the potential in the conventional methods is equivalent to finding the orbit space boundary, which is unique for each different representation. In our original works we used the Michel-Radicati conjecture for one irreducible representation (irrep) and the Gell-Mann-Slansky conjecture for two irreps as a guide to find the orbit space boundary. Later we found that much work has been done by mathematicians [15] on the structure of the orbit space for one irrep. Their results were derived without referring to invariants at all and, though general, are not too understandable for an average physicist. With our formalism many things become intuitively clear. The main result is that the orbit space consists of some l-

---

* In the solid-state physics the free energy need not be restricted to be a fourth degree polynomial of order parameters but in some cases it is important to go to higher degree [29].

dimensional volume occupied by the generic stratum of the lowest level symmetry group and all the other strata of higher symmetries forming the singular boundaries. The strata of the highest symmetries are the most singular.

As we shall see the absolute minimum of the Higgs potential occurs on the most protrudent portions of the projected orbit space boundary. Though there is no coherent logical relationship between singularity and protrusion of a stratum, we observe that most singular strata are normally most protrudent (at least locally though not globally). Consequently the absolute minimum of the potential is most likely to occur at the stratum of highest symmetries in accordance with the two conjectures above.

I.2 HIGGS PROBLEM AND ORBIT PARAMETERS

Though our method can be applied to any kind of Higgs potential, we will take a rather simple case to show the main ideas. In a non-abelian gauge theory, where the scalar potential has a symmetry $G \times reflection$ and the scalars transform as an n-dimensional irreducible representation R of G^*, the Higgs potential can be written as

$$V(\varphi) = -\frac{1}{2}m^2\sum_{i=1}^{n}\varphi_i^*\varphi_i + \frac{1}{4}A\left(\sum_{i=1}^{n}\varphi_i^*\varphi_i\right)^2 + \qquad (I.2.1)$$

$$+ \frac{1}{4}A_1 f_{ijkl}\varphi_i^*\varphi_j\varphi_k^*\varphi_l + \frac{1}{4}A_2 g_{ijkl}\varphi_i^*\varphi_j\varphi_k^*\varphi_l + \cdots .$$

$V(\varphi)$ is invariant under a group transformation

$$\varphi_j' = \sum_{i=1}^{n} T(\vartheta)_{ji}\varphi_i \ ,$$

where $T(\vartheta)$ is an n-dimensional matrix corresponding to a group element. In general

$$T(\vartheta) = \exp(-i\sum_{i=1}^{N}\vartheta_L X_L) \ ,$$

where X_L are generators of the group and ϑ_L are group parameters specifying an element of the group.

As is well known, due to the negative mass term the minimum of the potential occurs at some nonzero values v of φ. The vacuum, defined to be at the minimum of the potential, respects only a subgroup G' of the symmetry group G of the Lagrangian. Mathematically speaking, $T(\vartheta)\, v = v$ only if $T(\vartheta)$ is an element of $G' \subset G$, otherwise $T(\vartheta)\, v \neq v$.

---

* G is a semi-simple compact Lie group.

When one tries to find the minimum of the potential, one faces significant difficulties;

1) Finding the solution for arbitrary coupling coefficients by setting $\partial V/\partial \varphi_i = 0$ is very difficult because it requires us to solve simultaneous cubic equations of too many unknowns.

2) For numerically given values of the coefficients we may try to use some well-developed computer programs to minimize the potential. But it will not be helpful because the minimum occurs along valleys in φ space. To put it more clearly, we may choose $\varphi_1 = v$ and $\{X_1, X_2, X_3\}$ as our subgroup singlet and generators respectively, or we may equally well choose $\varphi_2 = v$ and $\{X_4, X_5, X_6\}$. In general there is a continuum of equivalent sets of φ_i and $\{X_L, X_M, X_N\}$. The Higgs potential is totally blind to such differences.

We will now introduce some useful group theoretical concepts. The _orbit_ of φ_a is defined to be the set of states $\varphi^{(a)}$ that can be expressed as $\varphi^{(a)} = T(\vartheta)\,\varphi_a$ with $T(\vartheta)$ an element of G. The _little group_ of φ_a is defined to be the subgroup G'_a of G that leaves φ_a invariant, $T(\vartheta)\varphi_a = \varphi_a$ for $T(\vartheta) \in G'_a \subset G$. Considering that $T(\vartheta)\varphi_a = T(\xi)\varphi_a$ is true if and only if $T(\vartheta) = T(\xi)T(\vartheta')$ with $T(\vartheta')$ an element of G'_a we see that the states of an orbit are in one-to-one correspondence with the coset G/G'_a. It can easily be shown that the little group G'_b of any state φ_b on the orbit of φ_a is conjugate to G'_a. If the $T(\vartheta)$ are unitary then all the states $\varphi^{(a)}$ have the same norm $\varphi_a^* \varphi_a$. In general, there is a continuum of distinct orbits respecting the same little group up to conjugation. The set of all such orbits is called the _stratum_ of the little group. Note that if the little groups of two orbits are distinct then the orbits are distinct. However the converse is not true, i.e., if two orbits are distinct their little groups are not necessarily different.

Two important theorems concerning invariants and orbits can be found in the literature:

Theorem 1; Invariant polynomials $P(\varphi)$ specify orbits of φ.

From this theorem [12] we see that each invariant polynomial in the Higgs potential is constant on an orbit and thus is a function of orbits. When we seek a solution to the Higgs problem, we are actually seeking the orbit that minimizes the potential, and its little group.

Theorem 2; There exists a set of invariant polynomials $I_a(\varphi)$, called the integrity basis such that every invariant polynomial $P(\varphi)$ can be expressed as a polynomial of I_a : $P(\varphi) = \overline{P}[I_a(\varphi)]$.

This is the celebrated theorem of Hilbert's [13]. The invariants in the integrity basis are not necessarily independent and indeed for some representations there are constraints among them. We will call the complete set of independent invariants, basic invariants. The number $(l+1)$ of basic invariants is different for each different representation $\underline{R}$. Thus we can visualize an orbit as a point in the $(l+1)$-dimensional space of I_a.

Our crucial observation is that the dimensionless ratios of invariants to the magnitude of the φ vector, for example

$$\lambda = f_{ijkl}\,\varphi_i^*\varphi_j\varphi_k^*\varphi_l / \big(\sum_{i=1}^{n} \varphi_i^*\varphi_i \big)^2, \qquad (I.2.2)$$

can also be used to specify strata, and yield a powerful tool in minimum problem. We will call the dimensionless ratios *orbit parameters*. They can be considered as a set of generalized angles containing all the directional information. From the definition we can readily see that their ranges are bounded and thus they occupy a localized region (called the *orbit space*)* in the orbit parameter space, which can be regarded as a l-dimensional vector space.

---

* We think Michel and Radicati [18] were the first physicists who constructed orbit spaces explicitly.

CHAPTER II ONE IRREDUCIBLE REPRESENTATION

II.1 OUTLOOK WITH AN EVEN DEGREE HIGGS POTENTIAL

Before we analyze the general scalar potential let us consider a simple case to develop general ideas. Suppose the scalar fields transform as an n-dimensional irreducible representation (irrep) $\underline{R}$ of a compact (or finite) group G and in addition have a reflection symmetry. Then the most general Higgs potential can be written as

$$V(\varphi) = -\frac{1}{2}m^2||\varphi|| + \frac{1}{4}||\varphi||^2[A + A_1\lambda_1(\widehat{\varphi}) + A_2\lambda_2(\widehat{\varphi}) + \cdots], \quad \text{(II.1.1)}$$

where

$$||\varphi|| = \sum_{i=1}^{n}\varphi_i^*\varphi_i,$$

$$\widehat{\varphi}_i = \varphi_i/||\varphi||^{\frac{1}{2}}.$$

Since we want the potential $V(\varphi)$ to increase to $+\infty$ as $||\varphi||\to\infty$, we impose a condition on the coupling coefficients;

$$A + A_1\lambda_1(\widehat{\varphi}) + A_2\lambda_2(\widehat{\varphi}) + \cdots > 0 \quad \text{for any } \lambda_i(\widehat{\varphi}) \quad . \quad \text{(II.1.2)}$$

Our new variables are $||\varphi||$ and $\lambda_i(\widehat{\varphi})$. Since the potential is made of quadratic and quartic invariants only, normally λ_i do not constitute the complete set of orbit parameters. However we shall soon see that these constitute the complete set of parameters needed to specify the absolute minimum of the potential.

If we choose a particular direction in φ space, then the orbit parameters will take definite values. We can easily see how the Higgs potential behaves in

this direction;

$$V = -\frac{1}{2}m^2||\varphi|| + \frac{1}{4}A'||\varphi||^2 , \qquad \text{(II.1.3)}$$

where m and A' are constant numbers. This function behaves like Fig. II.1.1.

The extremum for this particular choice of $\lambda_i(\widehat{\varphi})$ is found by setting

$$\frac{\partial V}{\partial ||\varphi||} = \frac{1}{2}[-m^2 + (A + A_1\lambda_1 + A_2\lambda_2 + \cdots)||\varphi||] \qquad \text{(II.1.4)}$$

equal to zero. We obtain

$$||\varphi||_0 = \frac{m^2}{A + A_1\lambda_1 + A_2\lambda_2 + \cdots} , \qquad \text{(II.1.5)}$$

which is automatically positive for $m^2 > 0$ due to the condition (II.1.2). Noting that

$$\frac{\partial^2 V}{\partial ||\varphi||^2} = \frac{1}{2}[A + A_1\lambda_1 + A_2\lambda_2 + \cdots] \qquad \text{(II.1.6)}$$

is always positive due to the condition (II.1.2), we see that eq.(II.1.5) is a local minimum (which we call the _directional minimum_ of the potential in the direction of φ specified by $\lambda_i(\widehat{\varphi})$.
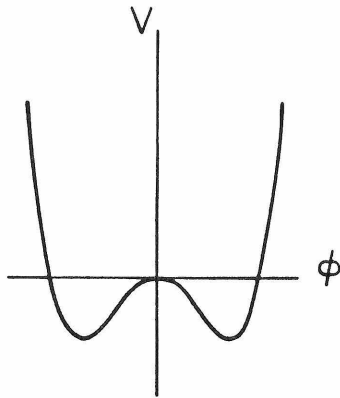
Fig. II.1.1
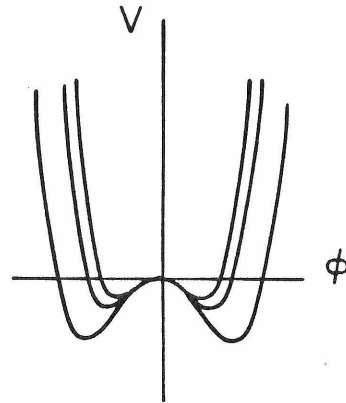
Fig. II.1.2

At the directional minimum

$$V_o(\varphi) = V(\varphi)\big|_{||\varphi||=||\varphi||_o}$$

$$= -\frac{1}{4}\frac{m^4}{(A + A_1\lambda_1 + A_2\lambda_2 + \cdots)} \tag{II.1.7}$$

$$= -\frac{m^2}{4}||\varphi||_o \ .$$

As we change the direction in φ space (i.e., the $\lambda_i(\hat{\varphi})$), the location of the minimum will move around as in Fig. II.1.2. To find the absolute minimum we just have to look for the lowest of those directional minima. Since

$$\frac{\partial V}{\partial \lambda_i} = \frac{1}{4}||\varphi||^2 A_i \ , \tag{II.1.8}$$

V is a monotonic function of λ_i. Thus the absolute minimum of V is _not_ at $\partial V/\partial \lambda_i = 0$, but at the boundary points of the region of "physical" λ_i.

To find these boundary points, note that the orbit parameters are dimensionless ratios of invariants such as eq.(I.2.2), i.e., they depend on $\hat{\varphi}$ whose magnitudes are less than one. These defining equations permit a precise determination of the region of "physical" λ_i. In particular it is immediately clear that for any configuration of $\hat{\varphi}$, the range of λ_i is bounded above and below:

$$\lambda_{i\ min} \le \lambda_i(\hat{\varphi}) \le \lambda_{i\ max} \ .$$

In an actual calculation the first practical task will be to calculate the physical region of $\lambda_i(\hat{\varphi})$, which we shall call the orbit space*.

---

* A proper description is the stratum space, which is a projection of the true orbit space. The choice was made because "Orbit Space" is close enough and phonetically sounds softer. Later we found that Michel and Radicati [18] named it the same way.

Suppose there are two orbit parameters λ_1 and λ_2. In the $\lambda_1 - \lambda_2$ plane, the orbit space will look like the warped polygon in Fig. II.1.3. It is important to note (*viz*, eq.(I.2.2)) that the orbit space is independent of Higgs coupling coefficients and masses, though it does depend on the group and the representation.

Turning our attention to the potential, let us put

$$C = A + A_1\lambda_1 + A_2\lambda_2 \ . \tag{II.1.9}$$

For given values of A, A_1, A_2 and C, this will represent a line in $\lambda_1 - \lambda_2$ space (Fig. II.1.3) According to condition (II.1.2) the line can only intersect orbit space when $C > 0$. As we increase C at fixed A, A_1, A_2, the line will sweep the orbit space. The minimum physical value of C will occur where the line first touches the orbit space. By eq.(II.1.6) this corresponds to the absolute minimum of the Higgs potential. Above the absolute minimum of V there is a continuous range of V and $||\varphi||_0$ where $\partial V/\partial ||\varphi|| = 0$ can be satisfied by some choice of λ_i. As we further increase C, the line finally leaves the orbit space at the highest of the directional minima where V has the form of the upper curve in Fig. II.1.2.
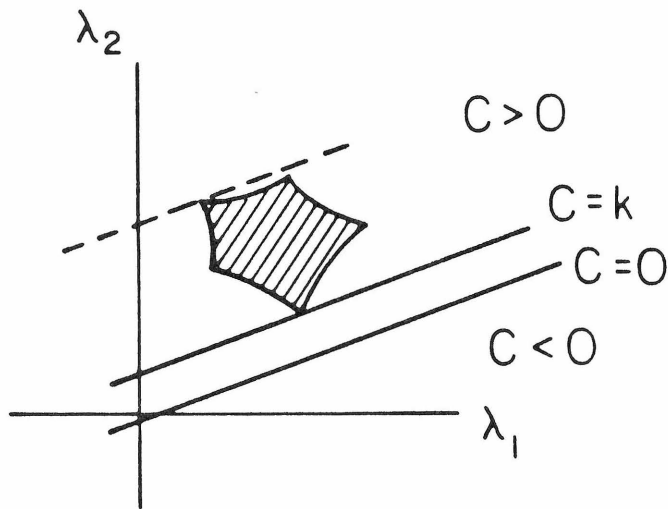
Fig. II.1.3

Our considerations with Fig. II.1.2 have suggested that V has no other extremum than the absolute minimum and the local maximum at $||\varphi|| = 0$.

For some special values of A_1 and A_2 the line can first touch the boundary of orbit space at two points. In such cases there are two different valleys of extrema (two orbits) that cannot be connected by a gauge transformation and the vacuum has an accidental degeneracy.

If there are more than two orbit parameters, then

$$C = A + A_1\lambda_1 + A_2\lambda_2 + \cdots + A_s\lambda_s \qquad (\text{II}.1.10)$$

represents a plane in λ space and the situation can be depicted as in Fig. II.1.4. The procedure to find the minimum will be the same as before. Since the absolute minimum always occurs at the boundary of the orbit space, we have to find the $(s-1)$ surface parameters and the value of the potential at the first contact point in the s-dimensional orbit parameter space. However the orbit space of a single irrep is normally conjectured to be star-shaped (Fig. II.1.4) and normally all we need to know is the location of the cusps. Detailed explanation will be presented in CIII.2-3 and CIV.
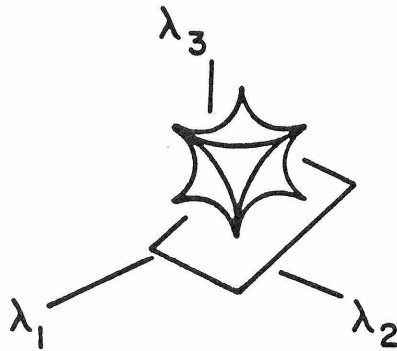
Fig. II.1.4

When the representation is complex, the potential can in general contain terms of the type

$$(H\, h_{ijkl}\, \varphi_i \varphi_j \varphi_k \varphi_l + complex\; conjugate\;)$$

$$= 2\, |H|\, \cos[h + \vartheta(\widehat{\varphi})]\, \eta(\widehat{\varphi}) ||\varphi||^2\; , \qquad\qquad (\text{II}.1.11)$$

where

$$|H| = \text{magnitude of } H\; ,$$

$$h = \text{argument of } H\; ,$$

$$0 \le \eta(\widehat{\varphi}) \le \eta_{max}\; .$$

At the minimum of the potential, $h + \vartheta = \pi$, and $\eta(\widehat{\varphi})$ is determined in the same way as the λ_i.

In problems where cubic potentials or effective potentials are considered, the potential takes the general form

$$V(\varphi) = \frac{1}{2} A ||\varphi|| + \frac{1}{3}[B_1 \beta_1(\widehat{\varphi}) + B_2 \beta_2(\widehat{\varphi}) + ...]||\varphi||^{3/2}$$

$$+ \frac{1}{4}[C + C_1 \gamma_1(\widehat{\varphi}) + ...]||\varphi||^2 + \frac{1}{5}[D_1 \delta_1(\widehat{\varphi}) + ...]||\varphi||^{5/2} + \cdots (\text{II}.1.12)$$

If we choose a direction in φ space, all the orbit parameters will become constant numbers and we can easily see how the function behaves in that direction of φ. However due to Theorem 2, some orbit parameters associated with higher degree (≥ 5) polynomial invariants are polynomials of lower degree parameters. Eventually the problem will become non-linear and one may expect that detailed solution will be far more complicated. However, as we shall see in CHV the problem can still be reduced to a form similar to the one presented in this chapter.

The classic paper of Li [19] dealt with single irreps of Higgsons in SU_n and SO_n. Only cases involving a single orbit parameter were considered, i.e., the orbit space was always a line $\lambda_{min} \leq \lambda(\hat{\varphi}) \leq \lambda_{max}$. The absolute minimum is found trivially by substituting the boundary value of the orbit parameter into eq. (II.1.6).

II.2 GENERAL FORMALISM

Let us start with a case where there is one cubic invariant polynomial and one non-trivial quartic invariant polynomial. As we will see our result can be trivially extended to a more general case where there are more cubic and quartic invariant polynomials.

To simplify the notation, we set

$$r \equiv ||\varphi||^{1/2} , \tag{II.2.1a}$$

$$A' \equiv A + A_1\alpha , \tag{II.2.1b}$$

$$B' \equiv B\beta . \tag{II.2.1c}$$

Then the Higgs potential takes the form,

$$V = -\frac{m^2}{2}r^2 + \frac{B'}{3}r^3 + \frac{A'}{4}r^4 . \tag{II.2.2}$$

We impose the positivity condition,

$$A + A_1\alpha(\hat{\varphi}) > 0 , \tag{II.2.3}$$

on the coupling coefficients in order to ensure that $V \to +\infty$ as $||\varphi|| \to \infty$.

As explained in the previous section, since the potential is a monotonic function of α and β we do not differentiate with respect to α and β to find the extremum of the potential. Differentiating with respect to r we obtain,

$$\frac{\partial V}{\partial r} = r \left(-m^2 + B'r + A'r^2\right) . \tag{II.2.4}$$

There are three extrema:

(i) $\qquad\qquad r_0 = 0$ \hfill (II.2.5a)

(ii)
$$r_0 = \frac{-B' + \sqrt{B'^2 + 4A'm^2}}{2A'} \qquad\qquad \text{(II.2.5b)}$$

(iii)
$$r_0 = \frac{-B' - \sqrt{B'^2 + 4A'm^2}}{2A'} \ . \qquad\qquad \text{(II.2.5c)}$$

To find out the nature of each extremum, let us check the second derivative,

$$\frac{\partial^2 V}{\partial r^2} = -m^2 + 2B'r + 3A'r^2 \ . \qquad\qquad \text{(II.2.6)}$$

The value of the second derivative at each extremum is:

(i)
$$-m^2 \qquad\qquad \text{(II.2.7a)}$$

(ii)
$$\frac{\sqrt{D}}{2A'}(\sqrt{D} - B') \qquad\qquad \text{(II.2.7b)}$$

(iii)
$$\frac{\sqrt{D}}{2A'}(\sqrt{D} + B') \qquad\qquad \text{(II.2.7c)}$$

where $D \equiv B'^2 + 4A'm^2$.

In order to prevent confusion, we will treat the three cases, $m^2 > 0$, $m^2 = 0$, and $m^2 < 0$, separately.

(a) $\underline{m^2 > 0}$

In this case, taking eq. (II.2.3) into account, D is automatically positive and greater than $|B'|$. Checking signs in eqs. (II.2.5) and (II.2.7) we find that solution **(i)** is a local maximum, solution **(iii)** is unphysical, and solution **(ii)** is a local minimum for either sign of B'. The local minimum is lower when $B' < 0$.

Substituting solution **(ii)** into eq. (II.2.2) we obtain

$$V_0 = -\frac{m^4}{4A'} - \frac{m^2 B'^2}{12A'^2} + \left(\frac{m^2 B'}{3A'} + \frac{B'^3}{12A'^2}\right)\left(\frac{-B' + \sqrt{B'^2 + 4A'm^2}}{2A'}\right)$$

$$\equiv -\frac{k}{4} \ , \qquad\qquad \text{(II.2.8)}$$

which is negative definite for $A' > 0$, $m^2 > 0$, and $B' < 0$. This equation defines a curve in the $\alpha-\beta$ plane (or $A'-B'$ plane). To get a rough idea, we have made computer generated plots of the contours for several k values for a particular case $(A, A_1, B, m^2 > 0)$ (Fig. II.2.1). Despite the complicated look of eq. (II.2.8), the contours turned out to have simple shapes. For a given k, the contour is a smooth curve with no extrema in the region $A + A_1\alpha > 0$. Each k contour passes through the point $[\alpha=(m^4/k-A)/A_1, \beta=0]$ to reach the point $[\alpha=-A/A_1, \beta=\sqrt{2/3}m^3/\sqrt{k}B]$ where A' goes negative. As k is reduced from $+\infty$, where the contour is the horizontal line $\alpha=-A/A_1$, the k contour rises up and slides to the right in the case $(A, A_1, B, m^2 > 0)$. When it makes the first contact with orbit space, it yields the absolute minimum of the potential. As k is further reduced, the k contour sweeps through the entire orbit space.
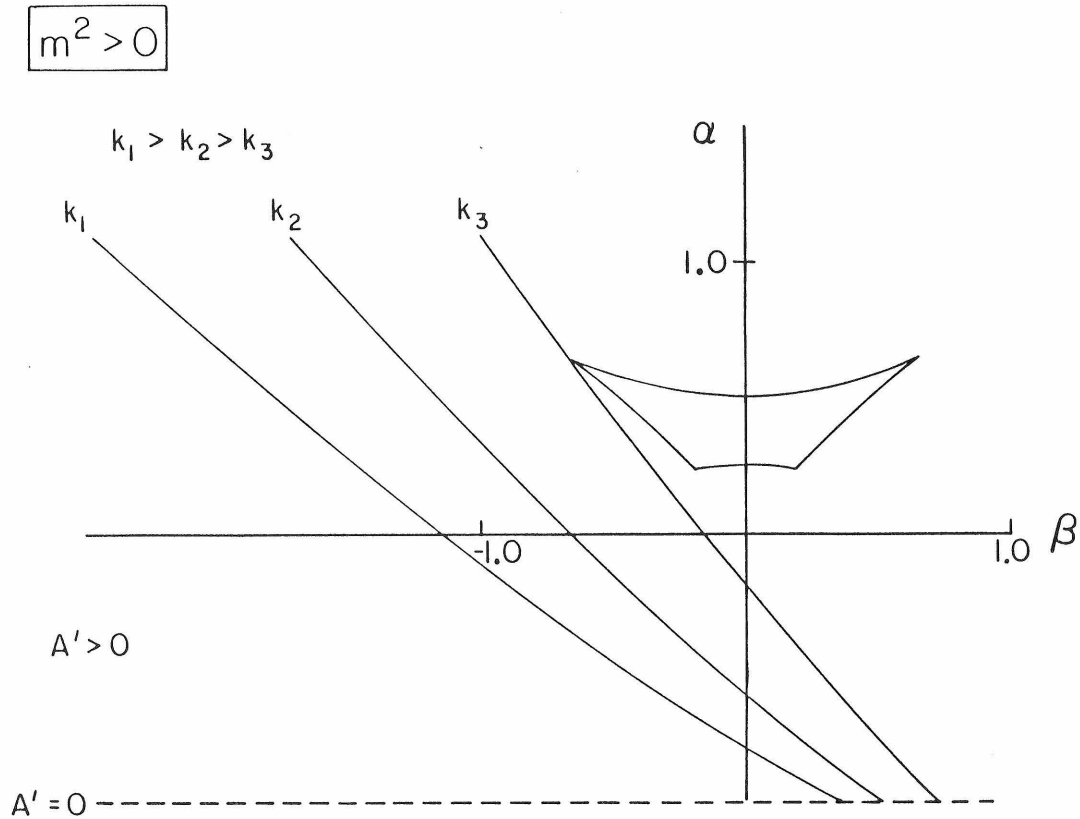
Fig. II.2.1

The above statements on the movement of the k contour are justified by checking the direction of the gradient vector $\nabla k = (\partial k / \partial \alpha, \partial k / \partial \beta)$. In terms of $p \equiv \sqrt{B'^2 + 4A'm^2} / |B'| > 1$, its components are:

$$-\frac{1}{4}\frac{\partial k}{\partial A'} = -\frac{1}{4A_1}\frac{\partial k}{\partial \alpha}$$

$$= \frac{m^4}{4A'^2} + \frac{m^2 B'^2}{6A'^3} - \left(\frac{2}{3}\frac{m^2 B'}{A'^2} + \frac{B'^3}{4A'^3}\right)\left(\frac{-B' + \sqrt{B'^2 + 4A'm^2}}{2A'}\right)$$

$$+ \left(\frac{m^2 B'}{3A'} + \frac{B'^3}{12A'^2}\right)\left(\frac{m^2}{A'\sqrt{B'^2 + 4A'm^2}}\right)$$

$$= \frac{m^4}{4A'^2}\left(\frac{p+1}{p-1}\right)^2 > 0 \ , \tag{II.2.9}$$

$$-\frac{1}{4}\frac{\partial k}{\partial B'} = -\frac{1}{4B}\frac{\partial k}{\partial \beta}$$

$$= \frac{m^2 |B'|}{6A'^2} + \left(\frac{m^2}{3A'} + \frac{B'^2}{4A'^2}\right)\left(\frac{|B'| + \sqrt{B'^2 + 4A'm^2}}{2A'}\right)$$

$$+ \left(\frac{m^2 |B'|}{3A'} + \frac{|B'|^3}{12A'^2}\right)\left(\frac{1 + \dfrac{|B'|}{\sqrt{B'^2 + 4A'm^2}}}{2A'}\right)$$

$$= \frac{m^2 |B'|}{6A'^2}\frac{(p+1)^2}{(p-1)} > 0 \ . \tag{II.2.10}$$

The orientation and direction of movement of the k contour as k decreases are summarized in Fig. II.2.2 for each sign of A_1 and B.
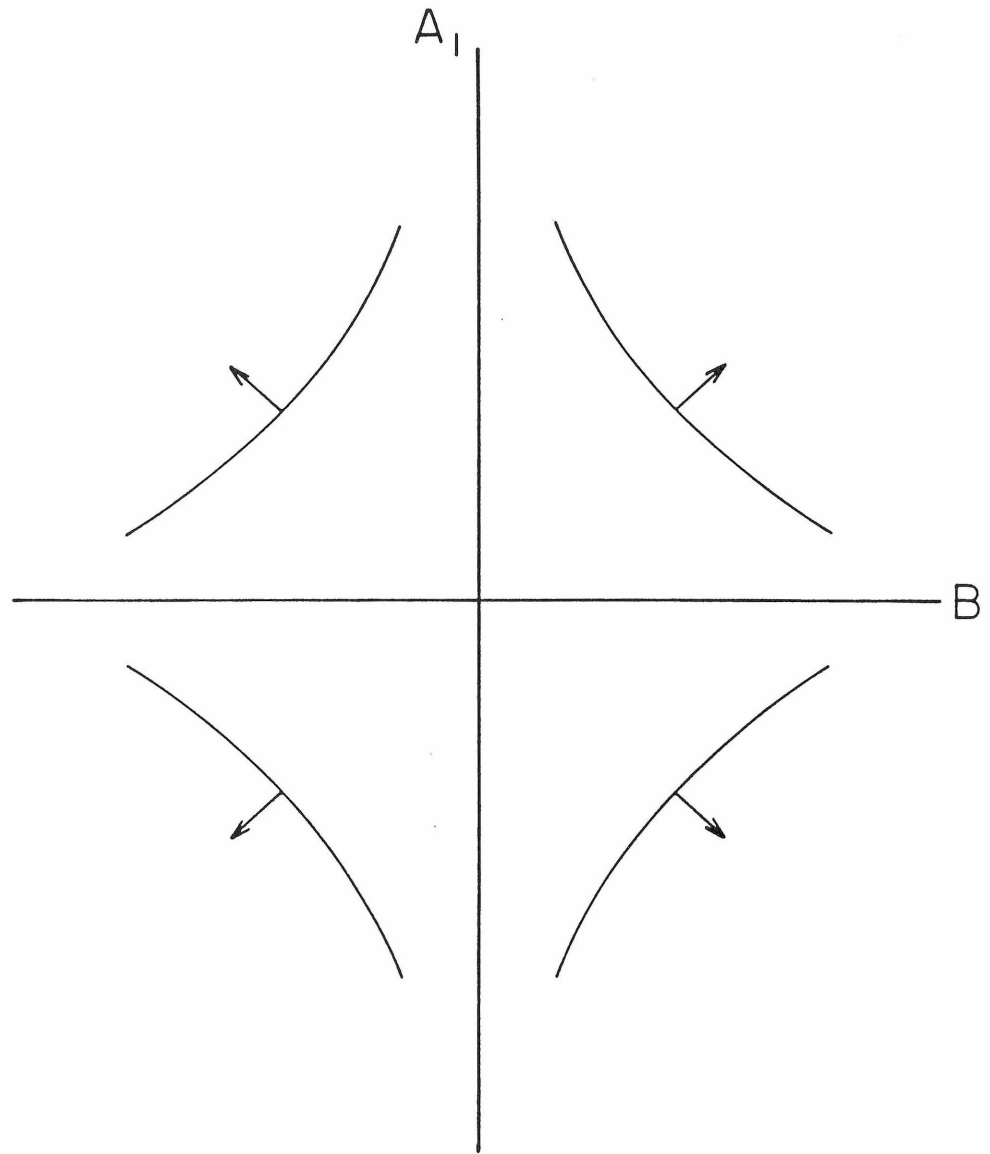
Fig. II.2.2

Using eqs. (II.2.9) and (II.2.10) one can compute the second derivative:

$$\frac{d^2 A'}{dB'^2} = - \frac{d}{dB'} \frac{(\partial k / \partial B')}{(\partial k / \partial A')}$$

$$= \frac{14}{9m^2} \frac{(p-1)}{p} > 0 \quad . \tag{II.2.11}$$

One finds that the k contour is always concave in the direction towards which it is moving.

(b) $m^2 = 0$

Though the potential has a simplified structure in this case, it still has directional extrema. Solution (**i**) is an inflection point and solution (**ii**) with $B' < 0$ is the directional minimum.

Eq. (II.2.8) reads, for $m^2 = 0$ and $B' < 0$, as follows:

$$V_0 = - \frac{|B'|^4}{12A'^3}$$

$$\equiv - \frac{k}{4} \tag{II.2.12}$$

which is negative definite. Solving eq. (II.2.12) for A' we obtain

$$A' = |B'|^{4/3} / (3k)^{1/3} \quad . \tag{II.2.13}$$

This is a familiar curve, somewhere between a straight line and a parabola, and thus gives some insight into the complicated k contour found in the other cases. We see that k is a measure of the flatness of the curve. As k is reduced, the curve becomes steeper or equivalently the k contour pivots about the point $(A'=0, B'=0)$ towards the A'-axis.

<u>(c)</u> $m^2 < 0$

In the region where $B'^2 - 4A'|m^2| > 0$, solution (i) is a local minimum, solution (ii) with $B' < 0$ is a local minimum, and solution (iii) with $B' < 0$ is a local maximum. If the cubic term is strong enough, solution (ii) will be the lower minimum. Otherwise solution (i) will be the lower. In the region where $B'^2 - 4A'|m^2| < 0$, there is only one local minimum at the origin.

Directional behavior of the potential is most complicated in this case. The evolution of the potential through the configurations listed above as k decreases is shown in Fig. II.2.3.
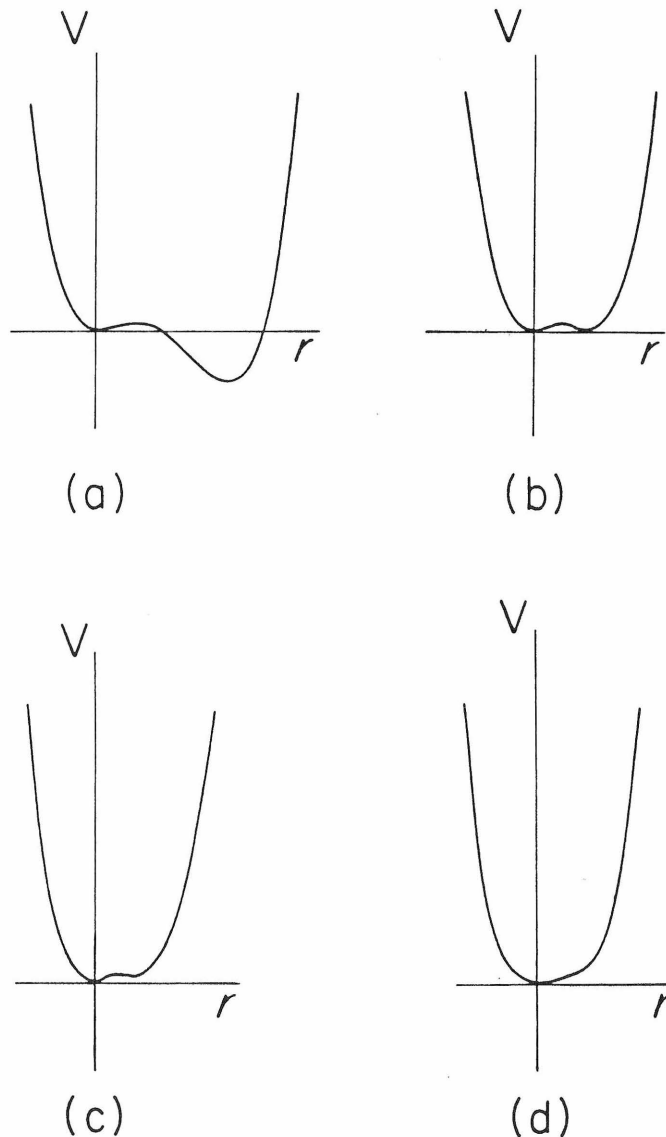
Fig. II.2.3
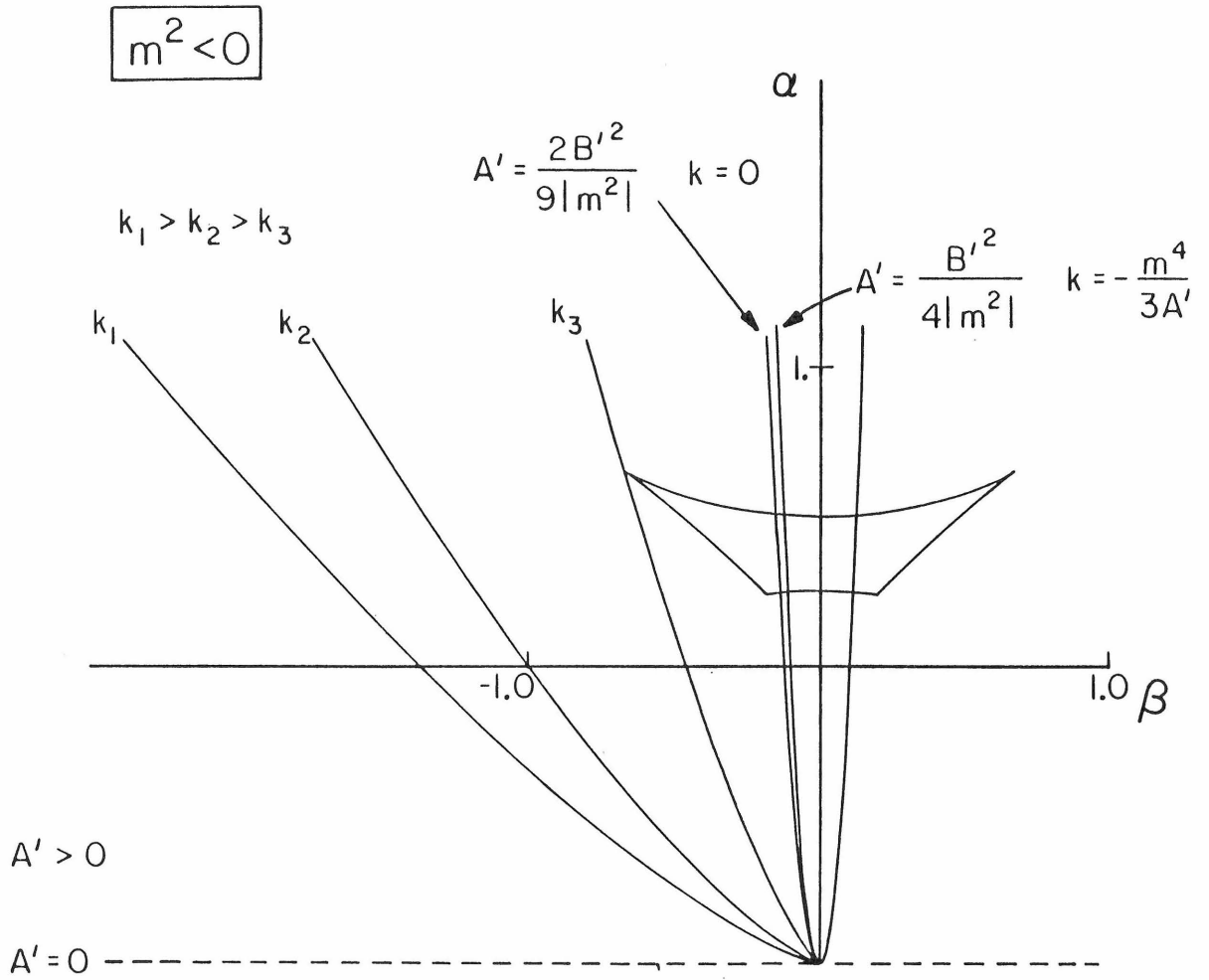
Fig. II.2.4

Eq. (II.2.8) reads, for $m^2 < 0$, and $B' < 0$, as follows:

$$V_0 = -\frac{m^4}{4A'} + \frac{|m^2||B'|^2}{12A'^2} + \left(\frac{|m^2||B'|}{3A'} - \frac{|B'|^3}{12A'^2}\right)\left(\frac{|B'| + \sqrt{B'^2 - 4A'|m^2|}}{2A'}\right)$$

$$= -\frac{m^4}{12A'(1-p^2)^2}(3p^4 + 8p^3 + 6p^2 - 1),$$

$$\equiv -\frac{k}{4} \tag{II.2.14}$$

which is not negative definite for $0 \le p \le 1$. Eqs. (II.2.9), (II.2.10), and (II.2.11) can be used for the $m^2 < 0$ case with m^2 replaced by $-|m^2|$ and $(p-1)$ by $(1-p)$. The direction of the gradient vector $\nabla k = (\partial k / \partial\alpha, \partial k / \partial\beta)$ is the same as before. The k contour is again concave. The k contour does not slide but pivots about the point $(\alpha = -A/A_1, \beta = 0)$. For simplicity let us concentrate on the case $A, A_1, B, -m^2 > 0$ (Fig. II.2.4). As k is reduced from $+\infty$ the k contour pivots clockwise until it meets the orbit space. As k is reduced to zero, which happens when $p = 1/3$, the contour becomes the parabola,

$$A' = \frac{2}{9}\frac{B'^2}{|m^2|}. \tag{II.2.15}$$

Beyond this point k takes on negative values. As the k contour touches and becomes identical to the parabola $B'^2 - 4A'|m^2| = 0$ at $k = -m^4/3A'$, the two extrema at $r_0 \ne 0$ coincide and become an inflection point leaving the origin as the only extremum, the absolute minimum.

If the first contact occurs with the $k = 0$ contour an interesting phenomenon occurs. In this case we have a spontaneous symmetry breaking at $r_0 \ne 0$ and no symmetry breaking at $r_0 = 0$ (Fig. II.2.3b). It will be interesting to see what kind of physics happens in such a degenerate vacuum.

The problem can again be reduced to the same form in cases involving one irreducible representation with more cubic and quartic invariants. To see this, note that the potential still has the form (II.2.2) in these cases, with A' and $\mathcal{B}$ dependent on more orbit parameters α_i and β_i but still linear in them. Eqs. (II.2.9) and (II.2.10) still hold for each $\partial k / \partial \alpha_i$ and $\partial k / \partial \beta_i$ and (II.2.11) still holds. We see that a hyper-k-surface approaches to the orbit space as k is reduced from $+\infty$. The k surface is again non-convex in the direction towards which it is moving. Again the first contact, i.e., the absolute minimum, can occur only on the non-concave segments of the orbit space boundary.

II.3 THE GENERAL STRUCTURE OF THE ORBIT SPACE OF ONE IRREDUCIBLE REPRESENTATION

Due to the monotonicity of the Higgs potential with respect to the orbit parameters the absolute minimum occurs on the boundary of orbit space, at the point of first contact with the potential minimizing k-surface. If the k-surface is flat (CHII.1) or concave in the direction towards which it is moving (CHII.2), its point of contact is further restricted to non-concave segments on the orbit space boundary. These features are universal to a general Higgs potential for scalar bosons belonging to an irreducible representation of the symmetry group. What is different for each different representation is that each has its own unique orbit space.

Although the structure of the orbit space for an irrep was unveiled [15] abstractly by a group of mathematicians, we derived the same result in a more intuitive way. An important clue leading to a general description of an orbit space is found in Michel's work. Michel and Radicati [17,18] were among the first who realized the importance of the orbit structure and of the conjugacy classes of subgroups. They took further steps in this direction and in addition studied the geometrical structure (in the field component space) of orbits. They conjectured that if the representation of the symmetry group G of a fourth degree Higgs potential is irreducible on the real, its minima preserve maximal little groups. This was based on a theorem by Michel [17] that when $||\varphi||$ is held constant, all invariant polynomials are stationary at a critical orbit, which is isolated in its stratum and has a maximal little group. This theorem amounts to saying that there is a cusp at each critical orbit point. If these cusps are the only non-concave portions of the boundary, the Michel-Radicati conjecture is proved. These considerations led us to anticipate that the orbit space of one irrep would be star-shaped (Fig. II.1.4).

Let us give somewhat more specific arguments on the structure of a complete orbit space of one irrep. First the dimension of a complete orbit space for one irrep is one less than the number of independent invariant polynomials. The latter number is equal to the number of simplified Higgs field components, which we have called φ_i so far. The two sets of parameters are equivalent ways of specifying a stratum point. The non-linear transformation rules among them are given by the definitions of the orbit parameters. Let us denote the ratios of the components as before, $r_i = \varphi_i / \varphi_{l+1}$. If we consider the Jacobian determinant $\partial(\alpha_1, \alpha_2, \cdots, \alpha_l) / \partial(r_1, r_2, \cdots, r_l)$, then we can easily deduce the necessary conditions for a boundary point:

At a point on the boundary point of the orbit space, the rank of the Jacobian determinant is less than or equal to $(l-1)$.

When the rank of the determinant is $(l-s)$ in some regions of the orbit space, the regions form $(l-s)$-dimensional surfaces. The regions are singular regions embedded in higher-dimensional space. Let us define $\vec{P} = (\alpha_1, \alpha_2, \cdots, \alpha_l)$ to describe the boundary conditions in more detail. When $s = l$ in some regions they correspond to singular points, i.e., cusps. Equations for them are

$$\frac{\partial \vec{P}}{\partial r_i} = 0 \ . \tag{II.3.1}$$

When $s = (l-1)$ in some regions they correspond to singular curves, i.e., edge curves. Equations for them are

$$\frac{\partial \vec{P}}{\partial r_1} \ // \ \frac{\partial \vec{P}}{\partial r_2} \ // \ \cdots \ // \ \frac{\partial \vec{P}}{\partial r_l} \ . \tag{II.3.2}$$

where $\partial \vec{P} / \partial r_i = 0$ is allowed for some i's but not for all. When $s = (l-2)$ in some regions they correspond to singular two-dimensional surfaces, i.e., warped surfaces. Equations for them are

$$\varepsilon_{ijk} \frac{\partial \alpha_a}{\partial r_i} \frac{\partial \alpha_b}{\partial r_j} \frac{\partial \alpha_c}{\partial r_k} = 0 \qquad for\ all\ (a,b,c) \tag{II.3.3}$$

where $\varepsilon_{ij}(\partial \alpha_a / \partial r_i)(\partial \alpha_b / \partial r_j) = 0$ is allowed for some (a,b) but not for all.

Eq. (II.3.1) imposes l conditions on l r_i's, implying that the stratum of the cusp has only one parameter, i.e., one singlet. This guarantees that the little group of the cusp is a maximal little group. Eq. (II.3.2) imposes $(l-1)$ conditions on l r_i's, leaving two parameters. The stratum of the curve has a semi-maximal* (or maximal) little group. Eq. (II.3.3) imposes $(l-2)$ conditions on l r_i's, leaving three parameters. The corresponding stratum commonly has a one-level lower little group.

From the above considerations and some examples (CHII.4, CHIV.1) we can picturize the complete orbit space of one irrep as follows; On the boundary of the complete orbit space there are cusps of maximal little groups, singular curves of semi-maximal little groups connecting the cusps, and singular surfaces of lower level little groups stretching between the curves, and so on. Inside the boundary all the points belong to a stratum, called the generic stratum, corresponding to a unique little group. It is noteworthy that the lower level little groups are subgroups of higher level little groups when the strata of the latter lie on the strata of the former. For example, when a cusp lies on two curves of different little groups they are subgroups of the little group of the cusp.

The main result of ref. [15] is that the generic stratum occupies some l-dimensional volume (an open, dense, and topologically connected region) and all the other lower dimensional strata form the singular boundaries of the generic stratum. It is noteworthy that this pattern repeats whichever stratum we start

---

* A little group is a subgroup whose sub-representations contain singlets. Maximal little groups are the largest little groups which do not contain each other. Semi-maximal little groups are second largest little groups whose sub-representations contain more singlets than maximal little groups. Semi-maximal little groups do not contain each other.

from. For example, if we start from a two-dimensional surface the curves close most of the boundary of the surface and the cusps close both the curves and the surface.

If the Michel-Radicati conjecture is to hold, the projected orbit space (constructed out of the invariants employed in the 4th degree Higgs potential) must have further properties; Cusps should be globally most protrudent. In other words, all the boundary surfaces must lie inside the polyhedron which is constructed by drawing straight lines between all the cusps. As we shall see in CHIV.1, the complete orbit spaces do not have this property. Whether or not the projected orbit spaces have the property remains to be seen.

However in the examples of CHIV.1 we find that the cusps are locally more protrudent than the curves, the curves are locally more protrudent than the two-dimensional surfaces and so on. We do not yet have a general proof or disproof of the observed hierarchy of concavities.

II.4 APPLICATION TO SU(N) ADJOINT REPRESENTATION

II.4.1 THE HIGGS POTENTIAL FOR SU(5) ADJOINT REPRESENTATION

In the spirit of doing simple things first and then extending to a general case we will first consider SU_5 adjoint [30] to show concretely how our method is applied. We will consider the most general Higgs potential invariant under SU_5 gauge transformation:

$$V(\varphi) = -\frac{m^2}{2} \sum_{i,j=1}^{5} \varphi^i{}_j \varphi^j{}_i + \frac{B}{3} \sum_{i,j,k=1}^{5} \varphi^i{}_j \varphi^j{}_k \varphi^k{}_i$$

$$+ \frac{A}{4} (\sum_{i,j=1}^{5} \varphi^i{}_j \varphi^j{}_i)^2 + \frac{A_1}{4} \sum_{i,j,k,l=1}^{5} \varphi^i{}_j \varphi^j{}_k \varphi^k{}_l \varphi^l{}_i \ . \tag{II.4.1}$$

Diagonalizing the traceless hermitian matrix $\varphi^i{}_j$, we obtain

$$V(\varphi) = -\frac{m^2}{2} \sum_{i=1}^{5} \varphi_i^2 + \frac{B}{3} \sum_{i=1}^{5} \varphi_i^3 + \frac{A}{4} (\sum_{i=1}^{5} \varphi_i^2)^2 + \frac{A_1}{4} \sum_{i=1}^{5} \varphi_i^4 \tag{II.4.2}$$

with

$$\varphi_i \equiv \varphi^i{}_i \ \text{ and } \ \varphi_5 = -\varphi_1 - \varphi_2 - \varphi_3 - \varphi_4 \ . \tag{II.4.3}$$

We further express the potential as

$$V(\varphi) = -\frac{m^2}{2} ||\varphi|| + \frac{B}{3} \beta(\widehat{\varphi}) ||\varphi||^{3/2} + \frac{1}{4} (A + A_1 \alpha(\widehat{\varphi})) ||\varphi||^2 \tag{II.4.4}$$

where

$$||\varphi|| \equiv \sum_{i=1}^{5} \varphi_i^2 \ , \tag{II.4.5}$$

$$\alpha \equiv \frac{\sum \varphi_i^4}{(\sum \varphi_i^2)^2} = \frac{r_1^4 + r_2^4 + r_3^4 + 1 + (r_1 + r_2 + r_3 + 1)^4}{[\ r_1^2 + r_2^2 + r_3^2 + 1 + (r_1 + r_2 + r_3 + 1)^2\ ]^2} \ , \tag{II.4.6}$$

$$\beta \equiv \frac{\sum \varphi_i^3}{(\sum \varphi_i^2)^{3/2}} = \pm \frac{r_1^3 + r_2^3 + r_3^3 + 1 - (r_1 + r_2 + r_3 + 1)^3}{[\, r_1^2 + r_2^2 + r_3^2 + 1 + (r_1 + r_2 + r_3 + 1)^2 \,]^{3/2}} \qquad (\text{II.4.7})$$

with $r_i = \varphi_i / \varphi_4$. Note that β can be positive or negative for the same α depending on the signs of the fields.

We impose the positivity condition,

$$A + A_1 \alpha(\hat{\varphi}) > 0 \;, \qquad (\text{II.4.8})$$

on the coupling coefficients in order to ensure that $V \to +\infty$ as $||\varphi|| \to \infty$.

II.4.2 MAXIMAL AND SEMI-MAXIMAL LITTLE GROUPS AND ORBIT SPACE

The maximal little groups and associated branching rules [22,31] of $\underline{24}$ are as follows:

$$SU_4 \times U_1: \quad 24 = 1(0) + 4(-5) + \overline{4}(5) + 15(0) \qquad (\text{II.4.9})$$

$$5 = 1(4) + 4(-1)$$

$$\varphi = \alpha(1,1,1,1,-4) \qquad (\text{II.4.10})$$

$$\alpha = 13/20$$

$$\beta = \pm\, 3/2\sqrt{5} \qquad (\text{II.4.11})$$

$$SU_3 \times SU_2 \times U_1: \quad 24 = (1,1)(0) + (1,3)(0) + (8,1)(0) + (3,2)(-5) + (\overline{3},2)(5) \qquad (\text{II.4.12})$$

$$5 = (3,1)(-2) + (1,2)(3)$$

$$\varphi = \alpha(2,2,2,-3,-3) \qquad (\text{II.4.13})$$

$$\alpha = 7/30$$

$$\beta = \pm\, 1/\sqrt{30} \qquad (\text{II.4.14})$$

where we also have listed the branching rule of $\underline{5}$, the form of φ which transforms as a singlet under the listed subgroup, and the orbit parameters for each case.

The semi-maximal little groups and associated branching rules of $\underline{24}$ are as follows:

$SU_3 \times U_1 \times U_1$:

$$24 = 1[0,0] + 1[0,0] + 1[0,2] + 1[0,-2] + 8[0,0]$$

$$+ 3[-5,1] + 3[-5,-1] + \bar{3}[5,1] + \bar{3}[5,-1] \qquad \text{(II.4.15)}$$

$$5 = 3[-2,0] + 1[3,1] + 1[3,-1]$$

$$\varphi = (a,a,a,b,-3a-b) \qquad \text{(II.4.16)}$$

$$\alpha = \frac{3a^4 + b^4 + (3a+b)^4}{[3a^2 + b^2 + (3a+b)^2]^2} \equiv \frac{3r^4 + 1 + (3r+1)^4}{[3r^2 + 1 + (3r+1)^2]^2} \qquad \text{(II.4.17)}$$

$$\beta = \frac{3a^3 + b^3 - (3a+b)^3}{[3a^2 + b^2 + (3a+b)^2]^{3/2}} \equiv \pm \frac{3r^3 + 1 - (3r+1)^3}{[3r^2 + 1 + (3r+1)^2]^{3/2}} , \qquad \text{(II.4.18)}$$

$SU_2 \times SU_2 \times U_1 \times U_1$:

$$24 = (1,1)[0,0] + (1,3)[0,0] + (1,1)[0,0] + (2,1)[0,3] + (2,1)[0,-3]$$

$$+ (3,1)[0,0] + (1,2)[-5,-2] + (2,2)[-5,1] + (1,2)[5,2] + (2,2)[5,-1] \qquad \text{(II.4.19)}$$

$$5 = (1,1)[-2,-2] + (2,1)[-2,1] + (1,2)[3,0]$$

$$\varphi = (a,a,b,b,-2a-2b) \qquad \text{(II.4.20)}$$

$$\alpha = \frac{2a^4+2b^4+(2a+2b)^4}{[2a^2+2b^2+(2a+2b)^2]^2} \equiv \frac{2r^4+2+(2r+2)^4}{[2r^2+2+(2r+2)^2]^2} \qquad (II.4.21)$$

$$\beta = \frac{2a^3+2b^3-(2a+2b)^3}{[2a^2+2b^2+(2a+2b)^2]^{3/2}} \equiv \pm \frac{2r^3+2-(2r+2)^3}{[2r^2+2+(2r+2)^2]^{3/2}} , \qquad (II.4.22)$$

where we have listed two U_1 charges in the brackets. We have underlined the singlets. The curves that represent the strata of these little groups are displayed in Fig. II.4.1.
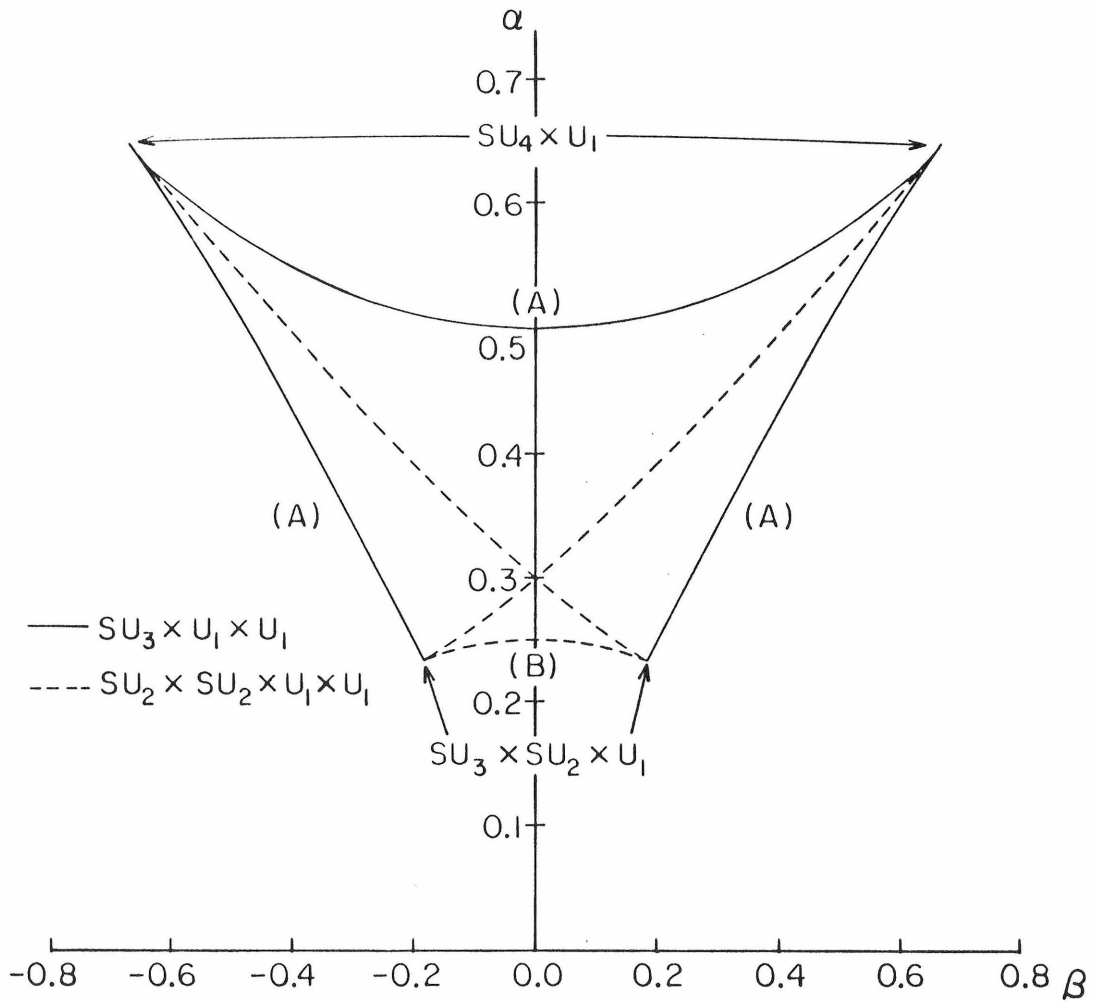
Fig. II.4.1

A simple-minded approach to finding the boundary of the orbit space is to extremize β for each α. Instead we can use the following idea. Consider a set of φ_i such that α, β lies on the boundary. Make an infinitesimal variation of one of the fields φ_i. The resulting change $\partial \alpha / \partial \varphi_i$, $\partial \beta / \partial \varphi_i$ forms a vector in α, β space. This vector cannot take us out of orbit space, therefore it must have vanishing component normal to the boundary. This requirement that the vector vanish or point along the orbit space boundary holds for infinitesimal variations in each φ_i, giving us the necessary condition for a boundary point;

At a boundary point, all field components φ_i must either satisfy

$$\partial \alpha / \partial r_i = \partial \beta / \partial r_i = 0 \qquad (\text{II}.4.23)$$

or must have a common value of

$$\frac{\partial \alpha / \partial r_i}{\partial \beta / \partial r_i} . \qquad (\text{II}.4.24)$$

Partial derivatives of α and β with respect to r_i are:

$$\frac{\partial \alpha}{\partial r_i} = \frac{4[r_i^3 + (r_1+r_2+r_3+1)^3]}{[r_1^2+r_2^2+r_3^2+1+(r_1+r_2+r_3+1)^2]^2} \qquad (\text{II}.4.25)$$

$$- \frac{4[r_i + (r_1+r_2+r_3+1)][r_1^4+r_2^4+r_3^4+1+(r_1+r_2+r_3+1)^4]}{[r_1^2+r_2^2+r_3^2+1+(r_1+r_2+r_3+1)^2]^3} ,$$

$$\frac{\partial \beta}{\partial r_i} = (\pm) \frac{3[r_i^2 - (r_1+r_2+r_3+1)^2]}{[r_1^2+r_2^2+r_3^2+1+(r_1+r_2+r_3+1)^2]^{3/2}} \qquad (\text{II}.4.26)$$

$$- \frac{3[r_i + (r_1+r_2+r_3+1)][r_1^3+r_2^3+r_3^3+1-(r_1+r_2+r_3+1)^3]}{[r_1^2+r_2^2+r_3^2+1+(r_1+r_2+r_3+1)^2]^{5/2}} .$$

We confirm that $\varphi = a(1,1,1,1,-4)$ and $\varphi = a(2,2,2,-3,-3)$ satisfy the condition (II.4.23); $\varphi = b(r,r,r,1,-3r-1)$ and $\varphi = b(r,r,1,1,-2r-2)$ satisfy the condition (II.4.24).

To ensure that these curves really form the boundaries, we have plotted several thousand random stratum points. No point was found outside the boundaries defined by the curves (A) and (B) of Fig. II.4.1.

II.4.3 LOCATION OF THE ABSOLUTE MINIMUM

Using the general formalism developed in CHII.2 we can locate the absolute minimum immediately. Since the k contours behave similarly for $m^2 \leq 0$ as for $m^2 > 0$, we can treat all three cases together.

Due to the concavity of the boundary curves of the orbit space and the concave shape of the k contour, the first contact can occur only at $(\alpha=13/20, \beta=\pm 3/2\sqrt{5})$, the stratum of $SU_4 \times U_1$, or at $(\alpha=7/30, \beta=\pm 1/\sqrt{30})$, the stratum of $SU_3 \times SU_2 \times U_1$, in agreement with the Michel-Radicati conjecture. When $A_1 > 0$, the absolute minimum may occur at either stratum depending on the values of the other coupling coefficients. When $A_1 < 0$, the absolute minimum occurs only at the stratum of $SU_4 \times U_1$. Note that of the two cusps with the same α, the one with $B' < 0$ gets the first contact because it yields a lower value of the potential.

II.4.4 SU(N) ADJOINT REPRESENTATION

The formalism for SU_5 24 can be extended trivially to the case of SU_N adjoint representation by extending the sums to N. What is different is that there are more maximal little groups and the orbit space boundary has more cusps as the group gets bigger.

The strata for the maximal little groups of SU_N adjoint representation are of the form

$$\varphi = \alpha \; (1,1,\cdots,1,\frac{-m}{N-m},\frac{-m}{N-m},\cdots,\frac{-m}{N-m}) \qquad \text{(II.4.27)}$$

where m elements have the common value a and the other $(N-m)$ elements have the common value $-am/(N-m)$. For fixed m eq. (II.4.27) represents the stratum of $SU_m \times SU_{N-m} \times U_1$. The orbit parameters for this stratum are:

$$\alpha = \frac{m + (N-m)\,(\frac{m}{N-m})^4}{[m + (N-m)\,(\frac{m}{N-m})^2]^2} \ , \tag{II.4.28a}$$

$$\beta = \pm\,\frac{m - (N-m)\,(\frac{m}{N-m})^3}{[m + (N-m)\,(\frac{m}{N-m})^2]^{3/2}} \ . \tag{II.4.28b}$$

The list of maximal little groups for SU_N adjoint representation is:

$SU_{N-1} \times U_1, \ SU_{N-2} \times SU_2 \times U_1, \cdots ,$

$SU_{(N-1)/2} \times SU_{(N+1)/2} \times U_1 \ (N \text{ odd}) \text{ or } SU_{N/2} \times SU_{N/2} \times U_1 \ (N \text{ even}). \tag{II.4.29}$

The strata for the semi-maximal little groups of SU_N adjoint representation are of the form

$$\varphi = a \ (r,r,\cdots,r,1,1,\cdots,1,\,-mr-(N-m-1)\,) \tag{II.4.30}$$

where m elements have the common value ar, $(N-m-1)$ elements have the common value a, and one element is the negative sum of all the other elements. For fixed m, eq. (II.4.30) represents the stratum of $SU_m \times SU_{N-m-1} \times U_1 \times U_1$. The orbit parameters for this stratum are:

$$\alpha = \frac{mr^4 + (N-m-1) + (mr + (N-m-1))^4}{[mr^2 + (N-m-1) + (mr + (N-m-1))^2]^2} \ , \tag{II.4.31a}$$

$$\beta = \pm\,\frac{mr^3 + (N-m-1) - (mr + (N-m-1))^3}{[mr^2 + (N-m-1) + (mr + (N-m-1))^2]^{3/2}} \ . \tag{II.4.31b}$$

It can easily be checked that eqs. (II.4.27) and (II.4.30) satisfy the necessary conditions for boundary points, eqs. (II.4.23) and (II.4.24), respectively. The cusps and curves of the boundary are shown in Fig. II.4.2 for several low N*. Again computer generated random stratum points never appeared outside the boundary.

It will be noted that the boundary curves corresponding to semi-maximal little groups in Fig. II.4.2 are all concave again. One sees, using the same k contour as in the previous section, that only the cusps corresponding to the maximal little groups can yield the absolute minimum, in agreement with the Michel-Radicati conjecture. Consideration of Figs. II.2.2 and II.4.2 together shows that when $A_1 < 0$, the absolute minimum occurs only at the stratum of $SU_{N-1} \times U_1$. When $A_1 > 0$, the absolute minimum may occur at any of the strata of maximal little groups, the choice depending on the value of the other coupling coefficients.

Again the Michel-Radicati conjecture is found to be true for any SU_N adjoint.

---

* No curve is shown for SU_3 because $\mathrm{Tr}\varphi^4$ is not independent of $(\mathrm{Tr}\varphi^2)^2$, i.e., there is no α, in this case.
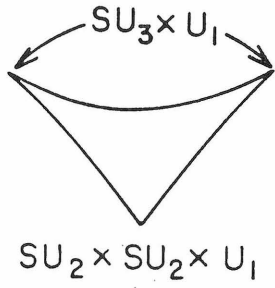
(a) SU$_4$
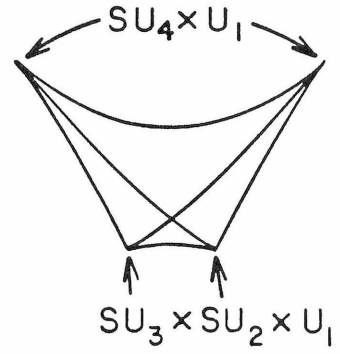
(b) SU$_5$
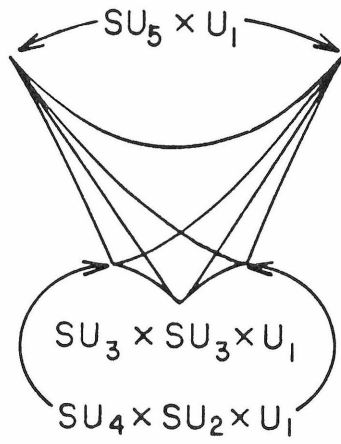
(c) SU$_6$
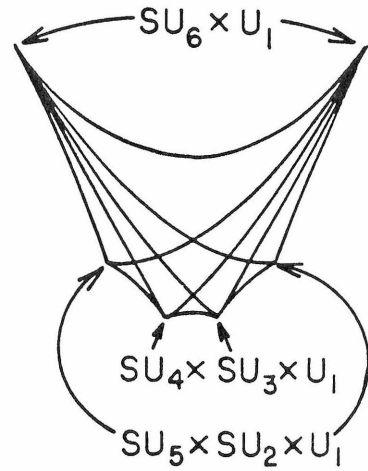
(d) SU$_7$

Fig. II.4.2

CHAPTER III   TWO IRREDUCIBLE REPRESENTATIONS

III.1 GENERAL FORMALISM

When there are two irreps, $\underline{R}$ and $\underline{S}$, of scalar bosons φ and χ the most general renormalizable Higgs potential invariant under $G \times reflection$ can be written as

$$V(\varphi,\chi) = -\frac{1}{2}M^2 ||\varphi|| - \frac{1}{2}m^2 ||\chi||$$

$$+ \frac{1}{4}[A + A_1\alpha_1(\widehat{\varphi}) + A_2\alpha_2(\widehat{\varphi}) + \cdots]||\varphi||^2$$

$$+ \frac{1}{4}[C + C_1\gamma_1(\widehat{\chi}) + C_2\gamma_2(\widehat{\chi}) + \cdots]||\chi||^2$$

$$+ \frac{1}{2}[B + B_1\beta_1(\widehat{\varphi},\widehat{\chi}) + \cdots]||\varphi||\,||\chi|| \ . \qquad \text{(III.1.1)}$$

While α_i and γ_i specify the orbits and associated little groups of $\underline{R}$ and $\underline{S}$, respectively, β_i specifies relative directions between orbits of $\underline{R}$ and orbits of $\underline{S}$. When χ moves on an orbit with the direction of φ fixed, the little group of the reducible representation $(\underline{R} + \underline{S})$ changes whereas the separate little groups of $\underline{R}$ and $\underline{S}$ remain the same. β_i specifies the location of χ on its orbit.

Let us define

$$A' \equiv A + A_1\alpha_1(\widehat{\varphi}) + A_2\alpha_2(\widehat{\varphi}) + \cdots \ ,$$

$$C' \equiv C + C_1\gamma_1(\widehat{\chi}) + C_2\gamma_2(\widehat{\chi}) + \cdots \ , \qquad \text{(III.1.2)}$$

$$B' \equiv B + B_1\beta_1(\widehat{\varphi},\widehat{\chi}) + \cdots \ .$$

Again we impose positivity conditions on coupling coefficients so that $V \to +\infty$ as

$||\varphi|| \to \infty$ and/or $||\chi|| \to \infty$;

$$A' > 0 \ ,$$

$$C' > 0 \ , \qquad\qquad\qquad \text{(III.1.3)}$$

$$B' > -\sqrt{A'C'} \ .$$

We will treat $||\varphi||$, $||\chi||$, $\alpha_i(\hat{\varphi})$, $\gamma_i(\hat{\chi})$, and $\beta_i(\hat{\varphi},\hat{\chi})$ as independent variables and extremize the potential with respect to these. The reasoning is similar to the one irrep case. If we choose a particular direction in $\varphi-\chi$ space, all the orbit parameters will be determined and the potential reduces to a function of $||\varphi||$ and $||\chi||$:

$$V = -\frac{1}{2}M^2||\varphi|| - \frac{1}{2}m^2||\chi||$$

$$+ \frac{1}{4}A'||\varphi||^2 + \frac{1}{4}C'||\chi||^2 + \frac{1}{2}B'||\varphi||\,||\chi|| \ . \qquad \text{(III.1.4)}$$

The directional behavior of the potential is schematically shown in Fig. III.1.1.
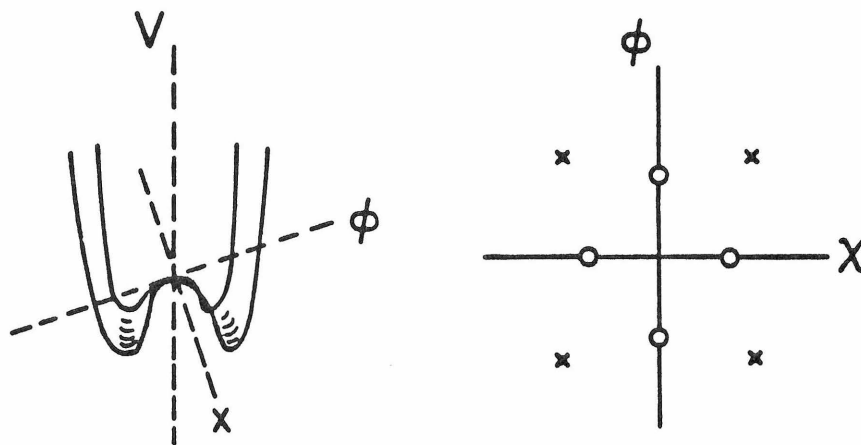
Fig. III.1.1

The extremum for the particular choice of orbit parameters, conveniently expressed in terms of the variables $r \equiv ||\varphi||^{\frac{1}{2}}$ and $s \equiv ||\chi||^{\frac{1}{2}}$, is given by the conditions

$$\frac{\partial V}{\partial r} = r \ (A'r^2 + B's^2 - M^2) = 0 \ ,$$

$$\frac{\partial V}{\partial s} = s \ (B'r^2 + C's^2 - m^2) = 0 \ . \qquad \text{(III.1.5)}$$

There are four solutions;

$$\text{I)} \quad r = s = 0 \ , \qquad \text{(III.1.6a)}$$

$$\text{II)} \quad r = 0 \ , \quad s^2 = m^2 / \ C' \ , \qquad \text{(III.1.6b)}$$

$$\text{III)} \quad s = 0 \ , \quad r^2 = M^2 / A' \ , \qquad \text{(III.1.6c)}$$

$$\text{IV)} \quad r^2 = ||\varphi||_0 = \frac{M^2C' - m^2B'}{A'C' - B'^2} \ , \quad s^2 = ||\chi||_0 = \frac{m^2A' - M^2B'}{A'C' - B'^2} \ . \qquad \text{(III.1.6d)}$$

To ascertain which solution is the minimum for this particular choice of direction in $\varphi - \chi$ space (i.e., the directional minimum), recall that at a minimum the second derivatives

$$\frac{\partial^2 V}{\partial r^2} = (A'r^2 + B's^2 - M^2) + 2 \ A'r^2 \ ,$$

$$\frac{\partial^2 V}{\partial s^2} = (B'r^2 + C's^2 - m^2) + 2 \ C's^2 \ , \qquad \text{(III.1.7)}$$

$$\frac{\partial^2 V}{\partial r \, \partial s} = 2 \ B'r \ s$$

must satisfy

$$\frac{\partial^2 V}{\partial r^2} > 0 \ , \qquad \text{(III.1.8a)}$$

$$\frac{\partial^2 V}{\partial s^2} > 0 \ , \qquad\qquad\qquad\qquad \text{(III.1.8b)}$$

$$\frac{\partial^2 V}{\partial r^2}\frac{\partial^2 V}{\partial s^2} > (\frac{\partial^2 V}{\partial r\,\partial s})^2 \ . \qquad\qquad\qquad \text{(III.1.8c)}$$

Of course solution I is not a minimum unless $M^2 < 0$ and $m^2 < 0$, a case we shall not be concerned with. We see from eqs.(III.1.6) - (III.1.8) that solution II (pure χ) is a directional minimum if

$$m^2 > 0 \ ,$$

$$m^2 B' > M^2 C' \ . \qquad\qquad\qquad\qquad \text{(III.1.9)}$$

Solution III (pure φ) is a directional minimum if

$$M^2 > 0 \ ,$$

$$M^2 B' > m^2 A' \ . \qquad\qquad\qquad\qquad \text{(III.1.10)}$$

Solution IV is a directional minimum if

$$M^2 C' > m^2 B' \ , \qquad\qquad\qquad\qquad \text{(III.1.11a)}$$

$$m^2 A' > M^2 B' \ , \qquad\qquad\qquad\qquad \text{(III.1.11b)}$$

$$A'C' > (B')^2 \qquad\qquad\qquad\qquad \text{(III.1.11c)}$$

for $A' > 0$ and $C' > 0$.

$||\varphi||_o > 0$ and $||\chi||_o > 0$ is guaranteed only if the conditions (III.1.11) are satisfied. This is in contrast to the case of one irrep where $||\varphi||_o \geq 0$ was ensured by the positivity conditions, $A' > 0$ and $m^2 > 0$. Relations (III.1.11) serve to replace the conditions $M^2 > 0$, $m^2 > 0$ which are overly strict because the Higgs fields φ and χ can both develop nonzero vacuum expectation values even with

$M^2 < 0$ or $m^2 < 0$ when $B' < 0$.

From another point of view $M^2 C' = m^2 B'$ and $m^2 A' = M^2 B'$ represent the boundaries where the directional minimum shifts from solution **IV** to solution **II** or **III** respectively. If solution **IV** is the directional minimum, extrema **II** and **III** are saddle points (assuming now $m^2 > 0$, $M^2 > 0$) as indicated in Fig. III.1.1b. In this case evaluation of the potential at the minimum yields

$$V_0(\widehat{\varphi}, \widehat{\chi}) = -\frac{1}{4} \frac{(m^4 A' + M^4 C' - 2 M^2 m^2 B')}{(A'C' - B'^2)} \qquad \text{(III.1.12)}$$

$$= -\frac{1}{4}(M^2 ||\varphi||_0 + m^2 ||\chi||_0).$$

When solution **IV** does not satisfy the conditions (III.1.11), it occupies a saddle point and either solution **II** (with $V_0 = -m^4/4C'$) or **III** (with $V_0 = -M^4/4A'$) becomes the directional minimum.

The foregoing discussion has been concerned with a particular direction in $\varphi-\chi$ space. As we now change the direction in $\varphi-\chi$ space (i.e., the α_i, β_i, and γ_i), the location of the minimum will move around. The absolute minimum will be the lowest of these directional minima. Since

$$\frac{\partial V}{\partial \alpha_i} = \frac{1}{4} ||\varphi||^2 A_i \ , \qquad \text{(III.1.13a)}$$

$$\frac{\partial V}{\partial \gamma_i} = \frac{1}{4} ||\chi||^2 C_i \ , \qquad \text{(III.1.13b)}$$

$$\frac{\partial V}{\partial \beta_i} = \frac{1}{2} ||\varphi|| ||\chi|| B_i \ , \qquad \text{(III.1.13c)}$$

V is a monotonic function of the orbit parameters α_i, β_i, and γ_i. Thus once

---

* The conditions (III.1.11) are only necessary conditions for solution **IV** to be the absolute minimum. There are additional conditions for sufficiency [see CHIII.3].

again the absolute minimum of V occurs at a boundary of the orbit space rather than at $\partial V / \partial \alpha_i = 0$, etc.

To illustrate how determination of the absolute minimum proceeds, let's look into the simple case where

$$A' = A + A_1 \alpha(\hat{\varphi}) \ ,$$

$$C' = C + C_1 \gamma(\hat{\chi}) \ , \qquad \qquad \text{(III.1.14)}$$

$$B' = B + B_1 \beta(\hat{\varphi}, \hat{\chi}) \ .$$

Let us set

$$V_0(\hat{\varphi}, \hat{\chi}) = -\frac{k}{4}. \qquad \qquad \text{(III.1.15)}$$

Then from eq.(III.1.12),

$$m^4(A + A_1\alpha) + M^4(C + C_1\gamma) - 2\, M^2 m^2 (B + B_1\beta)$$

$$= k \ [(A + A_1\alpha)(C + C_1\gamma) - (B + B_1\beta)^2] \ . \qquad \text{(III.1.16)}$$

It can easily be shown that the above equation represents a cone in $\alpha - \gamma - \beta$ space. That is, the potential minimizing k-surface is a cone in this problem. After some coordinate transformations, it reduces to

$$Z^2 = \frac{A_1 C_1}{2\, B_1^2} (X^2 - Y^2) \ , \qquad \qquad \text{(III.1.17)}$$

where

$$X = (X' + Y')/\sqrt{2} \ ,$$

$$Y = (X' - Y')/\sqrt{2} \ ,$$

$$X' = \alpha + \frac{A}{A_1} - \frac{M^4}{kA_1} \ , \qquad\qquad (\text{III}.1.18)$$

$$Y' = \gamma + \frac{C}{C_1} - \frac{m^4}{kC_1} \ ,$$

$$Z = \beta + \frac{B}{B_1} - \frac{M^2 m^2}{kB_1} \ .$$

While the coupling coefficients determine the shape and orientation of the cone, the value of k determines the location of the vertex of the cone which moves on a straight line in $\alpha - \gamma - \beta$ space as k varies. As we decrease k from $+\infty$, the cone begins to touch the orbit space at some k (Fig. III.1.2). This k gives the minimum energy, and the point of contact gives the orbit.
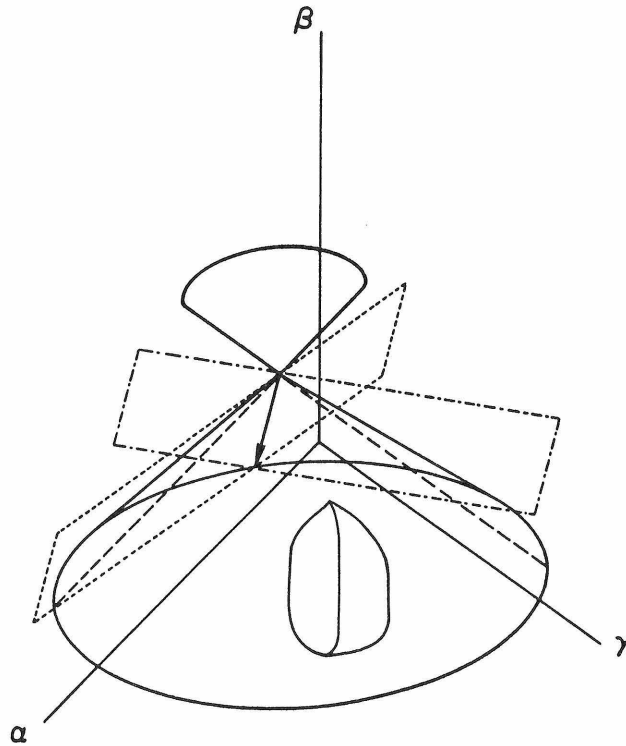
Fig. III.1.2

Some further details concerning the cone are as follows.

i) The straight line along which the vertex of the cone moves lies on the cone (i.e., it is a generating line of the cone.).

ii) The condition $A'C' = B'^2$ holds on the $k = \infty$ cone and $A'C' > B'^2$ holds inside it. Recalling that $A'C' > B'^2$ is a condition for solution **IV** (i.e., $||\varphi||_0$ and $||\chi||_0$ both nonzero), we see that when this solution gives the minimum energy, the orbit space lies entirely within the " forward " part of the cone, i.e., the part which narrows as k decreases (Fig. III.1.2).

iii) The line along which the vertex moves is also the intersection of the two planes

$$M^2 C' = m^2 B'$$

and

$$m^2 A' = M^2 B' \; ,$$

which formed the boundary between solutions **II** or **III** and **IV**. These planes slice the inside of the cone into three pieces. Only when the cone touches the orbit space on the $M^2 C' > m^2 B'$, $m^2 A' > M^2 B'$ side of these planes do we get type **IV** solutions. Such type **IV** solutions yield the absolute minimum energy if they occur at $k > M^4 / A'_0$ and $k > m^4 / C'_0$.

While the formalism in the preceding two paragraphs is universal to all the cases where there are three orbit parameters α, γ, and β, each different case will have a different orbit space and different physical meaning for the boundary surface. The formalism can be extended trivially to a general case where there are more α's, γ's, and β's. The k-surface will be a mixture of a plane and a cone in some hyper-space.

III.2 THE GENERAL STRUCTURE OF THE ORBIT SPACE OF TWO IRREDUCIBLE REPRESENTATIONS

While the trace of the hierarchical relationship between the levels of little groups and the concavities and dimensions of their strata observed in one irrep case is still visible in two irrep cases, the orbit space boundary of two irreps is more complex and things are pretty much mixed. The existence of a modified resemblance can be inferred from the observation that whereas orbit parameters associated with each irrep tend to form warped concave boundary surfaces, orbit parameters associated with both irreps tend to destroy such behavior because with the field components of one irrep fixed (consequently orbit parameters associated with that irrep are fixed.), one can always change the field components of the other irrep creating a volume traced by pencils. Moreover the volume occupied by the generic stratum is not always confined by the strata of higher symmetries but the generic stratum itself surfaces on the boundaries. This "looseness" stems from the non-compactness of the representation space.

Again an important clue leading to a description of an orbit space of two irreps is found in the Gell-Mann-Slansky conjecture [22] concerning the likely little groups of the absolute minimum of a 4th degree Higgs potential. Since the conjecture was made shortly before the current work started we restate it in the following.

To state the conjecture let us define the maxi-maximal little groups; Suppose there are two irreps R and S. First, we construct a list of maximal little groups and branching rules for R:

$$R = 1 + r_1 + r_2 + \cdots \qquad \text{for } G'_a \subset G$$

$$= 1 + r_3 + r_4 + \cdots \qquad \text{for } G'_b \subset G$$

$$= \cdots .$$

For each G'_i the branching rules of $\underline{S}$ will be

$$S = s_1 + s_2 + s_3 + \cdots \qquad \text{for } G'_a \subset G$$

$$= s_4 + s_5 + s_6 + \cdots \qquad \text{for } G'_b \subset G$$

$$= \cdots .$$

Then we make a list of maximal little groups and branching rules for each s_i:

$$s_1 = 1 + t_1 + t_2 + \cdots \qquad \text{for } G_\alpha^{(1)} \subset G'_a$$

$$= \cdots ,$$

$$s_2 = 1 + t_3 + t_4 + \cdots \qquad \text{for } G_\beta^{(2)} \subset G'_a$$

$$= \cdots ,$$

$$s_4 = 1 + t_5 + t_6 + \cdots \qquad \text{for } G_\gamma^{(4)} \subset G'_b$$

$$= \cdots ,$$

$$s_5 = 1 + t_7 + t_8 + \cdots \qquad \text{for } G_\delta^{(5)} \subset G'_b$$

$$= \cdots ,$$

$$\cdots .$$

This procedure yields a list, $\{ G_\alpha^{(1)} , \ldots ; G_\beta^{(2)} , \ldots ; G_\gamma^{(4)} , \ldots ; G_\delta^{(5)} , \ldots ; \cdots \}$, of *maxi–maximal little groups*. Repeating the same procedure staring from $\underline{S}$, we obtain another list of maxi-maximal little groups, which is different from the previous list.

The Gell-Mann-Slansky conjecture states that the minimum of a fourth degree Higgs potential will preserve no smaller subgroup than is in the list of

maxi-maximal little groups, which is made of the union of the two lists.

In the previous chapter we have seen that the potential minimizing k-surface for a Higgs potential of two irreps which has separate reflection symmetries in addition to the symmetry of the gauge group is a hyper-cone. This implies that if the Gell-Mann-Slansky conjecture is to hold for such a class of Higgs potentials then the strata of maxi-maximal little groups must occupy most protrudent portions, i.e., cusps, convex curves and surfaces etc., of the orbit space boundary. Specific examples will be given in the following chapters.

To help the reader to understand the abstract statements made above, let us briefly explain dimensionalities of strata of two irreps. Suppose the branching rules for two irreps, R and S, under $G' \subset G$ are

$$R = r_1 + r_2 + \cdots \quad ,$$

$$S = s_1 + s_2 + \cdots \quad .$$

If R contains one singlet and S one singlet of G', then the stratum will be a point in the orbit space. If R contains one singlet and S two singlets of G' or vice versa, the stratum will normally be a curve in the orbit space, though there are exceptions. If R contains one singlet and S three singlets of G' or vice versa, the stratum is likely to be a two-dimensional surface. If R contains two-singlets and S two singlets of G', the stratum is likely to occupy a three-dimensional volume. The occasions when we have more singlets than the parameters needed to specify the stratum are more common for two irrep than one irrep cases. These ambiguities will be partially clarified at the end of CHIII.4. Also the range of validity of the Gell-Mann-Slansky conjecture will be discussed later at the end of CHV.

III.3 APPLICATION TO SU(N) ADJOINT + VECTOR REPRESENTATIONS

III.3.1 HIGGS POTENTIAL FOR SU(5) $\underline{24}$ + $\underline{5}$

In this chapter we apply the general formalism derived in the previous chapter to the case of SU_5 adjoint + vector representations. This particular problem has been solved by many people [32] ever since Georgi and Glashow [6] formulated the grand unification theory based on SU_5 symmetry. In other branches of physics [9], namely in the second order phase transition occurring in order-disorder phenomenon [10], the spontaneous symmetry breaking problem already became so complicated that more powerful means were required. But in elementary particle physics it was the appearance of grand unification theories that prompted the need of more powerful methods than conventional ones. There was just no hope of minimizing the scalar potential with conventional methods when the representation of the scalar bosons is as huge as the ones introduced in SO_{10} or E_6 unification theories [33].

We will consider two scalar fields: $\varphi_i{}^j$, which transforms as the 24-dimensional adjoint representation, and χ_i, which transforms as the 5-dimensional (complex) vector representation. The most general renormalizable Higgs potential invariant under $SU_5 \times reflection$ is

$$V(\varphi,\chi) = -\frac{M^2}{2} \sum_{i,j=1}^{5} \varphi_i{}^j \varphi_j{}^i - \frac{m^2}{2} \sum_{i=1}^{5} \chi^{i*}\chi_i \qquad (\text{III.3.1})$$

$$+ \frac{A}{4} (\sum_{i,j=1}^{5} \varphi_i{}^j \varphi_j{}^i)^2 + \frac{A_1}{4} \sum_{i,j,k,l=1}^{5} \varphi_i{}^j \varphi_j{}^k \varphi_k{}^l \varphi_l{}^i$$

$$+ \frac{C}{4} (\sum_{i=1}^{5} \chi^{i*}\chi_i)^2$$

$$+ \frac{B}{2} (\sum_{i,j=1}^{5} \varphi_i{}^j \varphi_j{}^i)(\sum_{k=1}^{5} \chi^{k*}\chi_k) + \frac{B_1}{2} \sum_{i,j,k=1}^{5} \chi^{i*}\varphi_i{}^j \varphi_j{}^k \chi_k \ .$$

where we have represented the 24 as a 5×5 traceless hermitian matrix. Because φ_i^j is hermitian, we can always choose the coordinate system of $\varphi - \chi$ space in such a way that only χ and the diagonal elements of φ_i^j develop v.e.v. In terms of $\varphi_i \equiv \varphi_i^i$ the "potential" that we are going to minimize can be written as

$$V(\varphi,\chi) = -\frac{M^2}{2} \sum_{i=1}^{5} \varphi_i^2 - \frac{m^2}{2} \sum_{i=1}^{5} \chi_i^* \chi_i \qquad (\text{III.3.2})$$

$$+ \frac{A}{4} (\sum_{i=1}^{5} \varphi_i^2)^2 + \frac{A_1}{4} \sum_{i=1}^{5} \varphi_i^4$$

$$+ \frac{C}{4} (\sum_{i=1}^{5} \chi_i^* \chi_i)^2$$

$$+ \frac{B}{2} (\sum_{i=1}^{5} \varphi_i^2)(\sum_{k=1}^{5} \chi_i^* \chi_i) + \frac{B_1}{2} (\sum_{i=1}^{5} \varphi_i^2 \chi_i^* \chi_i)$$

with

$$\varphi_5 = -\varphi_1 - \varphi_2 - \varphi_3 - \varphi_4 \ . \qquad (\text{III.3.3})$$

We further express the potential in the simplest form as

$$V(\varphi,\chi) = -\frac{M^2}{2} ||\varphi|| - \frac{m^2}{2} ||\chi|| \qquad (\text{III.3.4})$$

$$+ \frac{1}{4}(A + A_1 \alpha(\widehat{\varphi})) ||\varphi||^2$$

$$+ \frac{1}{4} C ||\chi||^2$$

$$+ \frac{1}{2}(B + B_1 \beta(\widehat{\varphi},\widehat{\chi})) ||\varphi|| \, ||\chi||$$

where

$$\widehat{\varphi}_i \equiv \frac{\varphi_i}{(||\varphi||)^{\frac{1}{2}}}, \quad \widehat{\chi}_i \equiv \frac{\chi_i}{(||\chi||)^{\frac{1}{2}}} \qquad \text{(III.3.5)}$$

and the independent variables are now the field strengths

$$||\varphi|| \equiv \sum_{i=1}^{5} \varphi_i^2 , \qquad \text{(III.3.6a)}$$

$$||\chi|| \equiv \sum_{i=1}^{5} \chi_i^* \chi_i \qquad \text{(III.3.6b)}$$

and the orbit parameters

$$\alpha = \frac{\sum \varphi_i^4}{(\sum \varphi_i^2)^2} , \qquad \text{(III.3.7)}$$

$$\beta = \frac{\sum \varphi_i^2 \chi_i^* \chi_i}{(\sum \varphi_i^2)(\sum \chi_i^* \chi_i)} . \qquad \text{(III.3.8)}$$

III.3.2 ORBIT SPACE AND MAXI-MAXIMAL LITTLE GROUPS FOR SU(5) $\underline{24} + \underline{5}$

As we stated in the previous chapter the orbit space of two irreducible representations is made of pencils. The reason is as follows:

Assign a set of numerical values to φ_i. For the α thus determined, vary χ_i to obtain a range of β. Repeating the process, we eventually cover the entire orbit space.

We see from eq. (III.3.8) that the maximum of β is reached when χ_i points along the largest element of φ_i and the minimum when χ_i points along the smallest element of φ_i. These simple considerations yield three straight line sections of the boundary (Fig. III.3.1):

(I) If one of the φ_i is zero, then $\beta_{\min} = 0$. In this case

$$\frac{1}{4} \leq \alpha = \frac{\varphi_1^4 + \varphi_2^4 + \varphi_3^4 + (\varphi_1 + \varphi_2 + \varphi_3)^4}{(\varphi_1^2 + \varphi_2^2 + \varphi_3^2 + (\varphi_1 + \varphi_2 + \varphi_3)^2)^2} \leq \frac{7}{12} \ , \tag{III.3.9}$$

which is the α of the SU_4 adjoint representation.

(II) If $\varphi = a\,(1,1,1,1,-4)$, then α takes the maximum value $13/20$ and $1/20 \leq \beta \leq 4/5$.

(III) If $\varphi = a\,(2,2,2,-3,-3)$, then α takes the minimum value $7/30$ and $2/15 \leq \beta \leq 3/10$.
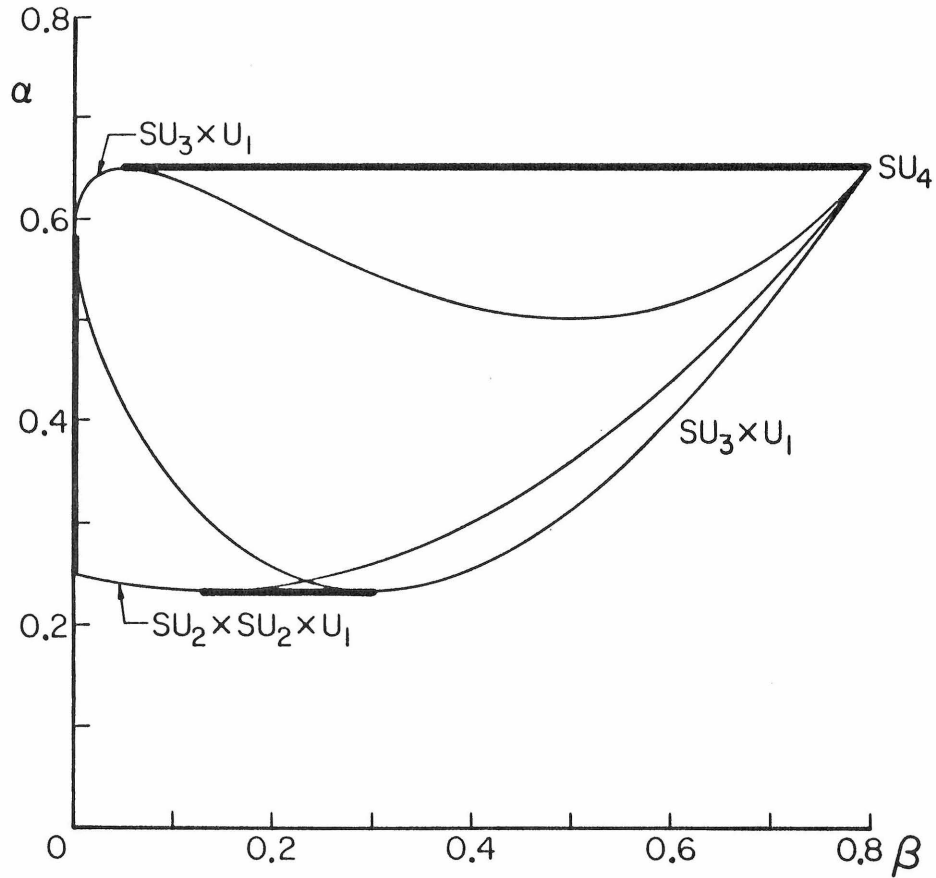
Fig. III.3.1

To find the remaining, curved sections of the boundary in Fig. III.3.1 we could extremize β for each α, but this method is very laborious. The second method of finding the boundary is to solve the equations for a boundary point, which were originally devised for this problem by Prof. Frautschi,

$$\frac{\partial \alpha}{\partial \varphi_i} = \frac{\partial \beta}{\partial \varphi_i} = 0 \qquad (\text{III.3.10})$$

and

$$\frac{\partial \alpha / \partial \varphi_1}{\partial \beta / \partial \varphi_1} = \frac{\partial \alpha / \partial \varphi_2}{\partial \beta / \partial \varphi_2} = \frac{\partial \alpha / \partial \varphi_3}{\partial \beta / \partial \varphi_3} = \frac{\partial \alpha / \partial \varphi_4}{\partial \beta / \partial \varphi_4} = \frac{\partial \alpha / \partial \varphi_5}{\partial \beta / \partial \varphi_5}. \qquad (\text{III.3.11})$$

Though this method is more civilized than the first one it is still not satisfactory because it requires us to solve high degree simultaneous algebraic equations of many unknowns. In the original work [25] we actually tried hard to solve these equations. Though we could find the wanted solutions we also found unwanted solutions and could not find the complete set of solutions. We realized that the best use of the above two equations is to confirm our final answers. The third method is to guess the answers assuming that the Gell-Mann-Slansky conjecture holds. As we explained at the end of the previous chapter, if the conjecture is to hold, the strata of maxi-maximal little groups must occupy most protrudent segments of the boundary of the projected orbit space built from the invariants employed in the 4th degree Higgs potential.

The maximal little groups of $\underline{24}$ and associated branching rules are:

$$24 = 1(0) + 4(-5) + \overline{4}(5) + 15(0) \qquad\qquad SU_4 \times U_1 \qquad (\text{III.3.12})$$

$$= (1,1)(0)+(8,1)(0)+(1,3)(0)+(\overline{3},2)(5)+(3,2)(-5) \quad SU_3 \times SU_2 \times U_1 (\text{III.3.13})$$

where the U_1 charges are displayed in an arbitrary normalization in the parentheses.

The branching rules of $\underline{5}$ under these subgroups are:

$$5 = 1(4) + 4(-1) \qquad\qquad SU_4 \times U_1 \qquad\qquad \text{(III.3.14)}$$

$$= (3,1)(-2) + (1,2)(3) \qquad\qquad SU_3 \times SU_2 \times U_1 \; . \qquad \text{(III.3.15)}$$

The maximal little groups of these sub-representations of $\underline{5}$ (for the listed subgroups), and the associated branching rules are:

$$\left\{ \begin{array}{l} 1(4) = 1 \qquad\qquad\qquad\qquad SU_4 \qquad\qquad \text{(III.3.16)} \\[2em] 4(-1) = 1(0) \;+\; 3(-1) \qquad\quad SU_3 \times U_1 \qquad\quad \text{(III.3.17)} \end{array} \right.$$

$$\left\{ \begin{array}{l} (3,1)(-2) = (1,1)(0) \;+\; (2,1)(-1) \qquad SU_2 \times SU_2 \times U_1 \qquad \text{(III.3.18)} \\[2em] (1,2)(3) = 1(0) \;+\; 1(3) \qquad\qquad\quad SU_3 \times U_1 \qquad\quad . \qquad \text{(III.3.19)} \end{array} \right.$$

Therefore we obtain a list of three maxi-maximal little groups, whose branching rules for $\underline{24}$ and $\underline{5}$ are

$$\underline{SU_4} : \; 5 = 1 + 4 \qquad\qquad\qquad\qquad\qquad\qquad \text{(III.3.20)}$$

$$24 = 1 + 4 + \overline{4} + 15$$

$$\underline{SU_3 \times U_1} : \; 5 = 1(0) + 1(3) + 3(-1) \qquad\qquad\qquad \text{(III.3.21)}$$

$$24 = 1(0) + 1(3) + \overline{3}(4) + 1(-3) + 3(-4)$$

$$+ \; 1(0) + 3(-1) + \overline{3}(1) + 8(0)$$

$$\underline{SU_2 \times SU_2 \times U_1} : \; 5 = (1,1)(0) + (1,2)(1) + (2,1)(-1) \qquad\qquad \text{(III.3.22)}$$

$$24 = (1,1)(0) + (1,2)(-1) + (2,1)(1) + (1,2)(1) + (2,1)(-1)$$

$$+ \; (1,1)(0) + (3,1)(0) + (1,3)(0) + (2,2)(2) + (2,2)(-2) \; .$$

Starting from the maximal little group of $\underline{5}$, SU_4, we obtain another list of maxi-maximal little groups along this route:

$$SU_4, \ SU_3 \times U_1, \ SU_2 \times SU_2 \times U_1, \ \text{and} \ SU_3 \ .$$

As we see in this example, lists of maxi-maximal little groups along two different routes are different in general.

Having found the list of maxi-maximal little groups let us find their strata, namely the field components transforming as the singlets of the little groups. The stratum of $\underline{SU_3 \times U_1}$ is found to be

$$\varphi = (a,a,a,b,-3a-b) \ , \ \chi = (0,0,0,0,f) \ . \tag{III.3.23}$$

which occupies a curve that can be characterized by the parameter $r = a/b$:

$$\alpha = \frac{3a^4+b^4+(3a+b)^4}{[3a^2+b^2+(3a+b)^2]^2} = \frac{3r^4+1+(3r+1)^4}{[3r^2+1+(3r+1)^2]^2} \ , \tag{III.3.24}$$

$$\beta = \frac{(3a+b)^2}{3a^2+b^2+(3a+b)^2} = \frac{(3r+1)^2}{3r^2+1+(3r+1)^2} \ . $$

The curve is displayed as a function of r in Fig. III.3.2. If r is eliminated, the curve can be expressed as

$$\alpha = \frac{107}{280} + \frac{35}{24}(\beta - \frac{13}{35})^2 \pm \frac{(4-5\beta)^{3/2}}{24}(3\beta)^{1/2} \ . \tag{III.3.25}$$

The stratum of $\underline{SU_2 \times SU_2 \times U_1}$ is found to be

$$\varphi = (a,a,b,b,-2a-2b) \ , \ \chi = (0,0,0,0,f) \ . \tag{III.3.26}$$

which occupies the curve

$$\alpha = \frac{2a^4+2b^4+(2a+2b)^4}{[2a^2+2b^2+(2a+2b)^2]^2} = \frac{2r^4+2+(2r+2)^4}{[2r^2+2+(2r+2)^2]^2} \ , \tag{III.3.27}$$

$$\beta = \frac{(2a+2b)^2}{2a^2+2b^2+(2a+2b)^2} = \frac{(2r+2)^2}{2r^2+2+(2r+2)^2} \ .$$

The curve is displayed as a function of r in Fig. III.3.2. If r is eliminated, the curve can be expressed as the part of the parabola

$$\alpha = \frac{7}{30} + \frac{15}{16}(\beta - \frac{2}{15})^2 \qquad\qquad (III.3.28)$$

running from $\beta = 0$ to $\beta = 4/5$.
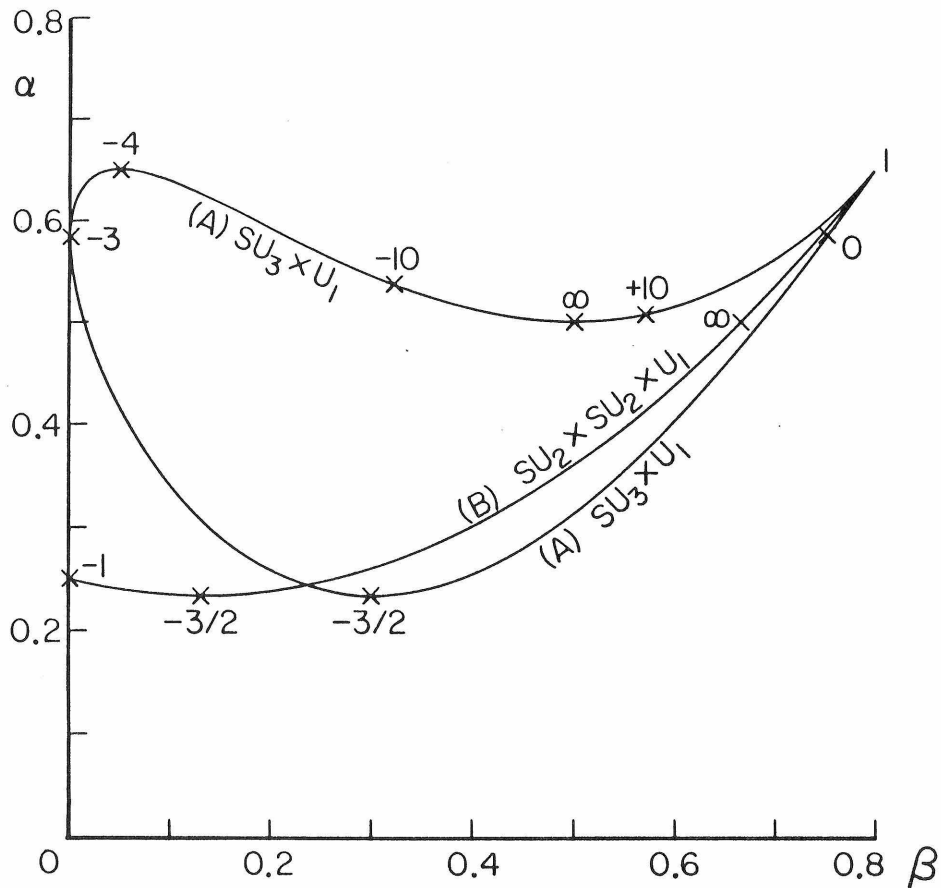
Fig. III.3.2

The stratum of $\underline{SU_4}$ is found to be

$$\varphi = a \ (1,1,1,1,-4) \ , \ \chi = (0,0,0,0,f) \ , \qquad \text{(III.3.29)}$$

which is located at

$$\alpha = 13/20 \ , \quad \beta = 4/5 \ . \qquad \text{(III.3.30)}$$

This stratum occupies the cusp at the upper right hand corner of orbit space, where the $SU_3 \times U_1$ curve, $SU_2 \times SU_2 \times U_1$ curve, and horizontal line all intersect.

The stratum of $\underline{SU_3}$ is found to be

$$\varphi = (a,a,a,b,-3a-b), \ \chi = (0,0,0,f,g) \ , \qquad \text{(III.3.31)}$$

which occupies the planar region confined by the $SU_3 \times U_1$ curve and the upper horizontal line (Fig. III.3.3). Note that the horizontal line, which is a one-dimensional stratum, belongs to the SU_3 stratum.
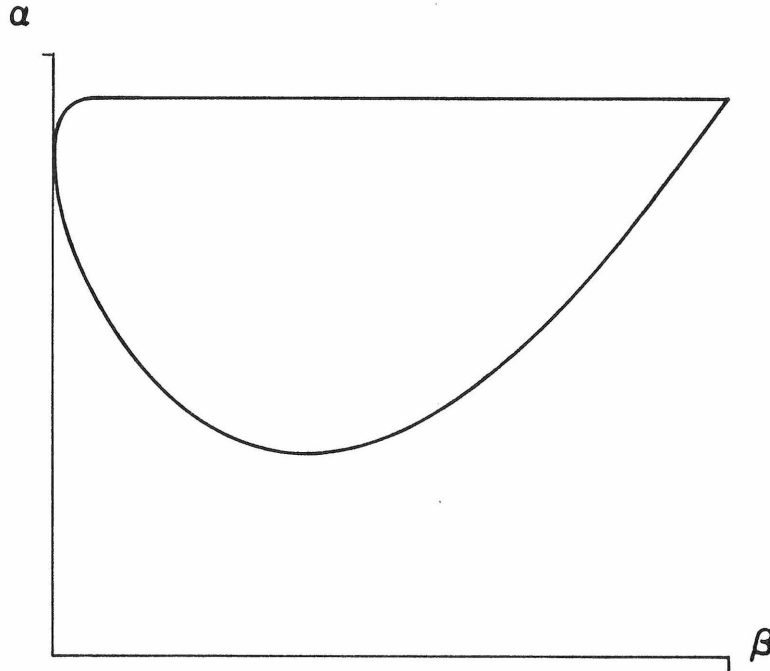
Fig. III.3.3

In order to see if these lines $(I - III)$ and curves form the boundary let us first check the boundary conditions. For purposes of varying α and β, we can replace φ by

$$\frac{\varphi}{\varphi_4} = (\, r_1, r_2, r_3, 1, -r_1 - r_2 - r_3 - 1\,) \qquad\qquad (III.3.32)$$

without loss of generality since α and β are dimensionless. It will suffice for our present needs to restrict χ to the " 5 direction " :

$$\chi = (\, 0, 0, 0, 0, f\,) \ . \qquad\qquad (III.3.33)$$

The reason is that we can always arrange r_i's such that the 5th component is the smallest or the largest yielding respectively left or right extreme values of β for fixed α. The form of α and β is now

$$\alpha = \frac{r_1^4 + r_2^4 + r_3^4 + 1 + (r_1 + r_2 + r_3 + 1)^4}{[\, r_1^2 + r_2^2 + r_3^2 + 1 + (r_1 + r_2 + r_3 + 1)^2\,]^2} \ , \qquad\qquad (III.3.34)$$

$$\beta = \frac{(r_1 + r_2 + r_3 + 1)^2}{r_1^2 + r_2^2 + r_3^2 + 1 + (r_1 + r_2 + r_3 + 1)^2} \ . \qquad\qquad (III.3.35)$$

Differentiating, one finds

$$\frac{\partial \alpha}{\partial r_i} = \frac{4[r_i^3 + (r_1 + r_2 + r_3 + 1)^3]}{[r_1^2 + r_2^2 + r_3^2 + 1 + (r_1 + r_2 + r_3 + 1)^2]^2} \qquad\qquad (III.3.36)$$

$$- \frac{4[r_i + (r_1 + r_2 + r_3 + 1)][r_1^4 + r_2^4 + r_3^4 + 1 + (r_1 + r_2 + r_3 + 1)^4]}{[r_1^2 + r_2^2 + r_3^2 + 1 + (r_1 + r_2 + r_3 + 1)^2]^3} \ ,$$

$$\frac{\partial \beta}{\partial r_i} = \frac{2(r_1 + r_2 + r_3 + 1)[r_1^2 + r_2^2 + r_3^2 + 1 - r_i(r_1 + r_2 + r_3 + 1)]}{[r_1^2 + r_2^2 + r_3^2 + 1 + (r_1 + r_2 + r_3 + 1)^2]^2} \ . \qquad\qquad (III.3.37)$$

To see that the curves and the lines we have found can form the orbit space boundary we have checked that eq. (III.3.10) is satisfied at the cusp representing

the SU_4 stratum and eq. (III.3.11) is satisfied on the one-dimensional strata, namely the curves representing the strata of $SU_3 \times U_1$, $SU_2 \times SU_2 \times U_1$. On the upper horizontal line belonging to the SU_3 stratum and the lower horizontal line belonging to the $SU_2 \times U_1$ stratum $\partial \alpha / \partial r_i = 0$, and on the vertical line $\partial \beta / \partial r_i = 0$.

To bolster our confidence that the curves and lines we have located really form the boundary of orbit space, we have plotted several thousand stratum points at random (Fig. III.3.4). They all lay within our boundary.

The main point of our observation is that most of the orbit space boundary is covered by the strata of maxi-maximal little groups but there are some portions belonging to lower level little groups. It is noteworthy that the most protrudent portions, namely the cusp and the convex portions, are covered exclusively by the strata of maxi-maximal little groups.
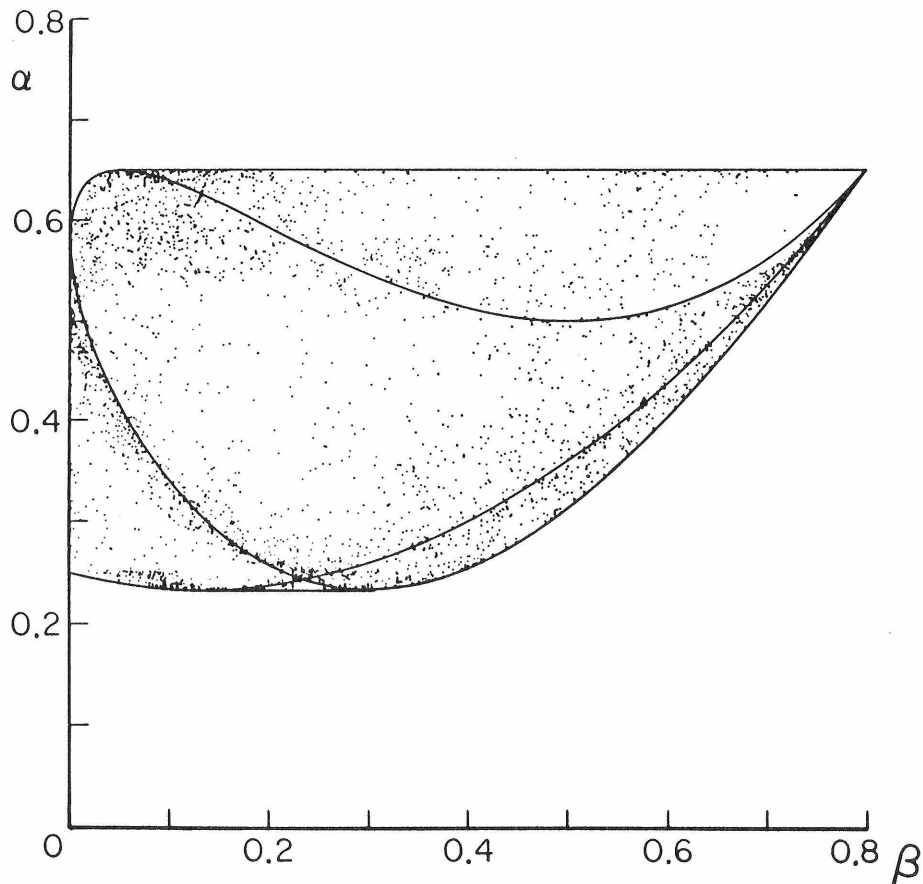
Fig. III.3.4

It is important to survey the orbit space structure a little further. The stratum of $SU_2 \times U_1$ is represented by

$$\varphi = (a,a,b,c,-2a-b-c) , \quad \chi = (0,0,0,f,g) . \qquad \text{(III.3.38)}$$

It is a three-dimensional stratum and occupies the whole orbit space. The branching rule of $\underline{5}$ under $SU_2 \times U_1$ is

$$5 = 2(1) + 1(0) + 1(-2) + 1(0) . \qquad \text{(III.3.39)}$$

It is immediately clear that this $SU_2 \times U_1$ is a subgroup of SU_3.

As we have seen in these examples various strata overlap each other or more accurately a stratum of a larger little group is included in the strata of smaller little groups that are subgroups of the larger, e.g., the stratum of SU_4 is the common point of the strata of all the little groups. This raises the issue of uniqueness of the little group corresponding to a stratum point. Since we are dealing with a projected space of the complete orbit space, it is natural for us to expect degeneracies. If we are provided with just two numbers, namely (α, β), then there is a set of φ_i's and χ_i's that yields these numbers. However if we are given additional conditions such as the boundary conditions, then we can determine the corresponding field configuration uniquely. We could establish the following result: On most of the boundary portions except for the vertical line the corresponding field configuration and thus the little group are uniquely determined, but to a point on the vertical line or to an interior point there corresponds a set of little groups none of which can be excluded in favor of the others.

III.3.3 MINIMIZING THE POTENTIAL

III.3.3.1 CONDITION FOR THE MINIMUM

The general formalism derived in CHIII.1 can be used for the case of SU_5 $\underline{24}$ + $\underline{5}$ with the following identification:

$$A' \equiv A + A_1 \, \alpha(\hat{\varphi}) \, , \tag{III.3.40}$$

$$B' \equiv B + B_1 \, \beta(\hat{\varphi}, \hat{\chi}) \, . $$

We shall concentrate on the normal Higgs case $m^2 > 0$, $M^2 > 0$. In this case solution I is the familiar local maximum at zero field, which we shall not be concerned with. Solution II is the Higgs minimum for a pure χ field and has energy

$$V_0 = - \frac{m^4}{4 \, C} \, . \tag{III.3.41}$$

Solution III is the Higgs minimum for a pure φ field and has energy

$$V_0 = - \frac{M^4}{4 \, A'} = - \frac{M^4}{4 \, [A + A_1 \alpha(\hat{\varphi})]} \, . \tag{III.3.42}$$

Solution IV has non-zero v.e.v. for both fields and is therefore the solution of principal interest to us. Its energy is

$$V_0(\hat{\varphi}, \hat{\chi}) = - \frac{(m^4 A' + M^4 C - 2 \, M^2 m^2 B')}{4(A'C - B'^2)} \tag{III.3.43}$$

$$= - \frac{1}{4}(M^2 ||\varphi||_0 + m^2 ||\chi||_0).$$

The energies for directional minima III and IV are orbit- dependent. The absolute minimum for solution III is obtained by varying $\hat{\varphi}$ to find the minimum of A', which is either at $\alpha_{\max} = 13/20$ or $\alpha_{\min} = 7/30$ depending on the sign of A_1.

The absolute minimum for solution **IV** is obtained by varying $\hat{\varphi}$ and $\hat{\chi}$ as discussed below. Comparison of the absolute minima for solutions **II**, **III** and **IV** then gives the lowest overall energy for the Higgs system.

III.3.3.2 GEOMETRY OF THE MINIMUM ENERGY CURVE

To determine the absolute minimum of solution **IV**, we begin by setting

$$V_o(\hat{\varphi},\hat{\chi}) = -\frac{k}{4}. \tag{III.3.44}$$

Then from eqs.(III.3.43), (III.3.44), and (III.3.40) one finds

$$m^4(A + A_1\alpha) + M^4C - 2\,M^2m^2(B + B_1\beta)$$

$$= k\,\left[(A + A_1\alpha)C - (B + B_1\beta)^2\right] . \tag{III.3.45}$$

We see that eq.(III.3.45) represents a parabola in $\alpha-\beta$ space. As k decreases from $+\infty$, the parabola moves in $\alpha-\beta$ space. The absolute minimum of solution **IV** for a given set of Higgs couplings and masses occurs at that k for which the parabola first touches a portion of the orbit space boundary satisfying the criteria of eqs.(III.1.11a-c), and the point of first encounter yields the orbit of minimum energy.

To visualize the movement of the parabola with k, it is useful to rewrite it as

$$(\beta + \frac{B}{B_1} - \frac{M^2m^2}{k\,B_1})^2 = \frac{A_1(C - m^4/k\,)}{B_1^2}(\alpha + \frac{A}{A_1} - \frac{M^4}{k\,A_1}) . \tag{III.3.46}$$

At $k = \infty$ the parabola has the limiting form

$$(\beta + \frac{B}{B_1})^2 = \frac{A_1C}{B_1^2}(\alpha + \frac{A}{A_1}) . \tag{III.3.47}$$

As k varies, the vertex of the parabola at

$$\alpha_o(k) = -\frac{A}{A_1} + \frac{M^4}{k\,A_1} \ , \quad \beta_o(k) = -\frac{B}{B_1} + \frac{M^2 m^2}{k\,B_1} \tag{III.3.48}$$

traces out the straight line trajectory

$$m^2 A_1[\alpha_o(k) - \alpha_o(\infty)] - M^2 B_1[\beta_o(k) - \beta_o(\infty)] = 0 \tag{III.3.49}$$

from $\alpha_o(\infty) = -A/A_1$, $\beta_o(\infty) = -B/B_1$ to infinity. Moreover as k is decreased the parabola narrows, flips orientation at $k = m^4/C$ where (III.3.46) becomes the vertical line

$$\beta = -\frac{B}{B_1} + \frac{M^2 C}{m^2 B_1} \ , \tag{III.3.50}$$

and then broadens again as k decreases further. Amidst all this movement every parabola, independent of k, passes through the intersection point of the vertex trajectory (III.3.49) and the vertical line (III.3.50):

$$\alpha_o^* = -\frac{A}{A_1} + \frac{M^4 C}{m^4 A_1} \ , \quad \beta_o^* = -\frac{B}{B_1} + \frac{M^2 C}{m^2 B_1} \ . \tag{III.3.51}$$

Thus the parabolas move with k as indicated in Fig. III.3.5: as k decreases from ∞ the parabolas remain entirely inside the $k = \infty$ parabola, narrowing to the vertical line at $k = m^4/C$, then flip to lie entirely outside the $k = \infty$ parabola at $k < m^4/C$, broadening to the limiting line

$$m^4(A + A_1\alpha) + M^4 C = 2\,M^2 m^2(B + B_1\beta) \tag{III.3.52}$$

at $k = 0$.
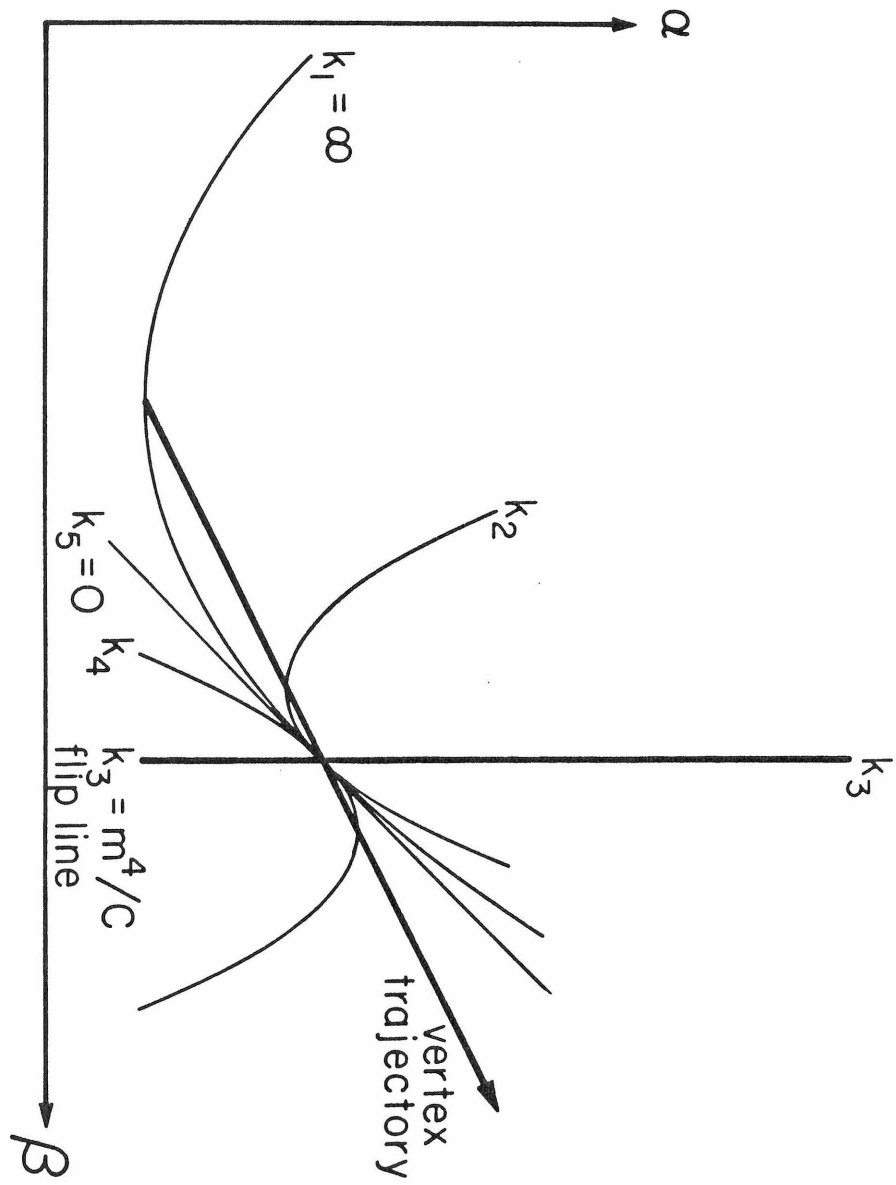
Fig. III.3.5

The relation of this complicated behavior of the minimum energy curve to the simpler behavior found in CHIII.1 for a case with 3 orbit parameters is described as follows. The two parameter case we have studied in this example corresponds to the $\gamma = 0$ plane of the 3 parameter case. The intersection of this plane with the cone yields a parabolic conic section (Fig. III.3.6a), while the planes $M^2 C' = m^2 B'$ and $m^2 A' = M^2 B'$ become straight lines and their intersection becomes the fixed point common to all solutions in the $\gamma = 0$ plane. As k decreases the vertex of the cone moves along the generating line <u>towards</u> the $\gamma = 0$ plane, causing the conic section to shrink, reduce to a line when the vertex reaches the plane at $k = m^4 / C$ (Fig. III.3.6b), and flip as the plane subsequently cuts into the other branch of the cone (Fig. III.3.6c).

(a)   (b)   (c)
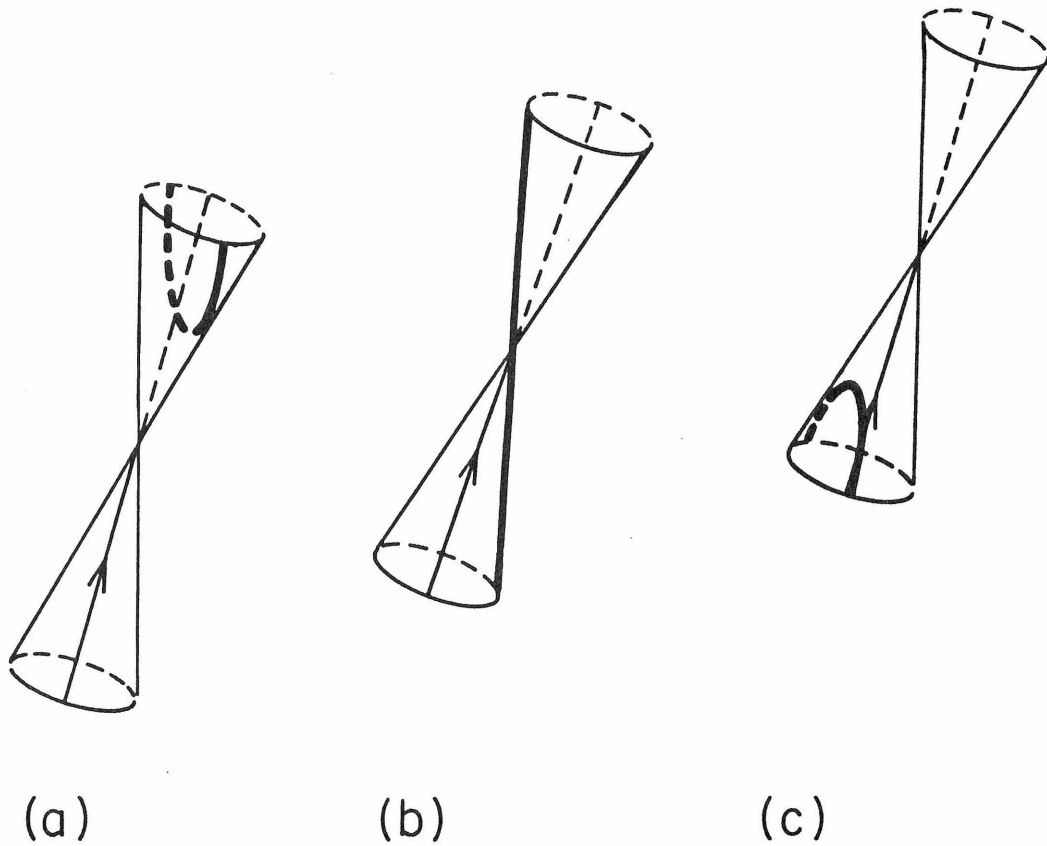
Fig. III.3.6

III.3.3.3 THE SUFFICIENCY CONDITION FOR SOLUTION IV TO BE THE ABSOLUTE MINIMUM

The inequalities (III.1.11) define a region in the $\alpha-\beta$ plane, which we will call the "allowed" region, where directional minima of type **IV** occur. The region is shown schematically in Fig. III.3.7a for the particular case $A_1 > 0$, $B_1 > 0$ with normal Higgs masses $m^2 > 0$, $M^2 > 0$. The equations for the parabola, the slant line, and the vertical line boundaries of the allowed region are given by replacing inequality signs with equality signs in relations (III.1.11c), (III.1.11b), and (III.3.11a) respectively. It is important to note that these are the same as eqs. (III.3.47), (III.3.49), and (III.3.50) for the $k = \infty$ parabola, the trajectory of parabola vertices, and the parabola flip line. Thus the dominant geometrical features of the previous chapter all have a simple physical interpretation.
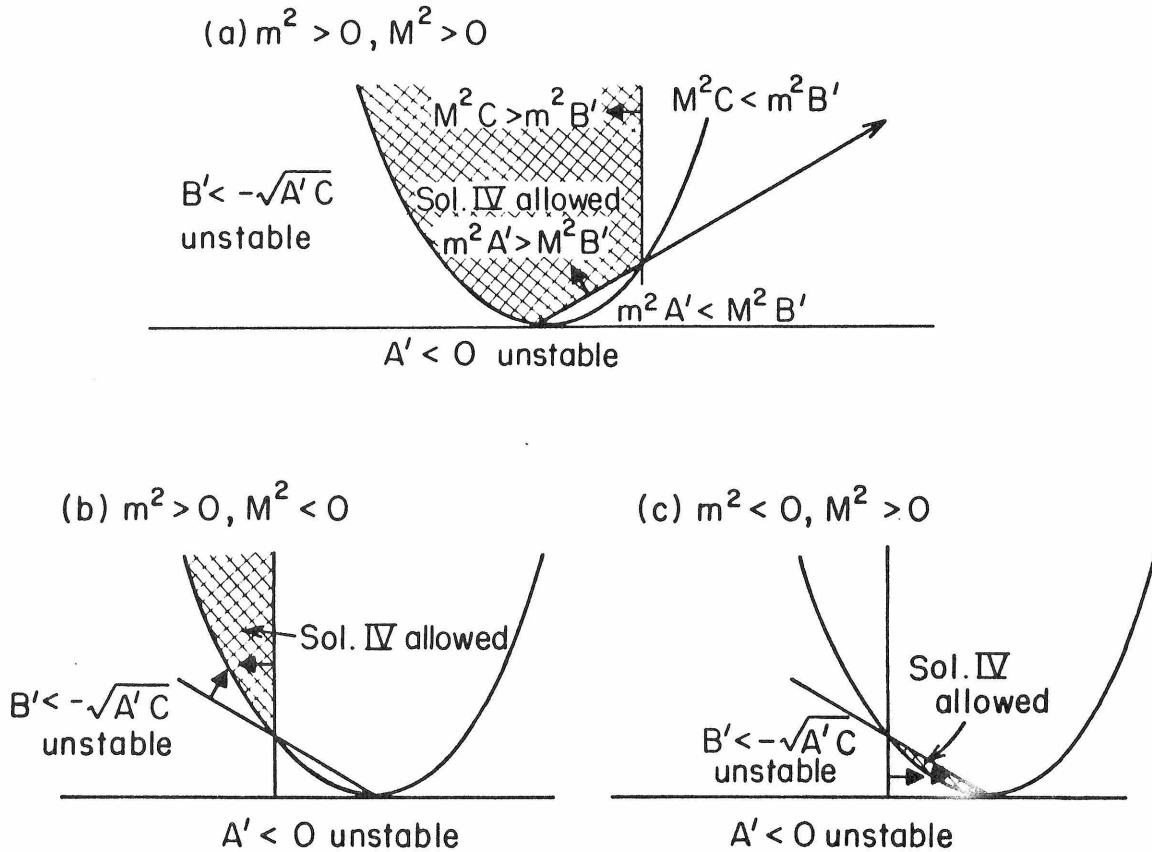
Fig. III.3.7

It is also possible to work out allowed regions for solution **IV** for the "semi-Higgs" potentials with $m^2 > 0$, $M^2 < 0$ and $m^2 < 0$, $M^2 > 0$. These are displayed in Fig.. III.3.7b and III.3.7c for the particular case $A_1 > 0$, $B_1 > 0$. Figs. III.3.7b and III.3.7c have the expected qualitative feature that although type-**IV** directional minima with both fields nonzero still exist when only one mass term has the Higgs sign [$B' < 0$ makes them possible], the allowed region for them is smaller.

The location of orbit space relative to the allowed region determines whether we obtain directional minima of type **IV** :

i)   If the orbit space is totally inside the allowed region, then directional minima of type **IV** occur everywhere in the orbit space.

ii) If the orbit space straddles the $B' = -\sqrt{A'C}$ branch of the parabola, which is the left branch in the case shown in Fig. III.3.7, then $||\varphi||_o \to +\infty$ and $||\chi||_o \to +\infty$ at stratum points along the parabola. Higgs couplings leading to this unstable result must be forbidden (positivity condition (III.1.3c)).

iii) If the orbit space straddles the slant and/or the vertical lines within the parabola, then directional minima of type **IV** occur at the stratum points within the allowed region. At nonallowed points of the orbit space, directional minima of type   **II** or **III** may occur.

iv) If the orbit space lies entirely outside the allowed region, no directional minima of type **IV** occur.

The absolute minimum of solution **IV** corresponds to the first contact of the moving parabola (III.3.46) with orbit space in the allowed region. However in case iii) of the preceding paragraph, directional minima of solutions **II** or **III** as well as **IV** are present and there is still the question of which solution gives the lowest energy. To settle this question we compare eqs. (III.3.41) and (III.3.42) to (III.3.43). First let us take the difference of eqs. (III.3.41) and (III.3.43) :

$$- \frac{m^4}{4C} + \frac{m^4 A' + M^4 C - 2 M^2 m^2 B'}{4(A'C - B'^2)} = \frac{(M^2 C - m^2 B')^2}{4C (A'C - B'^2)} \cdot \tag{III.3.53}$$

We see that at stratum points inside the parabola $(A'C > B'^2)$, type **IV** solutions always give a lower minimum than type **II**. Secondly let us take the difference of eqs. (III.3.42) and (III.3.43) :

$$- \frac{M^4}{4A'_m} + \frac{m^4 A' + M^4 C - 2 M^2 m^2 B'}{4(A'C - B'^2)} \tag{III.3.54}$$

$$= \frac{M^4}{4A'_m (A'C - B'^2)} [-B_1^2 (\beta + \frac{B}{B_1} - \frac{m^2 A'_m}{M^2 B_1})^2 + A_1 (C - \frac{m^4 A'_m}{M^4})(\alpha - \alpha_m)]$$

where $A'_m = A + \alpha_m A_1$, $\alpha_m = \alpha_{min}$ for $A_1 > 0$, and $\alpha_m = \alpha_{max}$ for $A_1 < 0$. Setting the right hand side of eq. (III.3.54) equal to zero again defines a parabola whose vertex is on the line $\alpha = \alpha_m$ and allows us a geometrical study which we leave the reader as an exercise.

The result is that in case i), there are always stratum points that make eq. (III.3.54) positive and a type **IV** solution gives the absolute minimum. In case iii), a type **IV** solution commonly gives the absolute minimum, but there is a range of Higgs coupling coefficients for which eq. (III.3.54) is negative at all the stratum points in the allowed region and a type **III** solution yields the absolute minimum.

III.3.3.4 CAN MINIMUM ENERGY ORBITS LIE ON STRAIGHT LINE ORBIT SPACE BOUNDARIES?

We now wish to show that although solution **IV** can be a directional minimum on the straight line segments of the orbit space boundary, the absolute minimum never lies on the horizontal line boundaries, and in only one degenerate case on the vertical line boundary.

At the point of first contact, the moving parabola must have the same slope as the boundary of orbit space (except at cusps). The horizontal boundary lines at α_{max}= 13/20 and α_{min}= 7/30 have slope $d\alpha/d\beta = 0$. Therefore the parabola can make its first contact with orbit space on one of these horizontal boundaries only if the contact occurs at the parabola vertex. But in the case $A_1 > 0$, $B_1 > 0$ depicted in Fig. III.3.8, the parabola already contacts other orbit space boundaries (Fig. III.3.8a) before its vertex reaches a horizontal boundary (Fig. III.3.8b). A horizontal boundary can be the last point touched (Fig. III.3.8c) but not the first. The same property is readily verified for the other possible ranges of A_1, B_1. Thus solution **IV** never gives the minimum energy at a horizontal line boundary.

The vertical boundary line at $\beta = 0$ has slope $d\alpha/d\beta = \infty$. The moving parabola has infinite slope only when it flips. Therefore (apart from the cusp at $\alpha = 1/4$, $\beta = 0$ which has no definite slope) the point of first contact can occur on the vertical boundary line only under special circumstances: the left-hand edge of orbit space must lie along the vertical line where the parabola flips, and the rest of orbit space must lie on its disallowed side (Fig. III.3.8d). In this case solution **IV** has $k = m^4/C$, degenerate in energy with solution **II**, and the field $||\varphi||_0$ of solution **IV** vanishes since $m^2B' = M^2C$ along the vertical line. Thus the vertical line never gives a minimum energy solution with two nonzero fields.
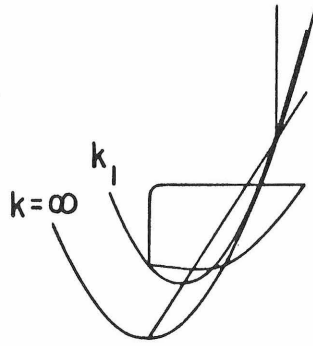
(a)
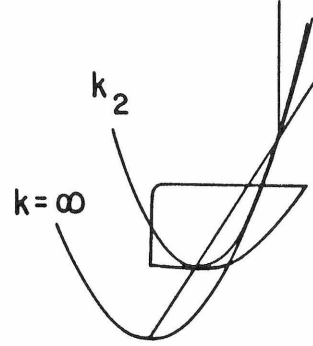
(b)
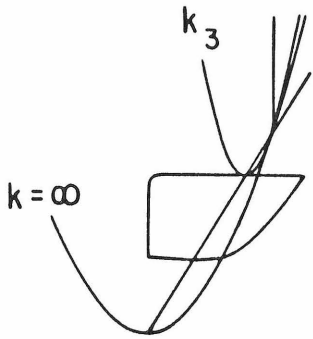
(c)
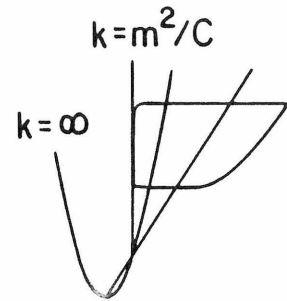
(d)

Fig. III.3.8

III.3.3.5 MINIMUM FOR VARIOUS RANGES OF HIGGS PARAMETERS

Throughout this chapter our illustrative figures have been specialized to the case $A_1 > 0$, $B_1 > 0$. In this case, the point of first contact of the parabola with an allowed portion of the orbit space (if any) occurs on the lower left boundary of orbit space . Here the minimum energy solution has residual symmetry $SU_2 \times SU_2 \times U_1$ with orbits characterized by $-3/2 < b/a \leq -1$ (Fig. III.3.2).

In the case $A_1 < 0$, $B_1 > 0$ the point of first contact (if any) occurs on the upper left boundary of orbit space. Here the minimum energy solution has residual symmetry $SU_3 \times U_1$ with orbits characterized by $-4 < b/a \leq -3$ (Fig. III.3.2).

Proceeding in this way, one finds that the four possible sign combinations of A_1, B_1 yield minimum energy solutions on the four corners of orbit space as summarized in Fig. III.3.9. These results agree with those of Buccella, Ruegg, and Savoy [20], who employed analytic methods.
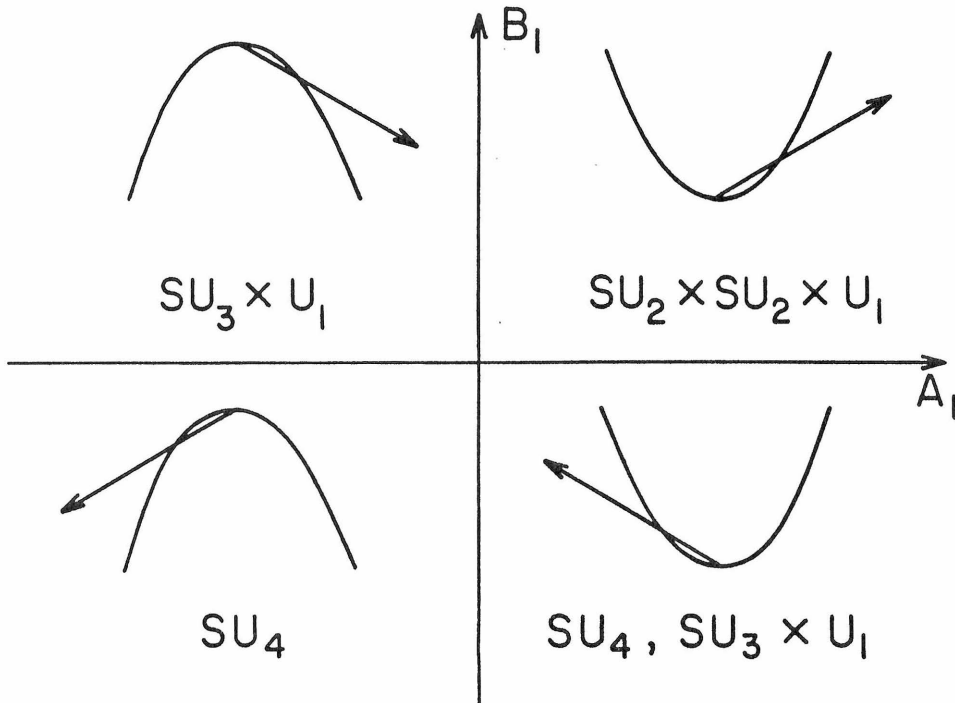
Fig. III.3.9

A_1 and B_1 are only two of the seven Higgs parameters A, A_1, B, B_1, C, m, and M. Ideally one would like to generalize Fig. III.3.9 to the full seven-dimensional Higgs parameter space, listing the exact boundaries of the unstable region where $||\varphi||$ and/or $||\chi|| \to \infty$ (positivity conditions (III.1.3) violated), the non-Higgs region $||\varphi|| = ||\chi|| = 0$ ($m^2 < 0$, $M^2 < 0$), the region of single-field Higgs solutions, and the region of two-field solutions (conditions (III.1.11) satisfied plus the sufficiency condition discussed in CHIII.3.3.3), together with the exact boundary separating SU_4 from $SU_3 \times U_1$ residual symmetries in the $A_1 > 0$, $B_1 < 0$ sector of Fig. III.3.9. The task of mapping these boundaries remains arduous, and we shall not carry it out here.

III.3.4 HIERARCHICAL SYMMETRY BREAKING via $SU_5 \to SU_3^c \times SU_2^w \times U_1 \to SU_3^c \times U_1^{em}$

If one begins with an SU_5-symmetric grand unification theory [6] and attempts to fit the phenomenological facts, one is led to introduce a hierarchical symmetry breaking [7]. First one assigns φ a huge v.e.v., which breaks the symmetry down to $SU_3^c \times SU_2^w \times U_1$ giving huge masses to gauge bosons not belonging to $SU_3^c \times SU_2^w \times U_1$. Then one assigns χ a much smaller v.e.v., which further breaks the symmetry down to $SU_3^c \times U_1^{em}$. One normally treats the second stage as a perturbation to the first stage.

There are four very restricted portions of the boundary curves (A) and (B) of Fig. III.3.2, where this conventional concept of perturbative hierarchical symmetry breaking is fully applicable:

i) Points at or near ($\alpha = 7/30$, $\beta = 3/10$) represent

$SU_5 \to SU_3^c \times SU_2^w \times U_1 \to SU_3^c \times U_1^{em}$,

ii)   points at or near ($\alpha = 7/30$, $\beta = 2/15$) represent

$$SU_5 \rightarrow SU_3^c \times SU_2^w \times U_1 \rightarrow SU_2 \times SU_2 \times U_1,$$

iii) points at or near ($\alpha = 13/20$, $\beta = 4/5$) represent

$$SU_5 \rightarrow SU_4 \times U_1 \rightarrow SU_3^c \times U_1^{em} \text{ or } SU_4,$$

iv)   points at or near ($\alpha = 13/20$, $\beta = 1/20$) represent

$$SU_5 \rightarrow SU_4 \times U_1 \rightarrow SU_3^c \times U_1^{em} .$$

The region of greatest phenomenological interest is the first one, near ($\alpha = 7/30$, $\beta = 3/10$).

However, our exact nonperturbative solution makes it clear that the condition $||\chi||_0 / ||\varphi||_0 \ll 1$ does not necessarily imply that gauge symmetry breaking occurs perturbatively and hierarchically. In general both fields should be treated with equal status. For example, while keeping $||\chi||_0 / ||\varphi||_0 \ll 1$ we can let the k-parabola first touch a point near the middle of one of the two convex portions of the curve (A), where α is far from its extrema corresponding to $SU_3^c \times SU_2^w \times U_1$ or $SU_4 \times U_1$.

Now let us examine our type-**IV** solution directly. We observe that

$$\frac{||\chi||_0}{||\varphi||_0} = \frac{(m^2/M^2)(A + A_1\alpha) - (B + B_1\beta)}{[C - (m^2/M^2)(B + B_1\beta)]} \tag{III.3.55}$$

can be made very small either by setting

$$m^2 A' \approx M^2 B' \tag{III.3.56a}$$

or by taking

$$C \gg A', |B'|, m^2/M^2 . \tag{III.3.56b}$$

Next, with an eye to the phenomenological situation, we take $A_1 > 0$, $B_1 < 0$, which places the first contact of the k parabola on the lower right $SU_3 \times U_1^{em}$

orbit space boundary. Near ($\alpha=7/30$, $\beta=3/10$) the slope of the orbit space boundary is very small, so $d\alpha/d\beta$ of the k parabola at first contact would have to be very small in this region. The general formula for the slope of the k parabola is

$$\frac{d\alpha}{d\beta} = \frac{2 B_1^2}{A_1(C - m^4/k)}(\beta + \frac{B}{B_1} - \frac{M^2 m^2}{k B_1})$$

$$= \frac{2 B_1^2}{A_1(C - m^4/k)}[\beta - \beta_0(k)] , \qquad (III.3.57)$$

where $\beta_0(k)$ refers to the parabola vertex at the given value of k. This slope can be made small either by taking

$$a) \qquad \qquad \beta - \beta_0(k) \approx 0 \qquad \qquad (III.3.58a)$$

or

$$b) \qquad \qquad \frac{B_1^2}{A_1(C - m^4/k)} \approx 0 . \qquad \qquad (III.3.58b)$$

In the first case the parabola vertex (slant line) passes very near the point ($\alpha=7/30$, $\beta=3/10$). In the second case the vertex can be far away but the k parabola is very flat in the vicinity of orbit space.

Case a) is identical with the first condition for making $||\chi||_0/||\varphi||_0$ small, ($m^2 A' \approx M^2 B'$). It requires what appears to be an unnaturally precise cancellation of coupling coefficients, a problem which has stimulated much research activity [4,7].

Case b) is compatible, but not identical, with the second condition for making $||\chi||_0/||\varphi||_0$ small ($C \gg A'$, $|B'|$, m^2/M^2). Therefore the possibility exists (as already stated) that, while $||\chi||_0/||\varphi||_0 \ll 1$, the point of first contact is far away from ($\alpha=7/30$, $\beta=3/10$) on the $SU_3 \times U_1^{em}$ boundary curve. In any event, very large C leads us to a strong coupling quantum field theory. It is a

possibility, but we do not know how to treat such a theory.

Up to now our analysis has been entirely classical, but a very important set of issues is raised by considering the radiative corrections. Whereas the classical Higgs potential is linear with respect to orbit parameters, radiative corrections are non-linear [34]. If these radiative correction terms are important then the absolute minimum can occur on the non-convex portions of the orbit space boundary (see CHV), in which case the little group will be smaller than maximaximal. The radiative correction terms are likely to play important roles in determining the symmetry of the vacuum if the gauge coupling coefficient is larger than the Higgs self-coupling coefficients, or if there is no quadratic term at all. Little groups smaller than maxi-maximal have not been noticed in the investigations of radiative corrections thus far [35], but no complete investigation has been performed yet and the danger is certainly present in the general case. The basic strategy for avoiding such a disaster is to prevent non-linear terms from playing major roles in determining the minimum of the effective potential*.

In general, radiative corrections will also introduce new orbit parameters into the effective potential (this possibility exists because in the classical Higgs potential we have been dealing with a subspace of the complete orbit space). The resulting increase in the dimensionality of orbit space complicates the problem but does not introduce difficulties of principle. Some aspects of the complete orbit space will be described in CHIV.

Thus far we have not been able to shed any light on the gauge hierarchy problem, but we will try to use our method to resolve some of the difficulties in a future work [36], where we will consider radiative corrections and renormalization group behavior [37] for several different values of m^2 and M^2.

---

* Our preliminary computation based on the effective potential in ref. [34], which contains only gauge boson loop contributions, indicates that the effective potential is monotonic with respect to α and β in the neighborhood of the point ($\alpha=7/30$, $\beta=3/10$).

III.3.5 GENERALIZATION TO SU(N) ADJOINT + VECTOR

The whole class of models SU_N adjoint + vector can be discussed by a trivial generalization of the techniques introduced in this paper for SU_5. The Higgs field φ_{ij}, which transforms as the (N^2-1) dimensional adjoint representation, is represented by an $N \times N$ traceless hermitian matrix which we put in the diagonal form $\varphi_{ij} = \delta_{ij} \varphi_i$. The Higgs field χ_i transforms as the N-dimensional (complex) vector representation. The potential $V(\varphi, \chi)$ and orbit parameters α and β retain the same forms (III.3.2), (III.3.7), and (III.3.8) with the sums extending from 1 to N.

In searching for the boundaries of orbit space, we consider a one-parameter stratum of the form

$$\varphi = (r, r, \cdots, 1, 1, \cdots, -nr - m) \tag{III.3.59}$$

(i.e., n elements r and m elements 1 with $n + m + 1 = N$) and

$$\chi = (0, 0, \cdots \cdots, 0, 1) \ . \tag{III.3.60}$$

One can readily show that this stratum satisfies the necessary condition (III.3.10-11) for a boundary curve. It has the symmetry SU_{N-1} for $m = 0$, $SU_{N-2} \times U_1$ for $m = 1$, and $SU_n \times SU_m \times U_1$ for $m \geq 2$. The whole range of subgroups SU_{N-1}, $SU_{N-2} \times U_1$, $\cdots$ down to $SU_{N/2} \times SU_{(N/2)-1} \times U_1$ (N even) or $SU_{(N-1)/2} \times SU_{(N-1)/2} \times U_1$ (N odd) occurs.

The stratum for $m = 0$ is the point

$$\alpha = \frac{n^3 + 1}{n(n+1)^2} \ ,$$

$$\beta = \frac{n}{n+1} \ . \tag{III.3.61}$$

Each stratum with $m \geq 1$ occupies a curve in orbit space which can be

characterized by the parameter r:

$$\alpha = \frac{n\,r^4 + m + (n\,r + m)^4}{[n\,r^2 + m + (n\,r + m)^2]^2} \quad,$$

$$\beta = \frac{(n\,r + m)^2}{n\,r^2 + m + (n\,r + m)^2} \quad. \tag{III.3.62}$$

A useful formula for the slope of the curve is

$$\frac{d\alpha}{d\beta} = \frac{\partial\alpha/\partial r}{\partial\beta/\partial r} = \frac{2(n^2-1)(r+\frac{m+1}{n})(r+\frac{m}{n+1})(r+\frac{m-1}{n-1})}{(r+\frac{m}{n})[nr^2 + m + (nr+m)^2]} \quad. \tag{III.3.63}$$

This formula exhibits all the turning points $\partial\alpha/\partial r = 0$ and $\partial\beta/\partial r = 0$ of the curve, except for the cusp factor $(r-1)$ which occurs in both $\partial\alpha/\partial r$ and $\partial\beta/\partial r$ and cancels out of their ratio. Substituting these values of r into eq. (III.3.62) we obtain the list of α and β at all turning points given in Table III.3.1.

Turning Point	r	α	β
α_{max}	1	$\dfrac{(m+n)^3+1}{(m+n)(m+n+1)^2}$	$\dfrac{m+n}{m+n+1}$
local min and	$\dfrac{-(m-1)}{n-1}$	$\dfrac{n(m-1)^4+m(n-1)^4+(n-m)^4}{[n(m-1)^2+m(n-1)^2+(n-m)^2]^2}$	$\dfrac{(n-m)^2}{n(m-1)^2+m(n-1)^2+(n-m)^2}$
local max of α	$\dfrac{-m}{n+1}$	$\dfrac{m^3+(n+1)^3}{m(n+1)(m+n+1)^2}$	$\dfrac{m}{(n+1)(m+n+1)}$
β_{min}	$\dfrac{-m}{n}$	$\dfrac{m^3+n^3}{nm(m+n)^2}$	0
α_{min}	$\dfrac{-(m+1)}{n}$	$\dfrac{(m+1)^3+n^3}{n(m+1)(m+n+1)^2}$	$\dfrac{n}{(m+1)(m+n+1)}$

Table III.3.1

If r is eliminated, the curve can be expressed as

$$\alpha = \beta^2 \left[1 + \frac{m^2 - mn + n^2}{mn(m+n)} + \frac{2(m^2 - 4mn + n^2)}{mn(m+n)^2} + \frac{m^2 - 6mn + n^2}{mn(m+n)^3} \right]$$

$$-2\beta \left[\frac{m^2 - mn + n^2}{mn(m+n)} + \frac{m^2 - 4mn + n^2}{mn(m+n)^2} \right]$$

$$+ \frac{m^2 - mn + n^2}{mn(m+n)}$$

$$\pm \frac{4(n-m)}{(n+m)^3} [n+m-(n+m+1)\beta]^{3/2} \left(\frac{\beta}{mn}\right)^{1/2} . \qquad \text{(III.3.64)}$$

In most cases this curve has the teardrop-type shape we found in $SU_5 \to SU_3 \times U_1$. An exception is the case $n=m$, where the coefficient of the square root vanishes and (III.3.64) simplifies to a parabola as in $SU_5 \to SU_2 \times SU_2 \times U_1$. Note that this only occurs for N odd.

A check with random stratum points for several low N verifies that the boundary of orbit space is formed by the curves (III.3.64) together with a vertical line at $\beta = 0$, a horizontal line at $\alpha_{\max}$, and (for N odd) a horizontal line at $\alpha_{\min}$ as in SU_5. The first few cases are depicted in Fig. III.3.10. Each of the subgroups SU_{N-1}, $SU_{N-2} \times U_1$, $\cdots$ occupies some portion of the orbit space boundary.

The k parabola described in CHIII.3.3 is the same for any SU_N adjoint + vector. The various sign combinations of A_1, B_1 control the orientation of the k parabolas as in CHIII.3.3.5 and yield minimum energy solutions on the four corners of orbit space as summarized in Fig. III.3.11. These results again agree with those obtained by Buccella, Ruegg, and Savoy [20]. And once again, symmetry subgroups found at minimum energy are maxi-maximal little groups in accordance with the Gell-Mann-Slansky conjecture.
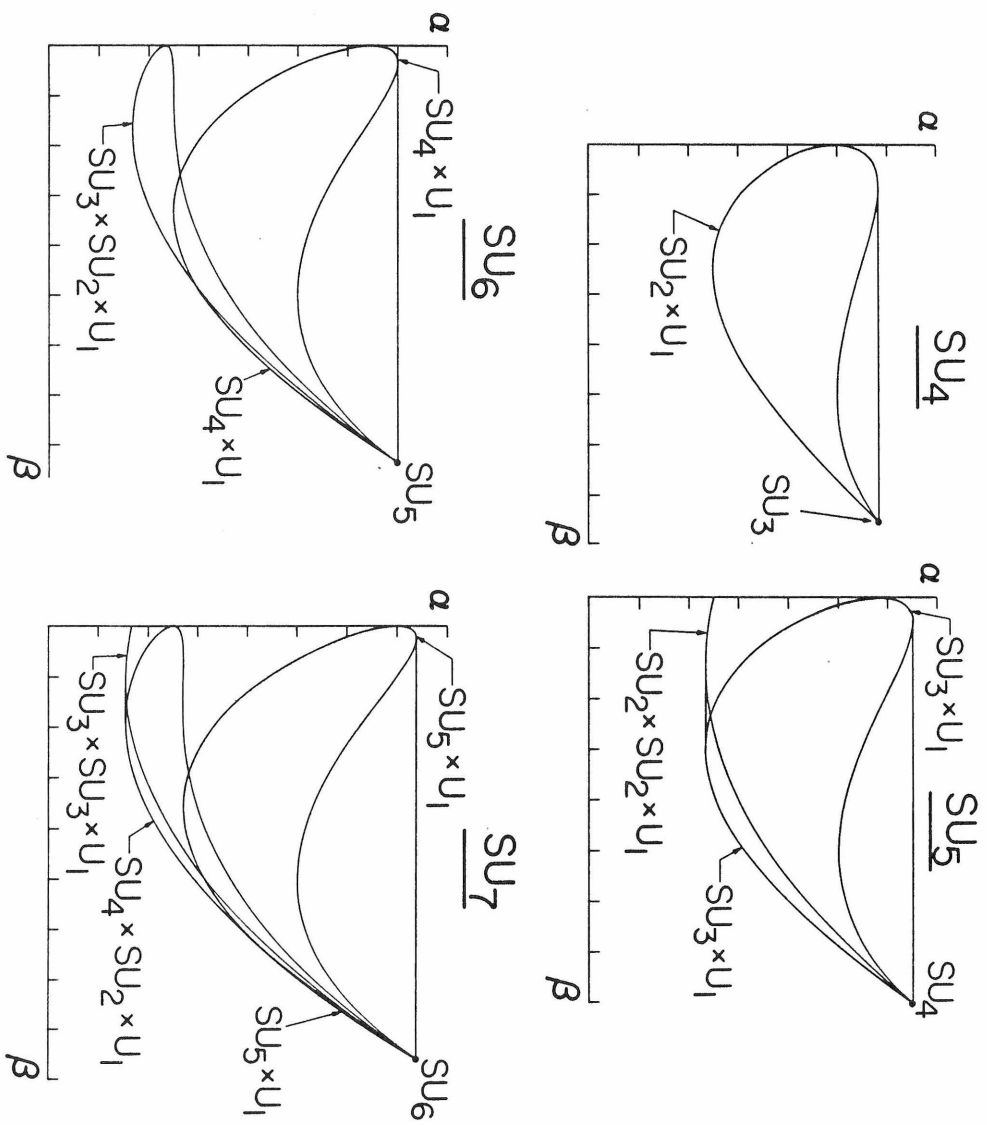
Fig. III.3.10
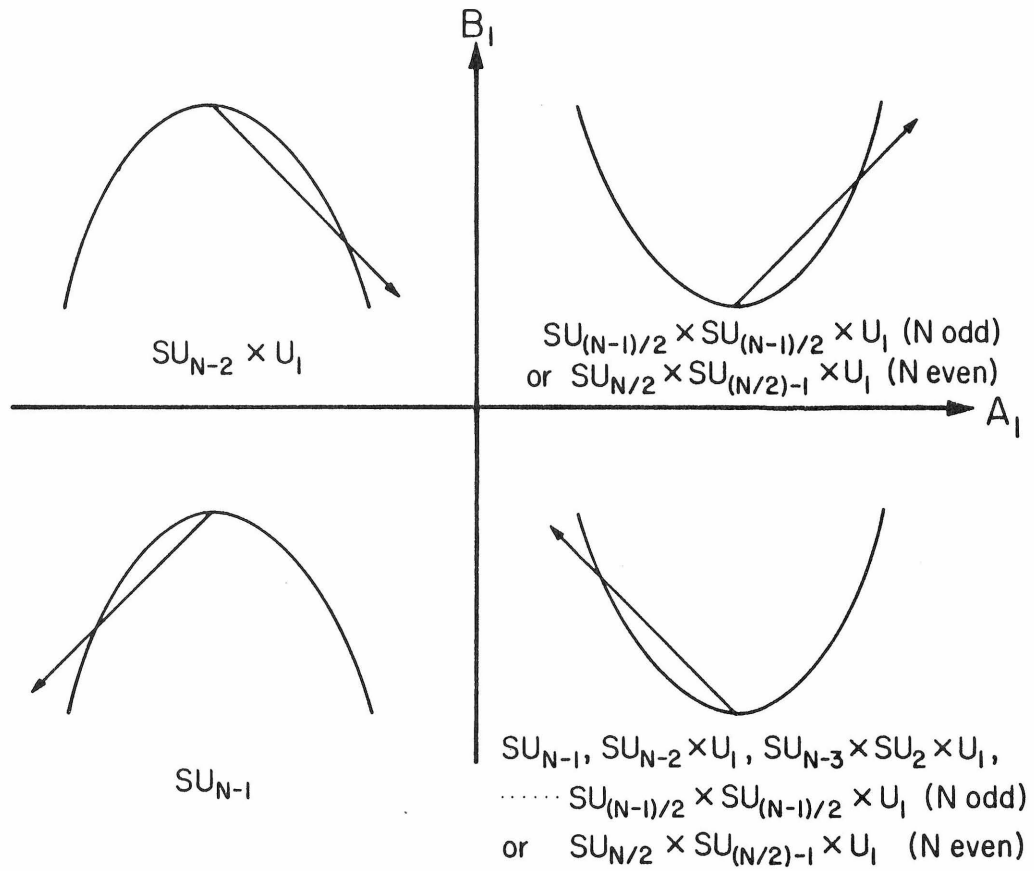
Fig. III.3.11

A new feature not found in SU_5 is the indented boundary segments found, e.g., in SU_6 near the intersection of the $SU_4 \times U_1$ and $SU_3 \times SU_2 \times U_1$ curves (Fig. III.3.10). The minimum energy stratum point cannot lie on these segments because the k parabola can never make its first contact there. A simple construction which indicates the restricted range of stratum points is to draw a straight line tangent to, e.g., the $SU_4 \times U_1$ and $SU_3 \times SU_2 \times U_1$ curves on the lower right boundary of SU_6 $\underline{35} + \underline{6}$ orbit space (Fig. III.3.12). The boundary segments closed in by this straight line never supply the lowest energy orbit.
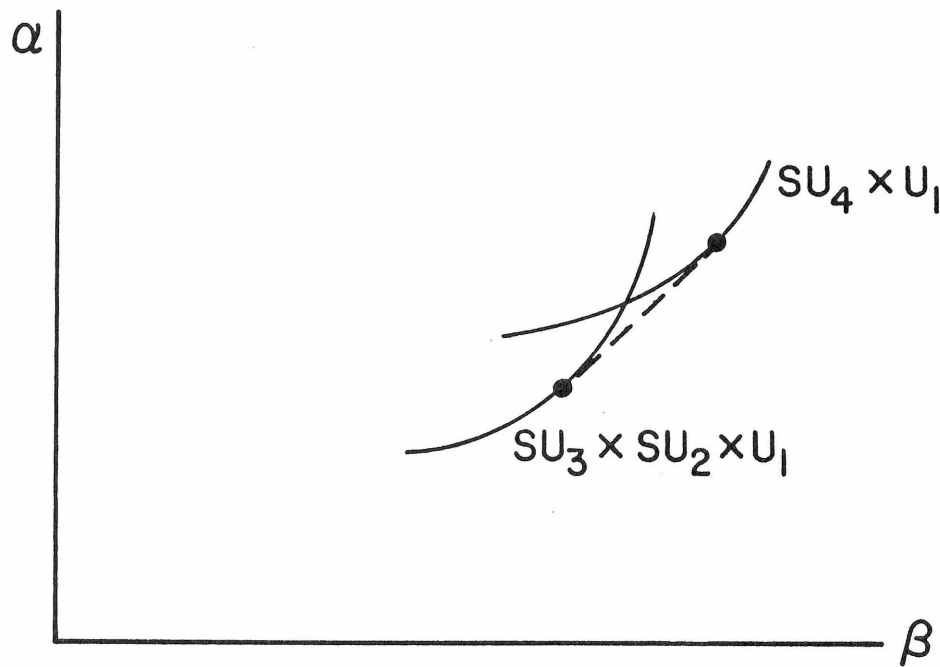
Fig. III.3.12

III.4 APPLICATION TO SO(N) ADJOINT + VECTOR REPRESENTATIONS

In this chapter we deal with the case of SO_N adjoint + vector representations. Though the same formalism as derived in the previous chapter is used for the minimizing procedure, its algebraic simplicity allows us to concentrate on the geometrical and group theoretical nature of the spontaneous symmetry breaking problem. We are going to observe a proliferation of maxi-maximal little groups. Though many of their strata lie inside the projected orbit space associated with the partial list of invariants employed in the classical Higgs potential and thus do not yield the absolute minimum, all of them have the equal geometrical status of being singular points, curves, and surfaces on the complete orbit space boundary. Also we are going to observe a proliferation of singlets. Some of them are grouped together and behave like one parameter.

We will treat the SO_{2n} and SO_{2n+1} cases separately because the two cases have somewhat different features. We treat SO_{10} as a prototype of the whole class of SO_{2n} cases, because SO_{10} is the smallest group that behaves like general SO_{2n} as we can see from Dynkin diagrams. The results are trivially extended to the SO_{2n} cases. We treat SO_7 as a prototype of the whole class of SO_{2n+1} cases for similar reasons. Again the results are trivially extended to the SO_{2n+1} cases.

III.4.1 HIGGS POTENTIAL FOR SO(10) 45 + 10

We will represent $\underline{45}$ by a 10×10 real antisymmetric matrix, φ_{ij}, and $\underline{10}$ by a 10-dimensional real vector, χ_i. Then the most general classical potential for the Higgs scalar fields, invariant under SO_{10}, can be written as follows*:

---

* Adjoint representations of small SO_{2n} groups, namely SO_4, SO_6, and SO_8, have additional invariant polynomials of a generic form $\varepsilon_{ij...kl} \, \varphi_{ij} \cdots \varphi_{kl}$, which are of degree less than 5. In such cases our Higgs potential, eq. (III.4.1), is not the most general one.

$$V(\varphi,\chi) = + \frac{M^2}{2} \sum_{i,j=1}^{10} \varphi_{ij} \varphi_{ji} - \frac{m^2}{2} \sum_{i=1}^{10} \chi_i \chi_i$$

$$+ \frac{A}{4} (\sum_{i,j=1}^{10} \varphi_{ij} \varphi_{ji})^2 + \frac{A_1}{4} \sum_{i,j,k,l=1}^{10} \varphi_{ij} \varphi_{jk} \varphi_{kl} \varphi_{li}$$

$$+ \frac{C}{4} (\sum_{i=1}^{10} \chi_i \chi_i)^2$$

$$- \frac{B}{2} (\sum_{i,j=1}^{10} \varphi_{ij} \varphi_{ji})(\sum_{k=1}^{10} \chi_k \chi_k) - \frac{B_1}{2} \sum_{i,j,k=1}^{10} \chi_i \varphi_{ij} \varphi_{jk} \chi_k \quad . \tag{III.4.1}$$

A gauge transformation, which is equivalent to an orthogonal transformation, can simplify v.e.v. of the fields into the following form:

$$\varphi = \begin{bmatrix} 0 & \varphi_1 & 0 & 0 & 0 & 0 \\ -\varphi_1 & 0 & & & & \\ & & 0 & \varphi_2 & 0 & 0 & 0 \\ 0 & & -\varphi_2 & 0 & & & \\ & & & 0 & \varphi_3 & 0 & 0 \\ 0 & & 0 & -\varphi_3 & 0 & & \\ & & & & 0 & \varphi_4 & 0 \\ 0 & 0 & 0 & & -\varphi_4 & 0 & \\ & & & & & 0 & \varphi_5 \\ 0 & 0 & 0 & 0 & & -\varphi_5 & 0 \end{bmatrix}$$

$$\equiv [\varphi_1, \varphi_2, \varphi_3, \varphi_4, \varphi_5] \quad , \tag{III.4.2}$$

$$\chi^T = (\chi_1, 0, \chi_2, 0, \chi_3, 0, \chi_4, 0, \chi_5, 0)$$

$$\equiv [\chi_1, \chi_2, \chi_3, \chi_4, \chi_5] \quad . \tag{III.4.3}$$

We have defined shorthand notations for the matrix and the row vector for convenience. In terms of this reduced set of components the potential takes a simpler form:

$$V(\varphi,\chi) = -M^2 \sum_{i=1}^{5} \varphi_i^2 - \frac{m^2}{2} \sum_{i=1}^{5} \chi_i^2$$

$$+ A \left(\sum_{i=1}^{5} \varphi_i^2\right)^2 + \frac{A_1}{2} \sum_{i=1}^{5} \varphi_i^4$$

$$+ \frac{C}{4}\left(\sum_{i=1}^{5} \chi_i^2\right)^2$$

$$+ B \left(\sum_{i=1}^{5} \varphi_i^2\right)\left(\sum_{k=1}^{5} \chi_i^2\right) + \frac{B_1}{2}\left(\sum_{i=1}^{5} \varphi_i^2 \chi_i^2\right) \qquad \text{(III.4.4)}$$

The orbit parameters are:

$$\alpha = \frac{\sum \varphi_{ij}\varphi_{jk}\varphi_{kl}\varphi_{li}}{(-\sum \varphi_{ij}\varphi_{ji})^2} = \frac{2\sum \varphi_i^4}{(2\sum \varphi_i^2)^2}$$

$$= \frac{r_1^4 + r_2^4 + r_3^4 + r_4^4 + 1}{2(r_1^2 + r_2^2 + r_3^2 + r_4^2 + 1)^2} , \qquad \text{(III.4.5)}$$

$$\beta = \frac{-\sum \chi_i \varphi_{ij}\varphi_{jk}\chi_k}{(-\sum \varphi_{ij}\varphi_{ji})(\sum \chi_i^2)} = \frac{\sum \varphi_i^2 \chi_i^2}{2(\sum \varphi_i^2)(\sum \chi_i^2)}$$

$$= \frac{r_1^2 s_1^2 + r_2^2 s_2^2 + r_3^2 s_3^2 + r_4^2 s_4^2 + 1}{2(r_1^2 + r_2^2 + r_3^2 + r_4^2 + 1)(s_1^2 + s_2^2 + s_3^2 + s_4^2 + 1)} . \qquad \text{(III.4.6)}$$

with $r_i = \varphi_i / \varphi_5$, $s_i = \chi_i / \chi_5$. In terms of $||\varphi|| \equiv -\sum \varphi_{ij}\varphi_{ji}$, $||\chi|| \equiv \sum \chi_i^2$, α, and β, we can write the potential in the simplest form:

$$V(\varphi,\chi) = -\frac{M^2}{2}||\varphi|| - \frac{m^2}{2}||\chi||$$

$$+ \frac{1}{4}(A + A_1\,\alpha(\hat{\varphi}))||\varphi||^2$$

$$+ \frac{1}{4}C\,||\chi||^2$$

$$+ \frac{1}{2}(B + B_1\,\beta(\hat{\varphi},\hat{\chi}))||\varphi||\,||\chi|| . \qquad \text{(III.4.7)}$$

III.4.2 MINIMIZATION OF THE HIGGS POTENTIAL FOR SO(10) $\underline{45} + \underline{10}$

In order to find the boundary of the orbit space, we simply anticipate the answers by looking for the strata of the maxi-maximal little groups of the Gell-Mann-Slansky conjecture. Then we verify our answers using the method given at the begining of CHIII.3.2 and by checking that they satisfy the necessary conditions for a boundary point. Since the group SO_{10} is fairly large, it is a rather lengthy procedure to find the maxi-maximal little groups. For our representations, $\underline{45} + \underline{10}$, it might look unnecessarily sophisticated. It looks even more so for higher SO_N. But if one considers other cases, e.g., $\underline{45} + \underline{16}$ [21] of SO_{10}, one realizes that simplifications like eqs. (III.4.2) and (III.4.3) are not possible in general and finds that the procedure is really a fool-proof way of finding the orbit space boundary. We refer the reader to Slansky's excellent review article [22] for the method of finding maxi-maximal little groups.

First let us consider the route starting with maximal little groups of $\underline{45}$. The maximal little groups [22,31] of $\underline{45}$, and the associated branching rules are:

a) $SU_5 \times U_1$:   (III.4.8)

$$45 = 1(0) + 10(4) + \overline{10}(-4) + 24(0)$$

$$10 = 5(2) + \bar{5}(-2)$$

b) $SO_8 \times U_1$:   (III.4.9)

$$45 = 1(0) + 8_v(2) + 8_v(-2) + 28(0)$$

$$10 = 1(2) + 1(-2) + 8_v(0)$$

c) $SU_2 \times SO_6 \times U_1$:   (III.4.10)

$$45 = (1,1)(2) + (1,1)(0) + (1,1)(-2) + (3,1)(0)$$

$$+(1,15)(0)+(2,6)(1)+(2,6)(-1)$$

$$10 = (2,1)(1)+(2,1)(-1)+(1,6)(0)$$

d) $\quad SO_4 \times SU_3 \times U_1$: $\hfill$ (III.4.11)

$$45 = (3,1,1)(0)+(1,3,1)(0)+(1,1,1)(0)+(1,1,3)(-4)$$

$$+(1,1,\bar{3})(4)+(1,1,8)(0)+(2,2,3)(2)+(2,2,\bar{3})(-2)$$

$$10 = (2,2,1)(0)+(1,1,3)(2)+(1,1,\bar{3})(-2)$$

We have adopted a $SU_2 \times SU_2$ notation for SO_4 sub-representations.

The maxi-maximal little groups along each of the four sub-routes are:
sub-route **a)** :

$$SU_4 \times U_1 :$$ $\hfill$ (III.4.12)

$$10 = 1(0)+4(1)+1(0)+\bar{4}(-1)$$

$$45 = 1(0)+4(1)+6(2)+\bar{4}(-1)+6(-2)+1(0)+4(1)+\bar{4}(-1)+15(0)$$

sub-route **b)** :

$$SO_8 :$$ $\hfill$ (III.4.13)

$$10 = 1+1+8_\nu$$

$$45 = 1+8_\nu+8_\nu+28$$

$$SO_7 \times U_1 :$$ $\hfill$ (III.4.14)

$$10 = 1(1)+1(-1)+1(0)+7(0)$$

$$45 = 1(0)+1(1)+7(1)+1(-1)+7(-1)+7(0)+21(0)$$

sub-route **c)** :

$$SO_8 \times U_1 \; : \tag{III.4.15}$$

$$10 = 1(1)+1(0)+1(0)+1(-1)+6(0)$$

$$45 = 1(1)+1(0)+1(-1)+1(1)+1(0)+1(-1)$$

$$+15(0)+6(1)+6(0)+6(0)+6(-1)$$

$$SU_2 \times SO_5 \times U_1 \; : \tag{III.4.16}$$

$$10 = (2,1)(1)+(2,1)(-1)+(1,1)(0)+(1,5)(0)$$

$$45 = (1,1)(2)+(1,1)(0)+(1,1)(-2)+(3,1)(0)+(1,5)(0)$$

$$+(1,10)(0)+(2,1)(1)+(2,5)(1)+(2,1)(-1)+(2,5)(-1)$$

sub-route **d)** :

$$SO_3 \times SU_3 \times U_1 \; : \tag{III.4.17}$$

$$10 = (3,1)(0)+(1,1)(0)+(1,3)(1)+(1,\bar{3})(-1)$$

$$45 = (3,1)(0)+(3,1)(0)+(1,1)(0)+(1,3)(-2)+(1,\bar{3})(2)$$

$$+(1,8)(0)+(3,3)(1)+(1,3)(1)+(3,\bar{3})(-1)+(1,\bar{3})(-1)$$

$$SO_4 \times SU_2 \times U_1 \; : \tag{III.4.18}$$

$$10 = (2,2,1)(0)+(1,1,2)(1)+(1,1,1)(0)+(1,1,2)(-1)+(1,1,1)(0)$$

$$45 = (3,1,1)(0)+(1,3,1)(0)+(1,1,1)(0)+(1,1,1)(-2)+(1,1,2)(-1)$$

$$+(1,1,1)(2)+(1,1,2)(1)+(1,1,1)(0)+(1,1,2)(1)+(1,1,2)(-1)$$

$$+(1,1,3)(0)+(2,2,1)(0)+(2,2,2)(1)+(2,2,1)(0)+(2,2,2)(-1)$$

Next let us consider the route starting with maximal little groups of $\underline{10}$. In this case the procedure is rather simple because $\underline{10}$ has only one maximal little group, SO_9. The branching rules are:

$$SO_9 : \qquad\qquad\qquad\qquad\qquad\qquad\qquad\qquad \text{(III.4.19)}$$

$$10 = 1+9$$

$$45 = 9+36$$

Following the same procedure, we obtain the list of the maxi-maximal little groups along this route: SO_8, $SO_7 \times U_1$, $SU_4 \times U_1$, $SU_2 \times SO_5 \times U_1$, $SO_3 \times SU_3 \times U_1$.

As we mentioned in CHIII.3.2, the lists of maxi-maximal little groups along two different routes are found to be different. The total list of maxi-maximal little groups, the forms of φ and χ which transform as singlets under them, and the orbit parameters for them are listed in Table III.4.1.

Maxi–maximal Little Group	Singlet Form	α	β
$SU_4 \times U_1$	$\varphi = [b,b,b,b,a]$ $\chi = [0,0,0,0,v]$	$\dfrac{1+4r^4}{2(1+4r^2)^2}$	$\dfrac{1}{2(1+4r^2)}$
SO_8	$\varphi = [0,0,0,0,a]$ $\chi = [0,0,0,0,v]$	$1/2$	$1/2$
$SO_7 \times U_1$	$\varphi = [0,0,0,0,a]$ $\chi = [0,0,0,v,0]$	$1/2$	0
$SO_6 \times U_1$	$\varphi = [0,0,0,b,a]$ $\chi = [0,0,0,0,v]$	$\dfrac{1+r^4}{2(1+r^2)^2}$	$\dfrac{1}{2(1+r^2)}$
$SU_2 \times SO_5 \times U_1$	$\varphi = [0,0,0,a,a]$ $\chi = [0,0,v,0,0]$	$1/4$	0
$SO_3 \times SU_3 \times U_1$	$\varphi = [a,a,a,0,0]$ $\chi = [0,0,0,0,v]$	$1/6$	$1/6$
$SO_4 \times SU_2 \times U_1$	$\varphi = [0,0,b,b,a]$ $\chi = [0,0,0,0,v]$	$\dfrac{1+2r^4}{2(1+2r^2)^2}$	$\dfrac{1}{2(1+2r^2)}$

Table III.4.1

The points and curves representing the strata of maxi-maximal little groups are shown in Fig. III.4.1. Unlike the case of SU_N adjoint + vector, strata of some maxi-maximal little groups are totally buried inside the orbit space and do not contribute to the boundary. This is because we are considering a projected space of the complete orbit space. We will come back to this issue in CHIII.4.5.

Using the minimization procedure of CHIII.3.3, one immediately finds that:

When $A_1 > 0$, $B_1 > 0$, the absolute minimum occurs at the stratum of $SU_4 \times U_1$;

when $A_1 > 0$, $B_1 < 0$, the absolute minimum occurs at the stratum of $SU_4 \times U_1$ or SO_8;

when $A_1 < 0$, $B_1 > 0$, the absolute minimum occurs at the stratum of $SO_7 \times U_1$;

when $A_1 < 0$, $B_1 < 0$, the absolute minimum occurs at the stratum of SO_8.
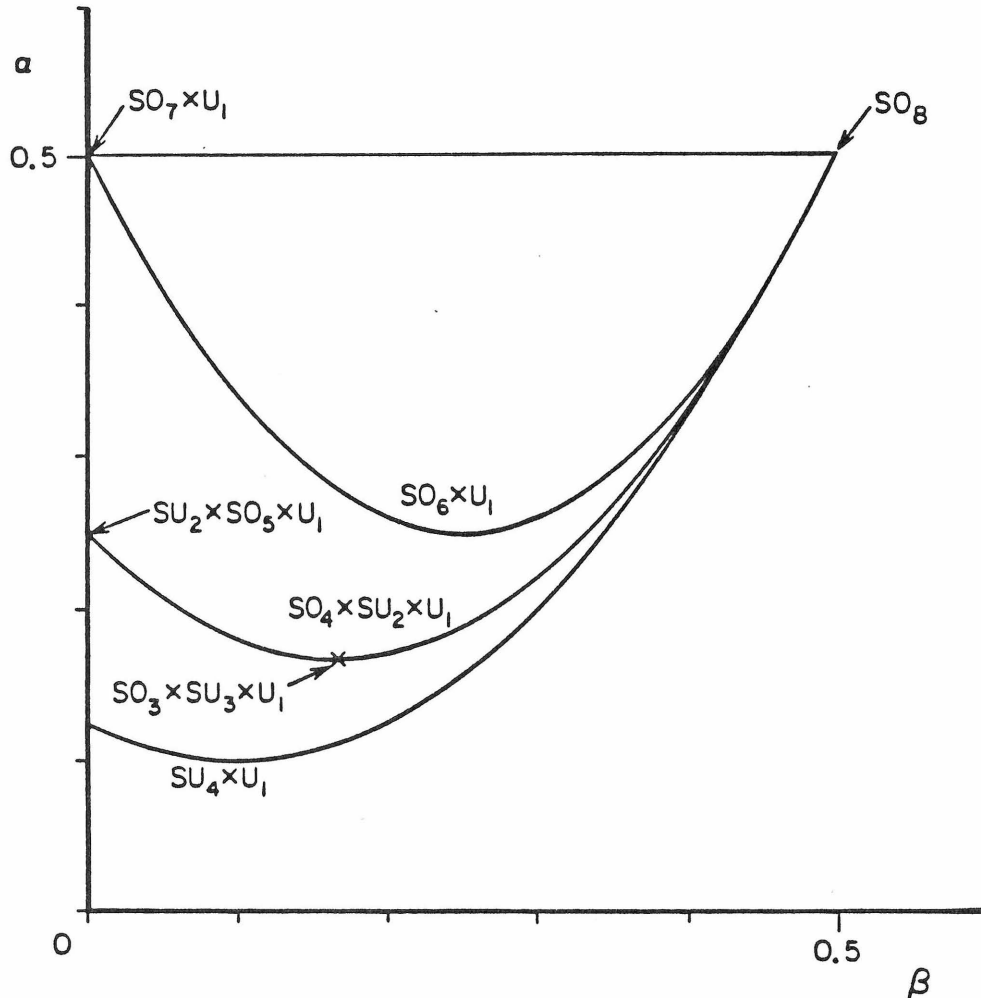
Fig. III.4.1

The number of maxi-maximal little groups grows rapidly as we go to higher n and the Gell-Mann-Slansky conjecture becomes less effective because the strata of more and more maxi-maximal little groups are totally buried inside the orbit space. However, the "usable" boundaries, where absolute minima occur, consist of the strata of just three maxi-maximal little groups;

$$SU_{n-1} \times U_1, \quad SO_{2n-2}, \quad SO_{2n-3} \times U_1 \quad . \tag{III.4.20}$$

Their strata are listed in Table III.4.2.

Thus the results of the SO_{10} case for absolute minima can be extended to SO_{2n} with $SU_4 \times U_1$ replaced by $SU_{n-1} \times U_1$, SO_8 by SO_{2n-2}, and $SO_7 \times U_1$ by $SO_{2n-3} \times U_1$.

Maxi–maximal Little Group	Singlet Form	α	β
$SU_{n-1} \times U_1$	$\varphi = [b,b,\cdots,b,a]$ $\chi = [0,0,\cdots,0,v]$	$\dfrac{1+(n-1)r^4}{2(1+(n-1)r^2)^2}$	$\dfrac{1}{2(1+(n-1)r^2)}$
SO_{2n-2}	$\varphi = [0,0,\cdots,0,a]$ $\chi = [0,0,\cdots,0,v]$	$1/2$	$1/2$
$SO_{2n-3} \times U_1$	$\varphi = [0,0,\cdots,0,0,a]$ $\chi = [0,0,\cdots,0,v,0]$	$1/2$	0

Table III.4.2

III.4.3 THE HIGGS POTENTIAL FOR SO(7) $\underline{21} + \underline{7}$

The Higgs potential for this case is of the same form as eq. (III.4.1) except that the upper limit of the sum is now 7. But after the gauge transformation the simplified v.e.v. of the fields take slightly different forms than before:

$$
\varphi = \begin{bmatrix}
0 & \varphi_1 & & & & & \\
-\varphi_1 & 0 & & 0 & & 0 & 0 \\
& & 0 & \varphi_2 & & & \\
& 0 & -\varphi_2 & 0 & & 0 & 0 \\
& & & & 0 & \varphi_3 & \\
& 0 & & 0 & -\varphi_3 & 0 & 0 \\
& 0 & & 0 & & 0 & 0
\end{bmatrix}
$$

$$
\equiv [\varphi_1, \varphi_2, \varphi_3] \; . \tag{III.4.21}
$$

$$
\chi^T = (\chi_1, 0, \chi_2, 0, \chi_3, 0, \chi_4)
$$

$$
\equiv [\chi_1, \chi_2, \chi_3, \chi_4] \; . \tag{III.4.22}
$$

Instead of eq. (III.4.4) we now have

$$
V(\varphi, \chi) = -M^2 \sum_{i=1}^{3} \varphi_i^2 - \frac{m^2}{2}(\sum_{i=1}^{3} \chi_i^2 + \chi_4^2)
$$

$$
+ A \left(\sum_{i=1}^{3} \varphi_i^2\right)^2 + \frac{A_1}{2} \sum_{i=1}^{3} \varphi_i^4
$$

$$
+ \frac{C}{4}(\sum_{i=1}^{3} \chi_i^2 + \chi_4^2)^2
$$

$$
+ B \left(\sum_{i=1}^{3} \varphi_i^2\right)(\sum_{i=1}^{3} \chi_i^2 + \chi_4^2) + \frac{B_1}{2}(\sum_{i=1}^{3} \varphi_i^2 \chi_i^2) \tag{III.4.23}
$$

The orbit parameters are:

$$
\alpha = \frac{\sum \varphi_{ij} \varphi_{jk} \varphi_{kl} \varphi_{li}}{(-\sum \varphi_{ij} \varphi_{ji})^2} = \frac{2 \sum \varphi_i^4}{(2 \sum \varphi_i^2)^2}
$$

$$= \frac{r_1^4 + r_2^4 + 1}{2\,(r_1^2 + r_2^2 + 1)^2}\,, \tag{III.4.24}$$

$$\beta = \frac{-\sum \chi_i \varphi_{ij} \varphi_{jk} \chi_k}{(-\sum \varphi_{ij} \varphi_{ji})(\sum \chi_i^2)} = \frac{\sum \varphi_i^2 \chi_i^2}{2\,(\sum \varphi_i^2)\,(\sum\limits_{i=1}^{3} \chi_i^2 + \chi_4^2)}$$

$$= \frac{r_1^2 s_1^2 + r_2^2 s_2^2 + 1}{2(r_1^2 + r_2^2 + 1)(s_1^2 + s_2^2 + 1 + s_4^2)}\,. \tag{III.4.25}$$

with $r_i = \varphi_i / \varphi_3$, $s_i = \chi_i / \chi_3$. Eq. (III.4.7) can be used without change.

III.4.4 MINIMIZATION OF THE HIGGS POTENTIAL FOR SO(7) $\underline{21} + \underline{7}$

As before we look for the strata of the maxi-maximal little groups to find the boundary of the orbit space. First let us consider the route starting with maximal little groups of $\underline{21}$. The maximal little groups of $\underline{21}$, and the associated branching rules are:

a) $SU_2 \times SO_3 \times U_1$: \hfill (III.4.26)

$$21 = (1,3)(0)+(3,1)(0)+(1,1)(2)+(1,1)(0)$$

$$+(1,1)(-2)+(2,3)(1)+(2,3)(-1)$$

$$7 = (1,3)(0)+(2,1)(1)+(2,1)(-1)$$

b) $SO_5 \times U_1$: \hfill (III.4.27)

$$21 = 1(0)+5(1)+5(-1)+10(0)$$

$$7 = 1(1)+1(-1)+5(0)$$

- 95 -

c) $SU_3 \times U_1$: $\qquad\qquad$ (III.4.28)

$$21 = 3(1)+\bar{3}(-1)+1(0)+3(-2)+\bar{3}(2)+8(0)$$

$$7 = 1(0)+3(1)+\bar{3}(-1)$$

The maxi-maximal little groups along each of the four sub-routes are:

sub-route **a)** :

$SU_2 \times U_1 \times U_1$: $\qquad\qquad$ (III.4.29)

$$7 = 1[0,1]+1[0,0]+1[0,-1]+2[1,0]+2[-1,0]$$

$$21 = 1[0,1]+1[0,0]+1[0,-1]+3[0,0]+1[2,0]+1[0,0]$$

$$+1[-2,0]+2[1,1]+2[1,0]+2[1,-1]+2[-1,1]+2[-1,0]+2[-1,-1]$$

$SO_3 \times U_1$: $\qquad\qquad$ (III.4.30)

$$7 = 3(0)+1(1)+1(0)+1(0)+1(-1)$$

$$21 = 3(0)+1(1)+1(0)+1(-1)+1(1)+1(0)$$

$$+1(-1)+3(1)+3(0)+3(0)+3(-1)$$

sub-route **b)** :

SO_5 : $\qquad\qquad$ (III.4.31)

$$7 = 1+1+5$$

$$21 = 1+5+5+10$$

$SO_4 \times U_1$: $\qquad\qquad$ (III.4.32)

$$7 = (1,1)(1)+(1,1)(-1)+(1,1)(0)+(2,2)(0)$$

$$21 = (1,1)(0)+(1,1)(1)+(2,2)(1)+(1,1)(-1)$$

$$+(2,2)(-1)+(1,3)(0)+(3,1)(0)+(2,2)(0)$$

sub-route **c**) :

$$SU_3 \times U_1 \; : \qquad\qquad\qquad\qquad\qquad\qquad\qquad (III.4.33)$$

$$7 = 1(0)+3(1)+\bar{3}(-1)$$

$$21 = 3(1)+\bar{3}(-1)+1(0)+3(-2)+\bar{3}(2)+8(0)$$

$$SU_2 \times U_1 \; : \qquad\qquad\qquad\qquad\qquad\qquad\qquad (III.4.34)$$

$$7 = 1(0)+1(0)+2(1)+1(0)+2(-1)$$

$$21 = 1(0)+2(1)+1(0)+2(-1)+1(0)+1(-2)+2(-1)$$

$$+1(2)+2(1)+1(0)+2(1)+2(-1)+3(0)$$

Next let us consider the route starting with maximal little groups of 7. 7 has only one maximal little group, SO_6. Following the same procedure, we obtain the list of maxi-maximal little groups along this route: $SO_5, SU_3 \times U_1, SO_4 \times U_1$.

The total list of maxi-maximal little groups, the forms of φ and χ which transform as singlets under them, and the orbit parameters for them are listed in Table III.4.3.

Maxi–maximal Little Group	Singlet Form	α	β
$SU_2 \times U_1 \times U_1$	$\varphi = [b,b,a]$ $\chi = [0,0,0,v]$	$\dfrac{1+2r^4}{2(1+2r^2)^2}$	0
$SO_3 \times U_1$	$\varphi = [0,b,a]$ $\chi = [0,0,v,0]$	$\dfrac{1+r^4}{2(1+r^2)^2}$	$\dfrac{1}{2(1+r^2)}$
SO_5	$\varphi = [0,0,a]$ $\chi = [0,0,v,0]$	$1/2$	$1/2$
$SO_4 \times U_1$	$\varphi = [0,0,a]$ $\chi = [0,0,0,v]$	$1/2$	0
$SU_3 \times U_1$	$\varphi = [a,a,a]$ $\chi = [0,0,0,v]$	$1/6$	0
$SU_2 \times U_1$	$\varphi = [b,b,a]$ $\chi = [0,0,v,w]$	$\dfrac{1+2r^4}{2(1+2r^2)^2}$	$\dfrac{1}{2(1+2r^2)(1+s^2)}$

Table III.4.3

The points and curves representing the strata of maxi-maximal little groups are shown in Fig. III.4.2.

Once again one easily finds that:

When $A_1 > 0$, $B_1 > 0$, the absolute minimum occurs at the stratum of $SU_3 \times U_1$;

when $A_1 > 0$, $B_1 < 0$, the absolute minimum occurs at the stratum of $SU_2 \times U_1$ or SO_5;

when $A_1 < 0$, $B_1 > 0$, the absolute minimum occurs at the stratum of $SO_4 \times U_1$;

when $A_1 < 0$, $B_1 < 0$, the absolute minimum occurs at the stratum of SO_5.
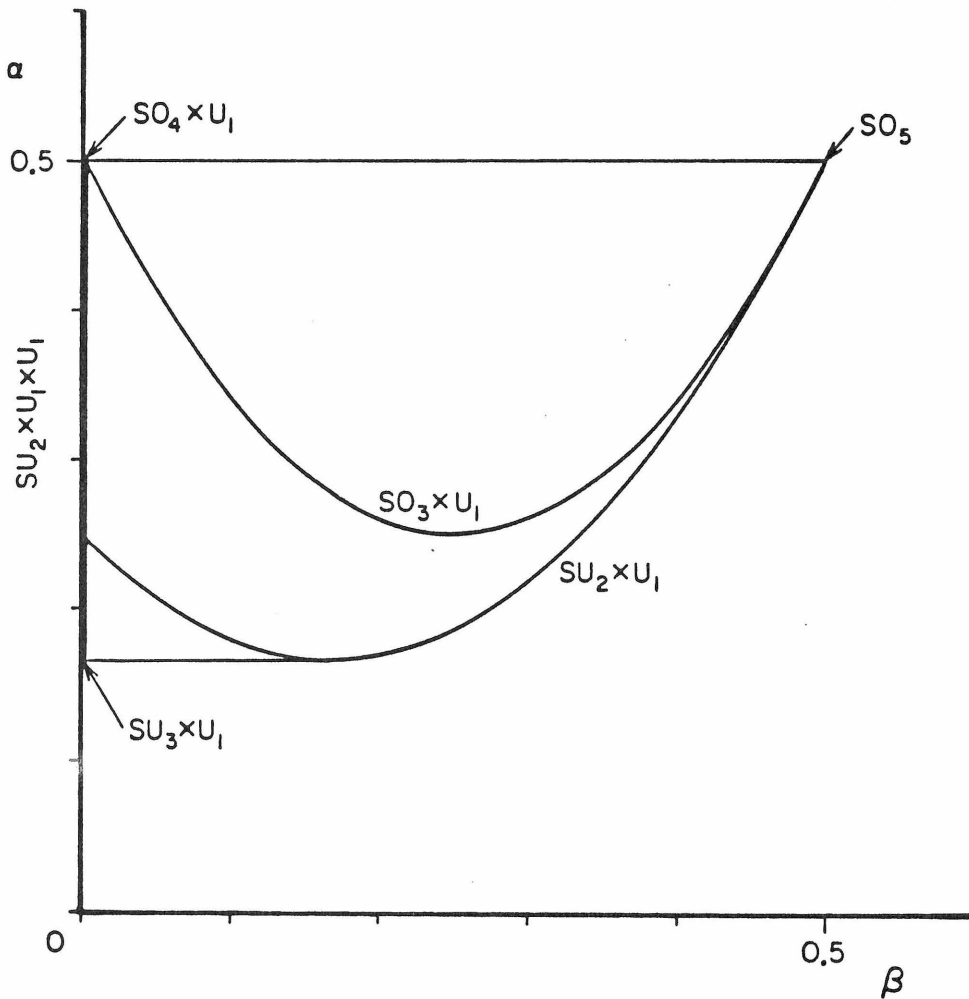
Fig. III.4.2

In this example the relationship between the signs of A_1 and B_1 and the strata of the absolute minimum is most transparent. When $B_1 > 0$, β is chosen to be zero and the minimum (maximum) value of α is chosen for $A_1 > 0$ $(A_1 < 0)$ to yield the lowest potential minimum. When $B_1 < 0$, the maximum allowed value of β is chosen to yield the lowest potential. The balancing between α and β is more delicate in this case because more options are available along the convex curved portion corresponding to $SU_2 \times U_1$. This property was used in ref. [20,21] to minimize the potential.

The generalization to the SO_{2n+1} adjoint + vector case is trivially done by using the results of the SO_7 case with $SU_3 \times U_1$ replaced by $SU_n \times U_1$, $SU_2 \times U_1$ by $SU_{n-1} \times U_1$, SO_5 by SO_{2n-1}, and $SO_4 \times U_1$ by $SO_{2n-2} \times U_1$. The strata of usable portions of the boundary are listed in Table III.4.4.

Maxi−maximal Little Group	Singlet Form	α	β
$SU_{n-1} \times U_1$	$\varphi = [b,b,\cdots,b,a]$ $\chi = [0,0,\cdots,0,v,w]$	$\dfrac{1+(n-1)r^4}{2(1+(n-1)r^2)^2}$	$\dfrac{1}{2(1+(n-1)r^2)(1+s^2)}$
SO_{2n-1}	$\varphi = [0,0,\cdots,0,a]$ $\chi = [0,0,\cdots,0,v,0]$	$1/2$	$1/2$
$SO_{2n-2} \times U_1$	$\varphi = [0,0,\cdots,0,a]$ $\chi = [0,0,\cdots,0,0,v]$	$1/2$	0
$SU_n \times U_1$	$\varphi = [a,a,\cdots,a,a]$ $\chi = [0,0,\cdots,0,0,v]$	$1/2n$	0

Table III.4.4

III.4.5 THE GEOMETRICAL SIGNIFICANCE OF MAXI-MAXIMAL LITTLE GROUPS

In CHII.4 we have seen that strata of maximal and semi-maximal little groups, namely singular points and curves on the complete orbit space boundary, are partially buried inside the projected orbit space used in the Higgs problem. Though it is hard to visualize the complete orbit space, the points and curves corresponding to some maxi-maximal little groups that are buried in the projected orbit space in the examples of present chapter are thought to lie on the boundary of the complete orbit space. In this chapter we list the complete set of basic invariants for the adjoint + vector representations of SO_{10} and SO_7 and compute the ranks of the Jacobian determinants for each stratum of the maxi-maximal little groups.

Let us consider SO_{10} adjoint + vector representations again. The complete set of elementary invariant polynomials for them is:

$$A_2 = Tr\,\varphi^2 = -2\sum\varphi_i^2, \quad A_4 = Tr\,\varphi^4 = 2\sum\varphi_i^4, \quad A_6 = Tr\,\varphi^6 = -2\sum\varphi_i^6, \tag{III.4.35}$$

$$A_8 = Tr\,\varphi^8 = 2\sum\varphi_i^8, \quad A_5 = \varepsilon_{ijklmnopqr}\,\varphi_{ij}\,\varphi_{kl}\,\varphi_{mn}\,\varphi_{op}\,\varphi_{qr} = 2^5\varphi_1\varphi_2\varphi_3\varphi_4\varphi_5,$$

$$C = \sum\chi_i^2, \tag{III.4.36}$$

$$B_2 = Tr\chi\varphi^2\chi = -2\sum\chi_i\varphi_i^2\chi_i, \quad B_4 = Tr\chi\varphi^4\chi = 2\sum\chi_i\varphi_i^4\chi_i, \tag{III.4.37}$$

$$B_6 = Tr\chi\varphi^6\chi = -2\sum\chi_i\varphi_i^6\chi_i, \quad B_8 = Tr\chi\varphi^8\chi = 2\sum\chi_i\varphi_i^8\chi_i.$$

We have confirmed that at the strata of SO_8, $SO_7\times U_1$, $SU_2\times SO_5\times U_1$, and $SO_3\times SU_3\times U_1$, the Jacobian determinant $\partial(\alpha_4,\alpha_6,\alpha_8,\alpha_5,\beta_2,\beta_4,\beta_6,\beta_8)/\partial(r_1,r_2,r_3,r_4,s_1,s_2,s_3,s_4)$ is of rank zero (i.e., eq. (II.3.1) is satisfied.), and at the strata of $SO_6\times U_1$, $SO_4\times SU_2\times U_1$, and $SU_4\times U_1$, the Jacobian determinant is of rank 1 (i.e., eq. (II.3.2) is satisfied.) with the orbit parameters deduced from the above invariant polynomials.

For SO_7 adjoint + vector representations, the complete set of elementary invariant polynomials is:

$$A_2 = Tr\,\varphi^2 = -2\sum\varphi_i^2, \quad A_4 = Tr\,\varphi^4 = 2\sum\varphi_i^4, \quad A_6 = Tr\,\varphi^6 = -2\sum\varphi_i^6, \tag{III.4.38}$$

$$C = \sum\chi_i^2 + \chi_4^2, \tag{III.4.39}$$

$$B_2 = Tr\chi\varphi^2\chi = -2\sum\chi_i\varphi_i^2\chi_i, \quad B_4 = Tr\chi\varphi^4\chi = 2\sum\chi_i\varphi_i^4\chi_i, \tag{III.4.40}$$

$$B_6 = Tr\chi\varphi^6\chi = -2\sum\chi_i\varphi_i^6\chi_i.$$

with i running from 1 to 3. We also have confirmed that at the strata of SO_5, $SO_4\times U_1$, and $SU_3\times U_1$, the appropriate Jacobian determinant is of rank zero, and at the strata of $SO_3\times U_1$, $SU_2\times U_1\times U_1$, and $SU_2\times U_1$ (with $w = 0$) it is of rank 1; and at the stratum of $SU_2\times U_1$, it is of rank 2.

The complete 3-dimensional orbit spaces of SO_5 and SU_3 adjoint + vector representations will be illustrated in CHIV.2.

III.4.6 COMMENTS

A careful reader may have noticed that the number of independent parameters is less than the number of singlets for a given maxi-maximal little group listed in eqs. (III.4.12)-(III.4.18) and eqs. (III.4.29)-(III.4.34). Generally, to specify a point in the complete l-dimensional orbit parameter space we need l parameters. We can use l dimensionless ratios of field components or l independent invariants with $||\varphi||$ and $||\chi||$ excluded for this purpose. These are the relevant parameters in determining the dimensionalities of cusps, curves, and surfaces of the complete orbit space. The most general stratum with full l independent parameters is called the generic stratum. Finding appropriate field components to describe the generic stratum of a representation is a non-trivial job [19] and the total number of them [38] is not necessarily small.

(Though Hilbert provided a systematic method of constructing a complete set of basic invariant polynomials for a general representation it has not been worked out explicitly except for adjoint representations of classical and exceptional Lie groups [39] and a few other simple cases. To construct invariant polynomials one needs a tractable method for computing Clebsch-Gordan coefficients, which is not available yet.)

Lacking these important pieces of information we cannot but work with singlets in practice. The stratum of a maximal little group of one irrep which has one singlet occupies a null-parameter subspace, that is, a point. The stratum of a semi-maximal (or maximal) little group of one irrep which has two singlets normally occupies a one-parameter subspace, that is, a curve. The stratum of a maxi-maximal little group which has one singlet from each of the two irreps occupies a null-parameter subspace. The stratum of a maxi-maximal little group which has one singlet from one irrep and two singlets from the other often (though not always) occupies a one-parameter subspace. When there are more singlets the stratum of a maxi-maximal little group occupies a higher dimensional subspace, e.g., the $SU_2 \times U_1$ of SO_7.

However in many cases, especially for smaller little groups there tend to be more singlets than the parameters needed to specify the stratum. This is because the extra singlets can be removed by global gauge transformations. In our dealing with adjoint representations so far we have used a diagonalized matrix form to specify the field components. If the matrix which is invariant under some subgroup contains some off-diagonal components, they can always be grouped together (via group transformation) with diagonal components and thus we see less parameters than we started with. (This simplification is achieved by choosing appropriate group parameters, which we called ϑ_L in CHI.2, and thus the maximum possible number of reduction is the number of

group generators. If the dimension of the representation is D and the exact number of reduction is D_r, then the dimension of the generic stratum, D_g, is $D_g = D - D_r - 1$ for one irrep and $D_g = D - D_r - 2$ for two irreps. As far as we know there is not yet a tractable way to compute D_r.) Consequently these field components that are grouped together appear as single entities in invariant polynomials. In such cases the number of singlets is misleading in determining the dimension of the stratum.

CHAPTER IV COMPLETE ORBIT SPACES

Now that we have given the general procedure for minimizing the Higgs potential the remaining problem is to survey the orbit spaces. Though most of the fourth degree Higgs potentials contain only a partial list of the complete orbit parameters, in more sophisticated problems more and more orbit parameters are included. In this regard and for the sake of completeness it will be instructive to survey the complete orbit spaces.

The general structure of the complete orbit space has been unveiled by a group of mathematicians [15]. It has been known that the generic stratum occupies some l-dimensional volume and the lower dimensional strata form the singular boundaries of this volume. Equivalently the generic stratum occupies an open, dense, topologically connected region and thus the boundaries must belong to the lower dimensional strata. We demonstrate this and also that lower dimensional strata always form the boundaries of higher dimensional strata in the specific examples that we have worked out. That is, the "openness" decreases as we go to lower dimensional strata and only the null-dimensional stratum is truely closed.

IV.1 COMPLETE ORBIT SPACES OF ADJOINT REPRESENTATIONS

Let us briefly review some group theoretical results [40] to set up our notation. For the algebra of order N and rank $(l+1)$ we choose a Cartan-Weyl basis, so that the commutation relations assume the standard form:

$$[H_i, H_j] = 0 \qquad i, j = 1, 2, \cdots, (l+1);$$

$$[H_i, E_{\pm\alpha}] = \pm r_i(\alpha)E_{\pm\alpha}, \qquad \alpha = 1, 2, \cdots, (N-l-1)/2; \qquad \text{(IV.1.1)}$$

$$[E_\alpha, E_{-\alpha}] = \sum_{i=1}^{l+1} r_i(\alpha)H_i;$$

$$[E_\alpha, E_\beta] = N_{\alpha\beta}E_{\alpha+\beta},$$

where $N_{\alpha\beta} \neq 0$ only if $\mathbf{r}(\alpha) + \mathbf{r}(\beta)$ is also a root. The matrices are normalized such that

$$TrH_iH_i = 1, \qquad TrE_\alpha E_{-\alpha} = 1,$$

with all the other combinations of matrices yielding zero. Furthermore the roots $\mathbf{r}(\alpha)$ satisfy the condition

$$\sum_\alpha r_i(\alpha)r_j(\alpha) = \delta_{ij}$$

Using the generalized Casimir operators derived by Racah [39], Gruber and O'Raifeartaigh [41] have derived forms for the Casimir invariants that are more useful in practice. It has also been known that the field components can be reduced by a group transformation to $(l+1)$ (number of rank) irreducible components which correspond to H_i's in the Cartan-Weyl basis. Utilizing these results we can readily write down the tractable form of each invariant.

The complete set of invariant polynomials for adjoint representations can be obtained by using the matrix form for the fields,

$$\varphi = \sum_{i=1}^{N} \varphi_i \, X_i \qquad\qquad\qquad (\text{IV}.1.2)$$

where φ_i is the ith component of φ in vector notation and X_i is the matrix corresponding to the ith generator. Note that X_i can be based on any representation. Using the notation

$$I_m = Tr\,\varphi^m, \qquad\qquad\qquad (\text{IV}.1.3)$$

we list the complete set of invariant polynomials in Table IV.1.1 along with other useful properties for each classical and exceptional Lie group. The I'_n of SO_{2n} is

of a form similar to A_5 in eq. (III.4.35). Using the convention

$$\varphi = \sum \varphi_i H_i \equiv [a_1, a_2, \cdots, a_l, a_{(l+1)}]$$
(IV.1.4)

where we have defined the square bracket as the diagonal elements of the matrix, we can directly write down the orbit parameters in the following generic form

$$\alpha_m \equiv \frac{Tr\,\varphi^m}{(Tr\,\varphi^2)^{m/2}},$$
(IV.1.5a)

$$\alpha'_m \equiv \frac{2^m\,a_1 a_2 \cdots a_m}{(Tr\,\varphi^2)^{m/2}}.$$
(IV.1.5b)

GROUP	INVARIANTS	ORDER	RANK
SU_{n+1}	$I_2, I_3, \cdots, I_{n+1}$	$n(n+2)$	n
SO_{2n+1}	$I_2, I_4, \cdots, I_{2n}$	$n(2n+1)$	n
Sp_{2n}	$I_2, I_4, \cdots, I_{2n}$	$n(2n+1)$	n
SO_{2n}	$I_2, I_4, \cdots, I_{2n-2}, I'_n$	$n(2n-1)$	n
G_2	I_2, I_6	14	2
F_4	I_2, I_6, I_8, I_{12}	52	4
E_6	$I_2, I_5, I_6, I_8, I_9, I_{12}$	78	6
E_7	$I_2, I_6, I_8, I_{10}, I_{12}, I_{14}, I_{18}$	133	7
E_8	$I_2, I_8, I_{12}, I_{14}, I_{18}, I_{20}, I_{24}, I_{30}$	248	8

Table IV.1.1

IV.1.1 GROUPS OF RANK TWO

There is only one orbit parameter for the adjoint representation of a group of rank 2 and thus the orbit space is a line.

SU(3)

We choose the vector representation for the basis of the matrices. The stratum of each little group is represented as follows:

$$\underline{SU_2 \times U_1} : \qquad 3 = 1[-2] + 2[1], \qquad\qquad\qquad (\text{IV}.1.6)$$

$$\varphi = [a, a, -2a],$$

$$\alpha_3 = \pm 1/\sqrt{6};$$

$$\underline{U_1 \times U_1} : \qquad \varphi = [a, b, -a-b], \qquad\qquad\qquad (\text{IV}.1.7)$$

$$\alpha_3 = \pm \frac{a^3 + b^3 - (a+b)^3}{(a^2 + b^2 + (a+b)^2)^{3/2}}.$$

The orbit space consists of two end points corresponding to $SU_2 \times U_1$ and the interior corresponding to $U_1 \times U_1$.

SO(5) and Sp(4)

We choose the 5-dimensional vector representation for the basis. The stratum of each little group is represented as follows:

$$\underline{SO_3 \times U_1} : \qquad 5 = 1[1] + 1[-1] + 3[0], \qquad\qquad\qquad (\text{IV}.1.8)$$

$$\varphi = [a, -a, 0, 0, 0],$$

$$\alpha_4 = 1/2;$$

$\underline{SU_2 \times U_1}$: $\qquad 5 = 1[0] + 2[1] + 2[-1],$ $\hfill$ (IV.1.9)

$$\varphi = [a, -a, a, -a, 0],$$

$$\alpha_4 = 1/4;$$

$\underline{U_1 \times U_1}$: $\qquad \varphi = [a, -a, b, -b, 0],$ $\hfill$ (IV.1.10)

$$\alpha_4 = \frac{2a^4 + 2b^4}{(2a^2 + 2b^2)^2}.$$

The orbit space consists of two end points corresponding to $SO_3 \times U_1$, $SU_2 \times U_1$ and the interior corresponding to $U_1 \times U_1$.

SO(4)

Although SO_4 may be considered to be a direct product group $SU_2 \times SU_2$ we include it for completeness. We choose the vector representation for the basis. The stratum of each little group is represented as follows:

$\underline{SU_2 \times U_1}$: $\qquad (2,2) = 2[1] + 2[-1],$ $\hfill$ (IV.1.11)

$$\varphi = [a, -a, a, -a],$$

$$\alpha'_2 = \pm 1;$$

$\underline{U_1 \times U_1}$: $\qquad \varphi = [a, -a, b, -b],$ $\hfill$ (IV.1.12)

$$\alpha'_2 = 2^2 \frac{ab}{2a^2 + 2b^2}.$$

The orbit space consists of two end points corresponding to $SU_2 \times U_1$ and the interior corresponding to $U_1 \times U_1$.

G(2)

We choose the 7-dimensional representation for the basis. The stratum of each little group is represented as follows:

$\underline{SO_3 \times U_1}$: $\qquad 7 = 3[0] + 2[1] + 2[-1],$ $\qquad\qquad$ (IV.1.13)

$$\varphi = [a, -a, a, -a, 0, 0, 0],$$

$$\alpha_6 = 1/16;$$

$\underline{SU_2 \times U_1}$: $\qquad 7 = 1[0] + 1[2] + 1[-2] + 2[1] + 2[-1],$ $\qquad$ (IV.1.14)

$$\varphi = [2a, 0, -2a, a, -a, a, -a,],$$

$$\alpha_6 = 33/128;$$

$\underline{U_1 \times U_1}$: $\qquad \varphi = [2a, 0, -2a, a+b, a-b, -a+b, -a-b],$ $\qquad$ (IV.1.15)

$$\alpha_6 = \frac{2(2a)^6 + 2(a+b)^6 + 2(a-b)^6}{[2(2a)^2 + 2(a+b)^2 + 2(a-b)^2]^3}.$$

The orbit space consists of two end points corresponding to $SO_3 \times U_1$, $SU_2 \times U_1$ and the interior corresponding to $U_1 \times U_1$.

IV.1.2 GROUPS OF RANK THREE

There are two orbit parameters for the adjoint representation of a Lie group of rank 3. The orbit space turns out to be a warped triangle.

SU(4) and SO(6)

We choose the 4-dimensional representation for the basis of the matrices. The stratum of each little group is represented as follows:

$$\underline{SU_3 \times U_1} : \qquad 4 = 1[-3] + 3[1], \qquad\qquad (IV.1.16)$$

$$\varphi = [a, a, a, -3a],$$

$$\alpha_3 = \pm 1/\sqrt{3},$$

$$\alpha_4 = 7/12;$$

$$\underline{SU_2 \times SU_2 \times U_1} : \qquad 4 = (2,1)[1] + (1,2)[-1], \qquad\qquad (IV.1.17)$$

$$\varphi = [a, a, -a, -a],$$

$$\alpha_3 = 0,$$

$$\alpha_4 = 1/4;$$

$$\underline{SU_2 \times U_1 \times U_1} : \qquad 4 = 1[1,1] + 1[1,-1] + 2[-1,0], \qquad\qquad (IV.1.18)$$

$$\varphi = [a, a, b, -2a - b],$$

$$\alpha_3 = \pm \frac{2a^3 + b^3 - (2a + b)^3}{[2a^2 + b^2 + (2a + b)^2]^{3/2}},$$

$$\alpha_4 = \frac{2a^4 + b^4 + (2a + b)^4}{[2a^2 + b^2 + (2a + b)^2]^2};$$

$$\underline{U_1 \times U_1 \times U_1} : \qquad \varphi = [a, b, c, -a - b - c], \qquad\qquad (IV.1.19)$$

$$\alpha_3 = \pm \frac{a^3+b^3+c^3-(a+b+c)^3}{[a^2+b^2+c^2+(a+b+c)^2]^{3/2}},$$

$$\alpha_4 = \frac{a^4+b^4+c^4+(a+b+c)^4}{[a^2+b^2+c^2+(a+b+c)^2]^2}.$$

The orbit space is shown in Fig. IV.1.1. It is a warped triangle. Two cusps $\pm$P1 of $[SU_3 \times U_1]$ and cusp P2 of $[SU_2 \times SU_2 \times U_1]$ are connected by the curve of $[SU_2 \times U_1 \times U_1]$. The cusps and the curve together form the boundary of the generic stratum of $[U_1 \times U_1 \times U_1]$ which occupies the interior.

Fig. IV.1.1

SO(7)

We choose the vector representation for the basis. The stratum of each little group is represented as follows:

$\underline{SO_5 \times U_1}$: $7 = 1[1] + 1[-1] + 5[0]$,   (IV.1.20)

$\varphi = [a, -a, 0, 0, 0, 0, 0]$,

$\alpha_4 = 1/2$,

$\alpha_6 = 1/4$;

$\underline{SU_2 \times SO_3 \times U_1}$: $7 = (1,3)[0] + (2,1)[1] + (2,1)[-1]$,   (IV.1.21)

$\varphi = [a, -a, a, -a, 0, 0, 0]$,

$\alpha_4 = 1/4$,

$\alpha_6 = 1/16$;

$\underline{SU_3 \times U_1}$: $7 = 1[0] + 3[1] + \bar{3}[-1]$,   (IV.1.22)

$\varphi = [a, -a, a, -a, a, -a, 0]$,

$\alpha_4 = 1/6$,

$\alpha_6 = 1/36$;

$\underline{SU_2 \times U_1 \times U_1}$: $7 = 1[0,0] + 1[0,1] + 1[0,-1] + 2[1,0] + 2[-1,0]$,   (IV.1.23)

$\varphi = [a, -a, a, -a, b, -b, 0]$,

$$\alpha_4 = \frac{4a^4 + 2b^4}{(4a^2 + 2b^2)^2},$$

$$\alpha_6 = \frac{4a^6 + 2b^6}{(4a^2 + 2b^2)^3};$$

$\underline{SO_3 \times U_1 \times U_1}$: $7 = 1[1,1] + 1[1,-1] + 1[-1,1] + 1[-1,-1] + 3[0,0],$ (IV.1.24)

$$\varphi = [a, -a, b, -b, 0, 0, 0],$$

$$\alpha_4 = \frac{2a^4 + 2b^4}{(2a^2 + 2b^2)^2},$$

$$\alpha_6 = \frac{2a^6 + 2b^6}{(2a^2 + 2b^2)^3};$$

$\underline{U_1 \times U_1 \times U_1}$: $\varphi = [a, -a, b, -b, c, -c, 0],$ (IV.1.25)

$$\alpha_4 = \frac{2a^4 + 2b^4 + 2c^4}{(2a^2 + 2b^2 + 2c^2)^2},$$

$$\alpha_6 = \frac{2a^6 + 2b^6 + 2c^6}{(2a^2 + 2b^2 + 2c^2)^3}.$$

The orbit space is shown in Fig. IV.1.2. It is again a warped triangle. Cusp P1 of $[SO_5 \times U_1]$ and cusp P2 of $[SU_2 \times SO_3 \times U_1]$ are connected by straight line L1 of $[SO_3 \times U_1 \times U_1]$. All three cusps including cusp P3 of $[SU_3 \times U_1]$ are connected by curve C2 of $[SU_2 \times U_1 \times U_1]$. All the cusps and L1 and C2 together form the boundary of the generic stratum $[U_1 \times U_1 \times U_1]$ which occupies the interior.
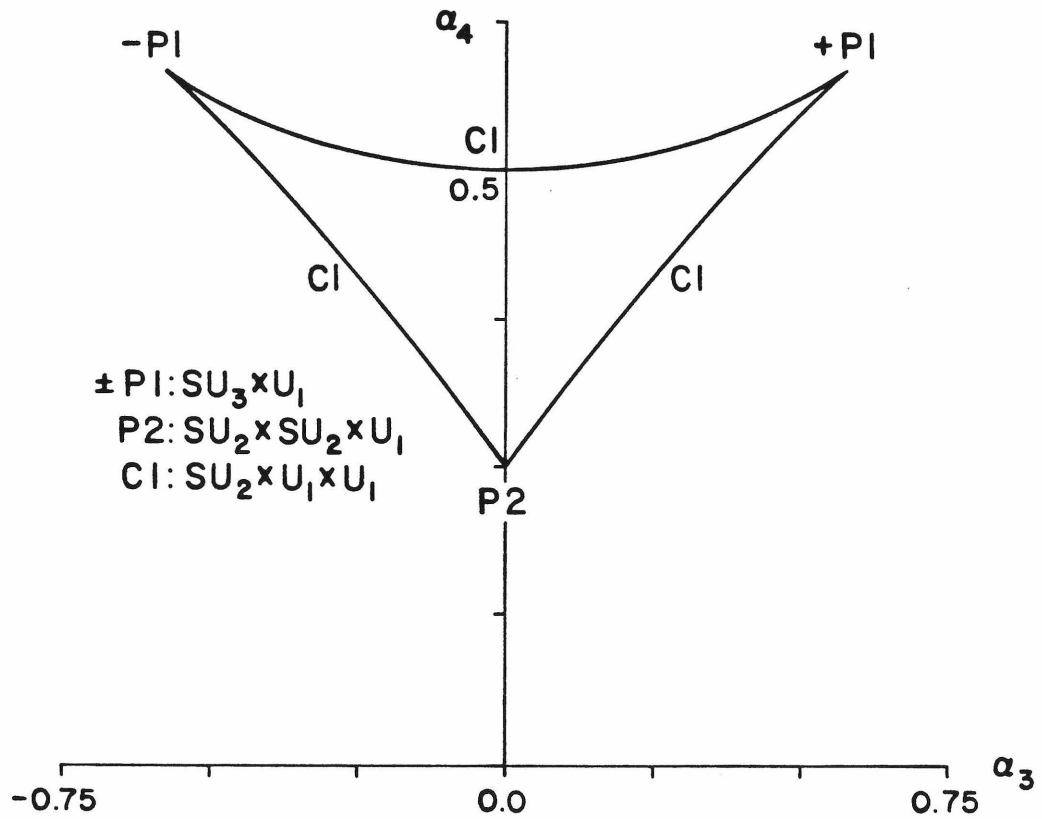

Fig. IV.1.2

Sp(6)

We choose the vector representation for the basis. The stratum of each little group is represented as follows:

$\underline{Sp_4 \times U_1}$: $\qquad$ $6 = 1[1] + 1[-1] + 4[0]$, $\qquad\qquad$ (IV.1.26)

$$\varphi = [a, -a, 0, 0, 0, 0],$$

$$\alpha_4 = 1/2,$$

$$\alpha_6 = 1/4;$$

$\underline{SU_2 \times SU_2 \times U_1}$: $\qquad$ $6 = (2,1)[0] + (1,2)[1] + (1,2)[-1]$, $\qquad$ (IV.1.27)

$$\varphi = [a, -a, a, -a, 0, 0],$$

$$\alpha_4 = 1/4,$$

$$\alpha_6 = 1/16;$$

$\underline{SU_3 \times U_1}$: $\qquad$ $6 = 3[1] + \overline{3}[-1]$, $\qquad\qquad$ (IV.1.28)

$$\varphi = [a, -a, a, -a, a, -a],$$

$$\alpha_4 = 1/6,$$

$$\alpha_6 = 1/36;$$

$\underline{SU_2 \times U_1 \times U_1\,(A)}$: $\qquad$ $6 = 1[0,1] + 1[0,-1] + 2[1,0] + 2[-1,0]$, $\qquad$ (IV.1.29)

$$\varphi = [a, -a, a, -a, b, -b],$$

$$\alpha_4 = \frac{4a^4 + 2b^4}{(4a^2 + 2b^2)^2},$$

$$\alpha_6 = \frac{4a^6 + 2b^6}{(4a^2 + 2b^2)^3};$$

$\underline{SU_2 \times U_1 \times U_1\ (B)}$: $\qquad$ $6 = 1[1,1] + 1[1,-1] + 1[-1,1] + 1[-1,-1] + 2[0,0],$ $\qquad$ (IV.1.30)

$$\varphi = [a,-a,b,-b,0,0],$$

$$\alpha_4 = \frac{2a^4 + 2b^4}{(2a^2 + 2b^2)^2},$$

$$\alpha_6 = \frac{2a^6 + 2b^6}{(2a^2 + 2b^2)^3};$$

$\underline{U_1 \times U_1 \times U_1}$: $\qquad$ $\varphi = [a,-a,b,-b,c,-c],$ $\qquad$ (IV.1.31)

$$\alpha_4 = \frac{2a^4 + 2b^4 + 2c^4}{(2a^2 + 2b^2 + 2c^2)^2},$$

$$\alpha_6 = \frac{2a^6 + 2b^6 + 2c^6}{(2a^2 + 2b^2 + 2c^2)^3}.$$

The orbit space is shown in Fig. IV.1.3. As we can see from Fig. IV.1.2 and Fig. IV.1.3 the orbit space of the Sp_6 adjoint is identical to that of the SO_7 adjoint. This identity persists between the Sp_{2n} adjoint and the SO_{2n+1} adjoint for any n because the orbit parameters are identically defined. Only the labeling of the little groups is different.
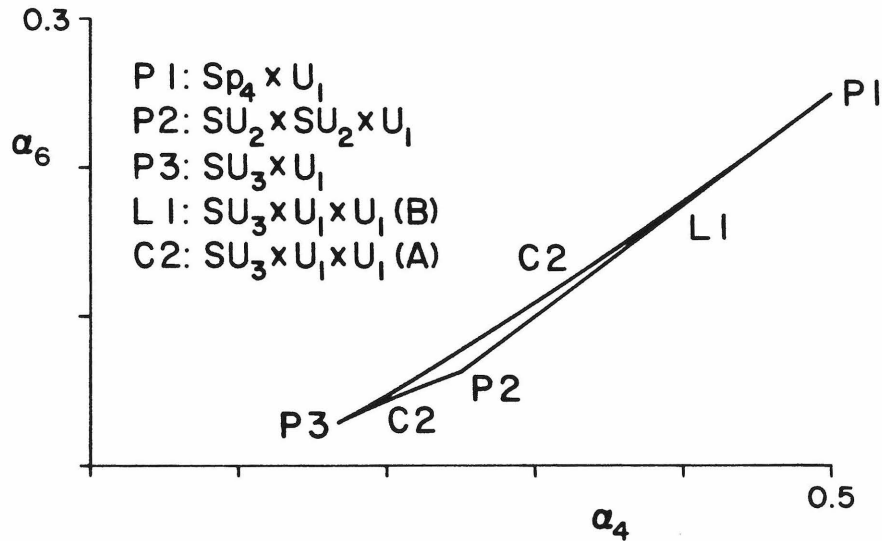
Fig. IV.1.3

IV.1.3 GROUPS OF RANK FOUR

There are three orbit parameters for the adjoint representation of a Lie group of rank 4. The orbit space turns out to be a warped tetrahedron.
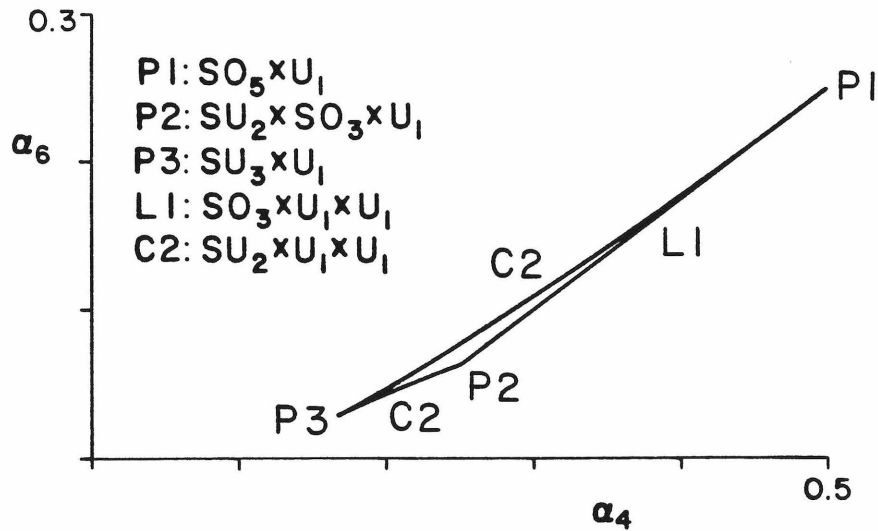
SU(5)

We choose the vector representation for the basis of the matrices. The stratum of each little group is represented as follows:

$$\underline{SU_4 \times U_1} : \qquad 5 = 1[-4] + 4[1], \qquad\qquad\qquad (IV.1.32)$$

$$\varphi = [a, a, a, a, -4a],$$

$$\alpha_3 = \pm\, 3/2\sqrt{5},$$

$$\alpha_4 = 13/20,$$

$$\alpha_5 = \pm\, 51/40\sqrt{5};$$

$$\underline{SU_3 \times SU_2 \times U_1} : \qquad 5 = (3,1)[2] + (1,2)[-3], \qquad\qquad (IV.1.33)$$

$$\varphi = [2a, 2a, 2a, -3a, -3a],$$

$$\alpha_3 = \pm\, 1/\sqrt{30},$$

$$\alpha_4 = 7/30,$$

$$\alpha_5 = \pm\, 13/30\sqrt{30};$$

$$\underline{SU_3 \times U_1 \times U_1} : \qquad 5 = 1[0,1] + 1[-3,-1] + 3[1,0], \qquad (IV.1.34)$$

$$\varphi = [a, a, a, b, -3a-b],$$

$$\alpha_3 = \pm\, \frac{3a^3 + b^3 - (3a+b)^3}{[3a^2 + b^2 + (3a+b)^2]^{3/2}},$$

$$\alpha_4 = \frac{3a^4+b^4+(3a+b)^4}{[3a^2+b^2+(3a+b)^2]^2},$$

$$\alpha_5 = \pm \frac{3a^5+b^5-(3a+b)^5}{[3a^2+b^2+(3a+b)^2]^{5/2}};$$

$\underline{SU_2 \times SU_2 \times U_1 \times U_1}$:

$$5=(1,1)[-2,-2]+(1,2)[1,0]+(2,1)[0,1], \qquad (IV.1.35)$$

$$\varphi = [a,a,b,b,-2a-2b],$$

$$\alpha_3 = \pm \frac{2a^3+2b^3-(2a+2b)^3}{[2a^2+2b^2+(2a+2b)^2]^{3/2}},$$

$$\alpha_4 = \frac{2a^4+2b^4+(2a+2b)^4}{[2a^2+2b^2+(2a+2b)^2]^2},$$

$$\alpha_5 = \pm \frac{2a^5+2b^5-(2a+2b)^5}{[2a^2+2b^2+(2a+2b)^2]^{5/2}};$$

$\underline{SU_2 \times U_1 \times U_1 \times U_1}$:

$$5=1[0,1,0]+1[0,0,1]+1[-2,-1,-1]+2[1,0,0], \qquad (IV.1.36)$$

$$\varphi = [a,a,b,c,-2a-b-c],$$

$$\alpha_3 = \pm \frac{2a^3+b^3+c^3-(2a+b+c)^3}{[2a^2+b^2+c^2+(2a+b+c)^2]^{3/2}},$$

$$\alpha_4 = \frac{2a^4+b^4+c^4+(2a+b+c)^4}{[2a^2+b^2+c^2+(2a+b+c)^2]^2},$$

$$\alpha_5 = \pm \frac{2a^5+b^5+c^5-(2a+b+c)^5}{[2a^2+b^2+c^2+(2a+b+c)^2]^{5/2}};$$

$\underline{U_1 \times U_1 \times U_1 \times U_1}$:

$$\varphi = [a,b,c,d,-a-b-c-d], \qquad (IV.1.37)$$

$$\alpha_3 = \pm \frac{a^3+b^3+c^3+d^3-(a+b+c+d)^3}{[a^2+b^2+c^2+d^2+(a+b+c+d)^2]^{3/2}},$$

$$\alpha_4 = \frac{a^4+b^4+c^4+d^4+(a+b+c+d)^4}{[a^2+b^2+c^2+d^2+(a+b+c+d)^2]^2},$$

$$\alpha_5 = \pm \frac{a^5+b^5+c^5+d^5-(a+b+c+d)^5}{[a^2+b^2+c^2+d^2+(a+b+c+d)^2]^{5/2}};$$

The orbit space is shown in Fig. IV.1.4. It is a thin warped tetrahedron. Cusps $\pm$ **P1** of $[SU_4 \times U_1]$ and cusps $\pm$ **P2** of $[SU_3 \times SU_2 \times U_1]$ are connected by both curves **C1** of $[SU_3 \times U_1 \times U_1]$ and curves **C2** of $[SU_2 \times SU_2 \times U_1 \times U_1]$. The two curves lie on the warped surfaces of $[SU_2 \times U_1 \times U_1 \times U_1]$. All these cusps, curves and surfaces together form the boundary of the generic stratum $[U_1 \times U_1 \times U_1 \times U_1]$ which occupies the interior.

The curves are all concave. One of the principal curvatures of each surface is zero (the surface is flat in this direction) and the other is negative (the surface is concave in this direction).
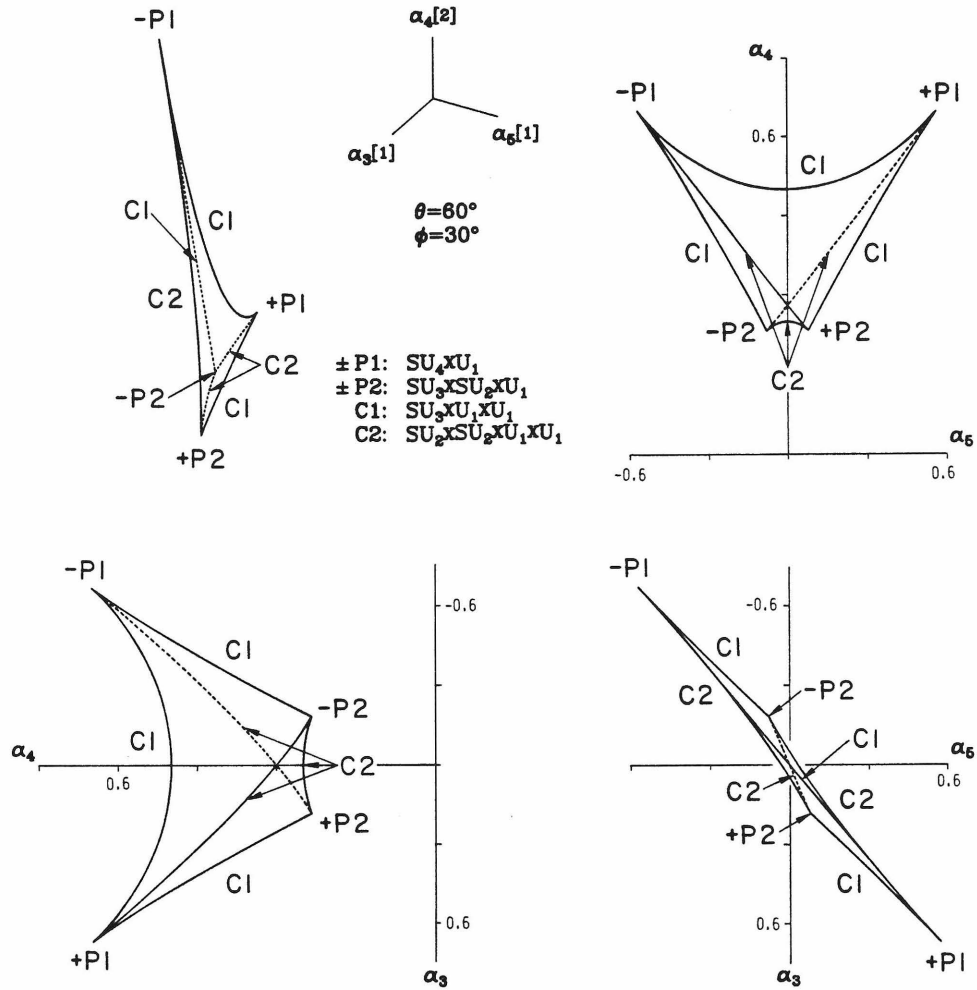
Fig. IV.1.4

The complete orbit space of the SU_5 adjoint representation. Shown at the upper left corner is a view from the direction oriented 30° from the α_3 axis and 60° from the α_4 axis. The numbers in the square brackets are the relative ratios of scale. Each projection is a view from the positive direction of the axis not shown in the picture. The dotted curves represent edges on the back (hidden) side of the orbit space.

SO(9)

We choose the vector representation for the basis. The stratum of each little group is represented as follows:

$$\underline{SO_7 \times U_1} : \quad 9 = 1[1] + 1[-1] + 7[0], \tag{IV.1.38}$$

$$\varphi = [\alpha, -\alpha, 0, 0, 0, 0, 0, 0, 0],$$

$$\alpha_4 = 1/2,$$

$$\alpha_6 = 1/4,$$

$$\alpha_8 = 1/8;$$

$$\underline{SO_5 \times SU_2 \times U_1} : \quad 9 = (5,1)[0] + (1,2)[1] + (1,2)[-1], \tag{IV.1.39}$$

$$\varphi = [\alpha, -\alpha, \alpha, -\alpha, 0, 0, 0, 0, 0],$$

$$\alpha_4 = 1/4,$$

$$\alpha_6 = 1/16,$$

$$\alpha_8 = 1/64;$$

$$\underline{SU_3 \times SU_2 \times U_1} : \quad 9 = (3,1)[1] + (\overline{3},1)[-1] + (1,3)[0], \tag{IV.1.40}$$

$$\varphi = [\alpha, -\alpha, \alpha, -\alpha, \alpha, -\alpha, 0, 0, 0],$$

$$\alpha_4 = 1/6,$$

$$\alpha_6 = 1/36,$$

$$\alpha_8 = 1/216;$$

$$\underline{SU_4 \times U_1} : \quad 9 = 1[0] + 4[1] + \overline{4}[-1], \tag{IV.1.41}$$

$$\varphi = [a, -a, a, -a, a, -a, a, -a, 0],$$

$$\alpha_4 = 1/8,$$

$$\alpha_6 = 1/64,$$

$$\alpha_8 = 1/512;$$

$\underline{SU_3 \times U_1 \times U_1}$: $9 = 1[0,0] + 1[0,1] + 1[0,-1] + 3[1,0] + \bar{3}[-1,0],$ (IV.1.42)

$$\varphi = [a, -a, a, -a, a, -a, b, -b, 0],$$

$$\alpha_4 = \frac{6a^4 + 2b^4}{(6a^2 + 2b^2)^2},$$

$$\alpha_6 = \frac{6a^6 + 2b^6}{(6a^2 + 2b^2)^3},$$

$$\alpha_8 = \frac{6a^8 + 2b^8}{(6a^2 + 2b^2)^4};$$

$\underline{SU_2 \times SU_2 \times U_1 \times U_1}$: $9 = (1,1)[0,0] + (2,1)[1,0] + (2,1)[-1,0]$ (IV.1.43)

$$+ (1,2)[0,1] + (1,2)[0,-1],$$

$$\varphi = [a, -a, a, -a, b, -b, b, -b, 0],$$

$$\alpha_4 = \frac{4a^4 + 4b^4}{(4a^2 + 4b^2)^2},$$

$$\alpha_6 = \frac{4a^6 + 4b^6}{(4a^2 + 4b^2)^3},$$

$$\alpha_8 = \frac{4a^8 + 4b^8}{(4a^2 + 4b^2)^4};$$

$\underline{SU_2 \times SO_3 \times U_1 \times U_1}$: $9 = (1,1)[0,1] + (1,1)[0,-1] + (2,1)[1,0]$ (IV.1.44)

$$+ (2,1)[-1,0] + (1,3)[0,0],$$

$$\varphi = [a,-a,a,-a,b,-b,0,0,0],$$

$$\alpha_4 = \frac{4a^4+2b^4}{(4a^2+2b^2)^2},$$

$$\alpha_6 = \frac{4a^6+2b^6}{(4a^2+2b^2)^3},$$

$$\alpha_8 = \frac{4a^8+2b^8}{(4a^2+2b^2)^4};$$

$\underline{SO_5 \times U_1 \times U_1}$: $9=1[1,0]+1[-1,0]+1[0,1]+1[0,-1]+5[0,0],$ (IV.1.45)

$$\varphi = [a,-a,b,-b,0,0,0,0,0],$$

$$\alpha_4 = \frac{2a^4+2b^4}{(2a^2+2b^2)^2},$$

$$\alpha_6 = \frac{2a^6+2b^6}{(2a^2+2b^2)^3},$$

$$\alpha_8 = \frac{2a^8+2b^8}{(2a^2+2b^2)^4};$$

$\underline{SU_2 \times U_1 \times U_1 \times U_1 \ (A)}$: $9=1[0,0,0]+1[0,1,0]+1[0,-1,0]$ (IV.1.46)

$$+1[0,0,1]+1[0,0,-1]+2[1,0,0]+2[-1,0,0],$$

$$\varphi = [a,-a,a,-a,b,-b,c,-c,0],$$

$$\alpha_4 = \frac{4a^4+2b^4+2c^4}{(4a^2+2b^2+2c^2)^2},$$

$$\alpha_6 = \frac{4a^6+2b^6+2c^6}{(4a^2+2b^2+2c^2)^3},$$

$$\alpha_8 = \frac{4a^8+2b^8+2c^8}{(4a^2+2b^2+2c^2)^4};$$

$\underline{SU_2 \times U_1 \times U_1 \times U_1 \ (B)}$: $9=1[1,0,0]+1[-1,0,0]+1[0,1,0]+1[0,-1,0]$ (IV.1.47)

$$+1[0,0,1]+1[0,0,-1]+3[0,0,0],$$

$$\varphi = [a,-a,b,-b,c,-c,0,0,0],$$

$$\alpha_4 = \frac{2a^4+2b^4+2c^4}{(2a^2+2b^2+2c^2)^2},$$

$$\alpha_6 = \frac{2a^6+2b^6+2c^6}{(2a^2+2b^2+2c^2)^3},$$

$$\alpha_8 = \frac{2a^8+2b^8+2c^8}{(2a^2+2b^2+2c^2)^4};$$

$\underline{U_1 \times U_1 \times U_1 \times U_1}$: $\qquad \varphi = [a,-a,b,-b,c,-c,d,-d,0],$ (IV.1.48)

$$\alpha_4 = \frac{2a^4+2b^4+2c^4+2d^4}{(2a^2+2b^2+2c^2+2d^2)^2},$$

$$\alpha_6 = \frac{2a^6+2b^6+2c^6+2d^6}{(2a^2+2b^2+2c^2+2d^2)^3},$$

$$\alpha_8 = \frac{2a^8+2b^8+2c^8+2d^8}{(2a^2+2b^2+2c^2+2d^2)^4};$$

The orbit space is shown in Fig. IV.1.5. It is a thin and sharp tetrahedron. Cusp P1 of $[SO_7 \times U_1]$ and cusp P2 of $[SO_5 \times SU_2 \times U_1]$ are connected by curve C1 of $[SO_5 \times U_1 \times U_1]$. Cusp P3 of $[SU_3 \times SU_2 \times U_1]$ and cusp P4 of $[SU_4 \times U_1]$ are connected by curve C2 of $[SU_3 \times U_1 \times U_1]$ which connects also P1 and P4. P2 and P4 are connected by curve C3 of $[SU_2 \times SU_2 \times U_1 \times U_1]$. P1, P2 and P3 are connected by curve C4 of $[SU_2 \times SO_3 \times U_1 \times U_1]$. The stratum of $[SU_2 \times U_1 \times U_1 \times U_1 \ (B)]$ occupies the warped triangular surface P1-P2-P3 bounded by C1 and C4. The stratum of $[SU_2 \times U_1 \times U_1 \times U_1 \ (A)]$ closes the rest of the boundary of the generic stratum $[U_1 \times U_1 \times U_1 \times U_1]$ which occupies the interior.

C1 and C3 are convex plane-curves and C2 and C4 are concave space-curves. Surface P1—P2—P3 is convex along its length but it meets with a $\alpha_4 = constant$ plane along a straight line. All the other surfaces meet with a

$\alpha_4 = constant$ plane along concave curves.   Surface P1–P3–P4 is totally concave. Each of surfaces P2–P3–P4 and P1–P2–P4 have two principal curvatures of opposite sign, i.e., the surfaces are saddle-shaped.

P1: SO_7xU_1
P2: $SO_5xSU_2xU_1$
P3: $SU_3xSU_2xU_1$
P4: SU_4xU_1
C1: $SO_5xU_1xU_1$
C2: $SU_3xU_1xU_1$
C3: $SU_2xSU_2xU_1xU_1$
C4: $SU_2xSO_3xU_1xU_1$
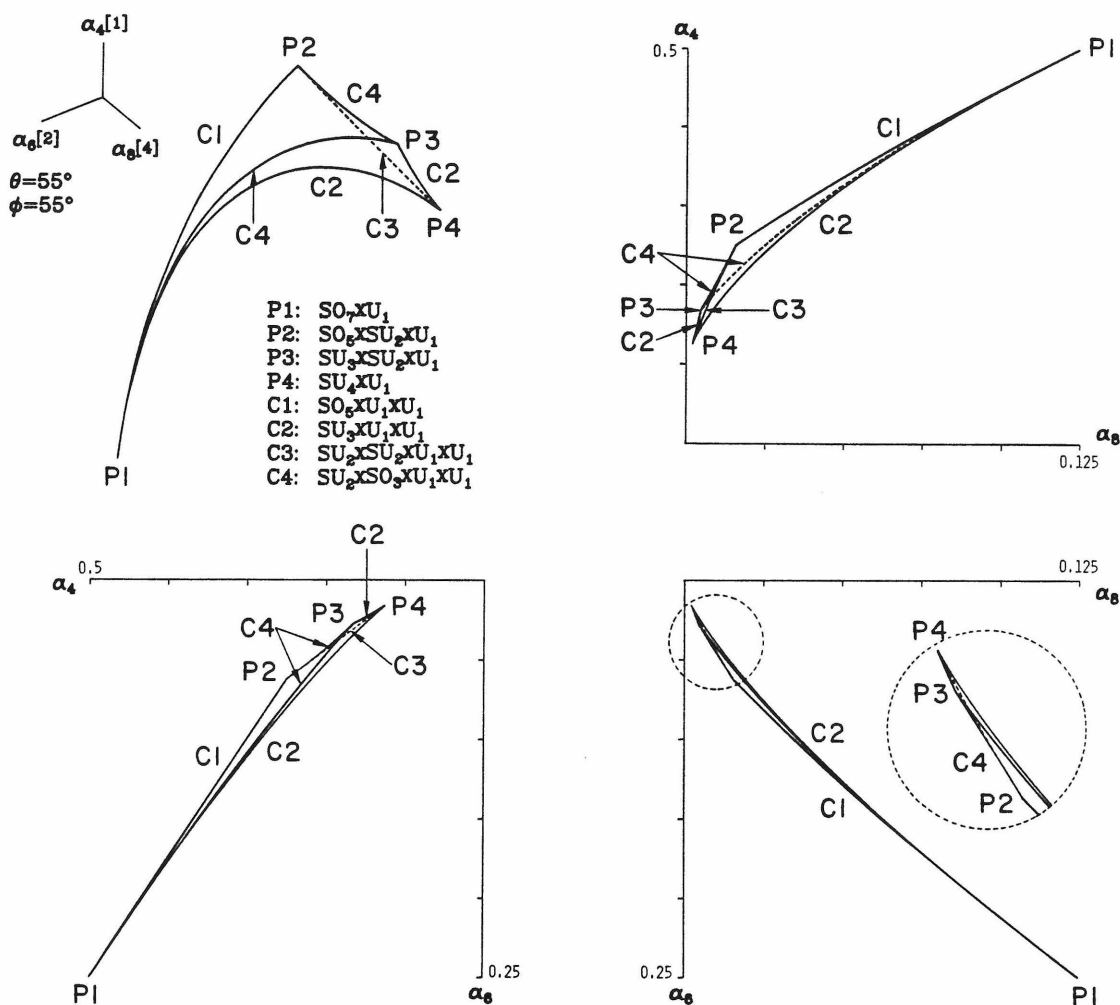
Fig. IV.1.5

The complete orbit space of the SO_9 adjoint representation. Shown at the upper left corner is a view from the direction oriented 55° from the α_6 axis and 55° from the α_4 axis. The numbers in the square brackets are the relative ratios of scale. Each projection is a view from the positive direction of the axis not shown in the picture. The dotted curves represent edges on the back (hidden) side of the orbit space.

Sp(8)

We choose the vector representation for the basis, The stratum of each little group is represented as follows:

$\underline{Sp_6 \times U_1}$: $8 = 1[1] + 1[-1] + 6[0]$,   (IV.1.49)

$\varphi = [a, -a, 0, 0, 0, 0, 0, 0]$,

$\alpha_4 = 1/2$,

$\alpha_6 = 1/4$,

$\alpha_8 = 1/8$;

$\underline{Sp_4 \times SU_2 \times U_1}$: $8 = (4,1)[0] + (1,2)[1] + (1,2)[-1]$,   (IV.1.50)

$\varphi = [a, -a, a, -a, 0, 0, 0, 0]$,

$\alpha_4 = 1/4$,

$\alpha_6 = 1/16$,

$\alpha_8 = 1/64$;

$\underline{SU_3 \times SU_2 \times U_1}$: $8 = (3,1)[1] + (\bar{3},1)[-1] + (1,2)[0]$,   (IV.1.51)

$\varphi = [a, -a, a, -a, a, -a, 0, 0]$,

$\alpha_4 = 1/6$,

$\alpha_6 = 1/36$,

$\alpha_8 = 1/216$;

$\underline{SU_4 \times U_1}$: $8 = 4[1] + \bar{4}[-1]$,   (IV.1.52)

$$\varphi = [a,-a,a,-a,a,-a,a,-a],$$

$$\alpha_4 = 1/8,$$

$$\alpha_6 = 1/64,$$

$$\alpha_8 = 1/512;$$

$\underline{SU_3 \times U_1 \times U_1}$: $8 = 1[0,1]+1[0,-1]+3[1,0]+\bar{3}[-1,0],$ (IV.1.53)

$$\varphi = [a,-a,a,-a,a,-a,b,-b],$$

$$\alpha_4 = \frac{6a^4+2b^4}{(6a^2+2b^2)^2},$$

$$\alpha_6 = \frac{6a^6+2b^6}{(6a^2+2b^2)^3},$$

$$\alpha_8 = \frac{6a^8+2b^8}{(6a^2+2b^2)^4};$$

$\underline{SU_2 \times SU_2 \times U_1 \times U_1 \ (A)}$: $8 = (1,2)[1,0]+(1,2)[-1,0]+(2,1)[0,1]+(2,1)[0,-1],$ (IV.1.54)

$$\varphi = [a,-a,a,-a,b,-b,b,-b],$$

$$\alpha_4 = \frac{4a^4+4b^4}{(4a^2+4b^2)^2},$$

$$\alpha_6 = \frac{4a^6+4b^6}{(4a^2+4b^2)^3},$$

$$\alpha_8 = \frac{4a^8+4b^8}{(4a^2+4b^2)^4};$$

$\underline{SU_2 \times SU_2 \times U_1 \times U_1 \ (B)}$: $8 = (1,1)[0,1]+(1,1)[0,-1]+(1,2)[0,0]$ (IV.1.55)

$$+(2,1)[1,0]+(2,1)[-1,0],$$

$$\varphi = [a,-a,a,-a,b,-b,0,0],$$

$$\alpha_4 = \frac{4a^4 + 2b^4}{(4a^2 + 2b^2)^2},$$

$$\alpha_6 = \frac{4a^6 + 2b^6}{(4a^2 + 2b^2)^3},$$

$$\alpha_8 = \frac{4a^8 + 2b^8}{(4a^2 + 2b^2)^4};$$

$\underline{Sp_4 \times U_1 \times U_1}$: $\quad 8 = 1[1,0] + 1[-1,0] + 1[0,1] + 1[0,-1] + 4[0,0],$ $\qquad$ (IV.1.56)

$$\varphi = [a, -a, b, -b, 0, 0, 0, 0],$$

$$\alpha_4 = \frac{2a^4 + 2b^4}{(2a^2 + 2b^2)^2},$$

$$\alpha_6 = \frac{2a^6 + 2b^6}{(2a^2 + 2b^2)^3},$$

$$\alpha_8 = \frac{2a^8 + 2b^8}{(2a^2 + 2b^2)^4};$$

$\underline{SU_2 \times U_1 \times U_1 \times U_1 \,(A)}$: $\quad 8 = 1[0,1,0] + 1[0,-1,0] + 1[0,0,1] + 1[0,0,-1]$ $\qquad$ (IV.1.57)

$$+2[1,0,0] + 2[-1,0,0],$$

$$\varphi = [a, -a, a, -a, b, -b, c, -c],$$

$$\alpha_4 = \frac{4a^4 + 2b^4 + 2c^4}{(4a^2 + 2b^2 + 2c^2)^2},$$

$$\alpha_6 = \frac{4a^6 + 2b^6 + 2c^6}{(4a^2 + 2b^2 + 2c^2)^3},$$

$$\alpha_8 = \frac{4a^8 + 2b^8 + 2c^8}{(4a^2 + 2b^2 + 2c^2)^4};$$

$\underline{SU_2 \times U_1 \times U_1 \times U_1 \,(B)}$: $\quad 8 = 1[1,0,0] + 1[-1,0,0] + 1[0,1,0] + 1[0,-1,0]$ $\qquad$ (IV.1.58)

$$+1[0,0,1] + 1[0,0,-1] + 2[0,0,0],$$

$$\varphi = [a, -a, b, -b, c, -c, 0, 0],$$

$$\alpha_4 = \frac{2a^4 + 2b^4 + 2c^4}{(2a^2 + 2b^2 + 2c^2)^2},$$

$$\alpha_6 = \frac{2a^6 + 2b^6 + 2c^6}{(2a^2 + 2b^2 + 2c^2)^3},$$

$$\alpha_8 = \frac{2a^8 + 2b^8 + 2c^8}{(2a^2 + 2b^2 + 2c^2)^4};$$

$$U_1 \times U_1 \times U_1 \times U_1: \quad \varphi = [a, -a, b, -b, c, -c, d, -d], \tag{IV.1.59}$$

$$\alpha_4 = \frac{2a^4 + 2b^4 + 2c^4 + 2d^4}{(2a^2 + 2b^2 + 2c^2 + 2d^2)^2},$$

$$\alpha_6 = \frac{2a^6 + 2b^6 + 2c^6 + 2d^6}{(2a^2 + 2b^2 + 2c^2 + 2d^2)^3},$$

$$\alpha_8 = \frac{2a^8 + 2b^8 + 2c^8 + 2d^8}{(2a^2 + 2b^2 + 2c^2 + 2d^2)^4};$$

The orbit space is shown in Fig. IV.1.6. Again it is identical to the SO_9 case. Thus we omit further details.
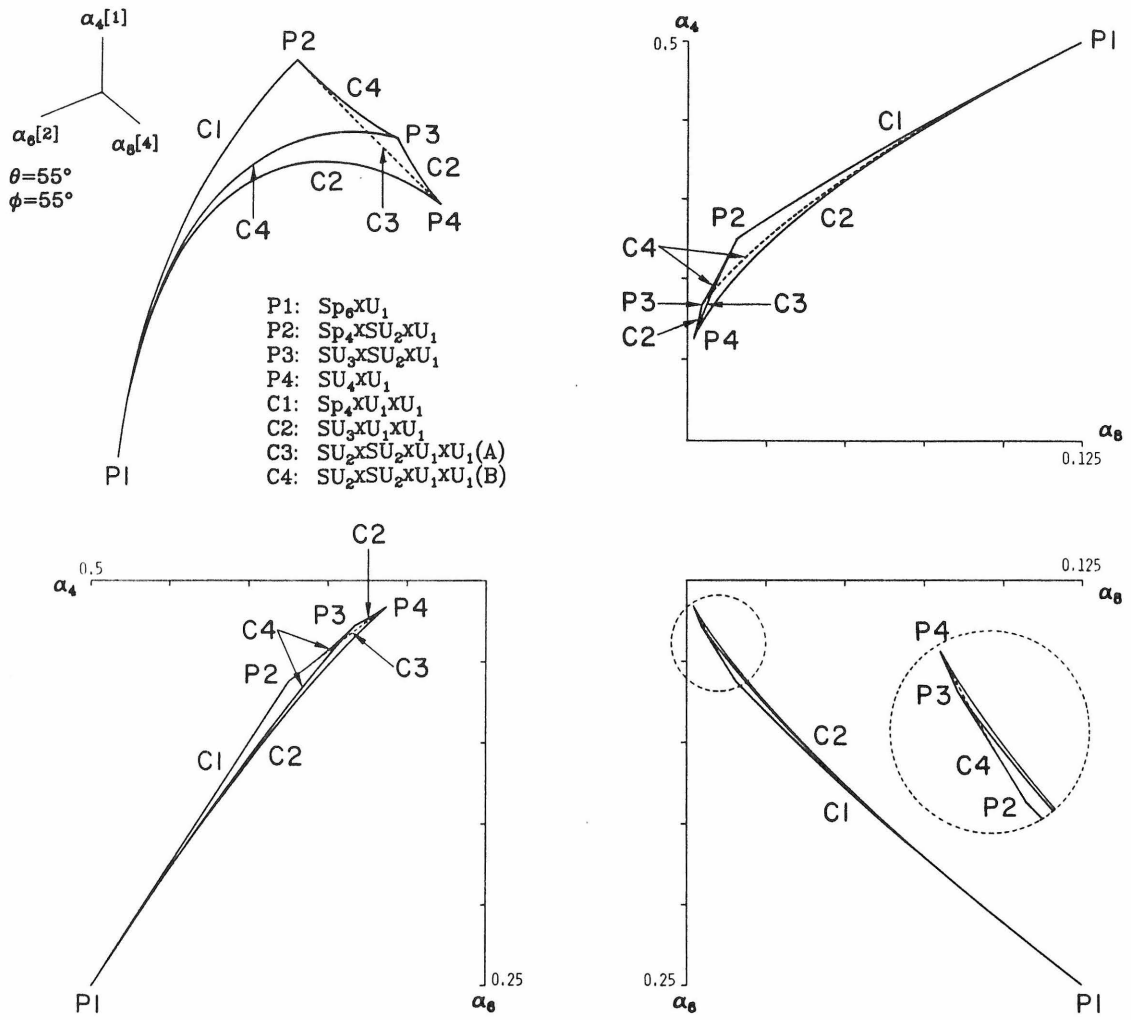
Fig. IV.1.6

The complete orbit space of the Sp_8 adjoint representation. It is identical to that of the SO_9 adjoint.

SO(8)

We choose the vector representation for the basis. The stratum of each little group is represented as follows:

$$\underline{SO_6 \times U_1} : \quad 8 = 1[1] + 1[-1] + 6[0], \quad\quad (IV.1.60)$$

$$\varphi = [a, -a, 0, 0, 0, 0, 0, 0],$$

$$\alpha_4 = 1/2,$$

$$\alpha_6 = 1/4,$$

$$\alpha'_4 = 0;$$

$$\underline{SO_4 \times SU_2 \times U_1} : \quad 8 = (2,1,1)[1] + (2,1,1)[-1] + (1,2,2)[0], \quad\quad (IV.1.61)$$

$$\varphi = [a, -a, a, -a, 0, 0, 0, 0],$$

$$\alpha_4 = 1/4,$$

$$\alpha_6 = 1/16,$$

$$\alpha'_4 = 0;$$

$$\underline{SU_4 \times U_1} : \quad 8 = 4[1] + \overline{4}[-1], \quad\quad (IV.1.62)$$

$$\varphi = [a, -a, a, -a, a, -a, a, -a],$$

$$\alpha_4 = 1/8,$$

$$\alpha_6 = 1/64,$$

$$\alpha'_4 = \pm 1/4;$$

$$\underline{SU_3 \times U_1 \times U_1} : \quad 8 = 1[0,1] + 1[0,-1] + 3[1,0] + \overline{3}[-1], \quad\quad (IV.1.63)$$

$$\varphi = [a, -a, a, -a, a, -a, b, -b],$$

$$\alpha_4 = \frac{6a^4 + 2b^4}{(6a^2 + 2b^2)^2},$$

$$\alpha_6 = \frac{6a^6 + 2b^6}{(6a^2 + 2b^2)^3},$$

$$\alpha'_4 = \pm \frac{2^4 a^3 b}{(6a^2 + 2b^2)^2};$$

$\underline{SU_2 \times SU_2 \times U_1 \times U_1}$: $8 = (2,1)[1,0] + (2,1)[-1,0] + (1,2)[0,1] + (1,2)[0,-1],$ (IV.1.64)

$$\varphi = [a, -a, a, -a, b, -b, b, -b],$$

$$\alpha_4 = \frac{4a^4 + 4b^4}{(4a^2 + 4b^2)^2},$$

$$\alpha_6 = \frac{4a^6 + 4b^6}{(4a^2 + 4b^2)^3},$$

$$\alpha'_4 = \pm \frac{2^4 a^2 b^2}{(4a^2 + 4b^2)^2};$$

$\underline{SO_4 \times U_1 \times U_1}$: $8 = (1,1)[1,0] + (1,1)[-1,0] + (1,1)[0,1] + (1,1)[0,-1]$ (IV.1.65)

$$+ (2,2)[0,0],$$

$$\varphi = [a, -a, b, -b, 0, 0, 0, 0],$$

$$\alpha_4 = \frac{2a^4 + 2b^4}{(2a^2 + 2b^2)^2},$$

$$\alpha_6 = \frac{2a^6 + 2b^6}{(2a^2 + 2b^2)^3},$$

$$\alpha'_4 = 0 ;$$

$\underline{SU_2 \times U_1 \times U_1 \times U_1}$: $8 = 1[0,1,0] + 1[0,-1,0] + 1[0,0,1] + 1[0,0,-1]$ (IV.1.66)

$$+2[1,0,0]+2[-1,0,0],$$

$$\varphi = [a,-a,a,-a,b,-b,c,-c],$$

$$\alpha_4 = \frac{4a^4+2b^4+2c^4}{(4a^2+2b^2+2c^2)^2},$$

$$\alpha_6 = \frac{4a^6+2b^6+2c^6}{(4a^2+2b^2+2c^2)^3},$$

$$\alpha'_4 = \frac{2^4a^2bc}{(4a^2+2b^2+2c^2)^2};$$

$$\underline{U_1{\times}U_1{\times}U_1{\times}U_1} : \quad \varphi = [a,-a,b,-b,c,-c,d,-d], \qquad \text{(IV.1.67)}$$

$$\alpha_4 = \frac{2a^4+2b^4+2c^4+2d^4}{(2a^2+2b^2+2c^2+2d^2)^2},$$

$$\alpha_6 = \frac{2a^6+2b^6+2c^6+2d^6}{(2a^2+2b^2+2c^2+2d^2)^3},$$

$$\alpha'_4 = \frac{2^4abcd}{(2a^2+2b^2+2c^2+2d^2)^2};$$

The orbit space is shown in Fig. IV.1.7. It is a warped tetrahedron. Cusp P1 of $[SO_6{\times}U_1]$ and cusp P2 of $[SO_4{\times}SU_2{\times}U_1]$ are connected by line L1 of $[SO_4{\times}U_1{\times}U_1]$. Cusps $\pm$P3 of $[SU_4{\times}U_1]$ and P2 are connected by line L2 of $[SU_2{\times}SU_2{\times}U_1{\times}U_1]$. P1 and $\pm$P3 are connected by curve C3 of $[SU_3{\times}U_1{\times}U_1]$. The stratum of $[SU_2{\times}U_1{\times}U_1{\times}U_1]$ closes the boundary of the generic stratum $[U_1{\times}U_1{\times}U_1{\times}U_1]$ which occupies the interior.

The projected orbit space $\alpha_4-\alpha_6$ is not closed by the one-dimensional strata L1, L2 and C3. The concave punctured portion belongs to the two-dimensional stratum. This is related to the fact that the triangular surface P2 $-$ +P3 $-$ $-$P3 is convex in the direction +P3 $\to$ $-$P3 but concave in the direction normal to it. All the surfaces that contain cusp P2 are saddle-shaped. Surface P1 $-$ +P3 $-$ $-$P3 is totally concave.
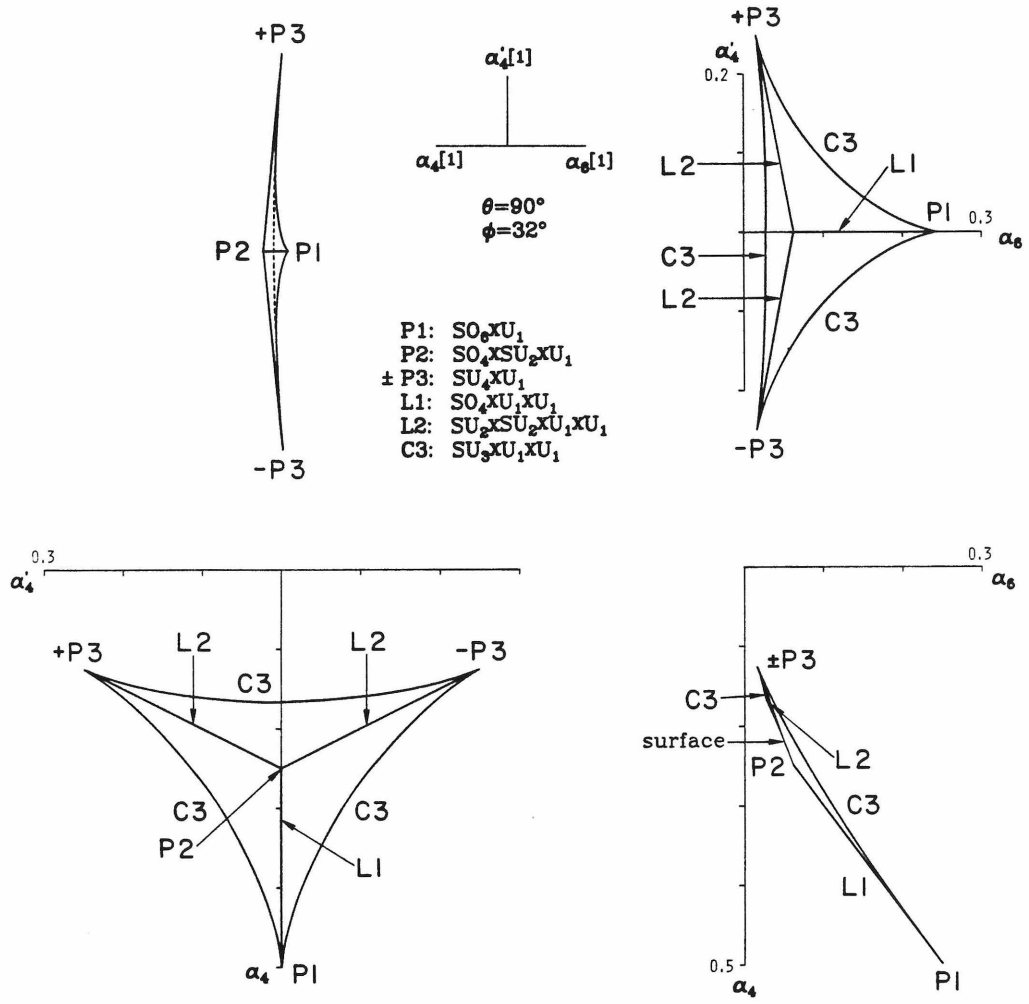
Fig. IV.1.7

The complete orbit space of the SO_8 adjoint representation. Shown at the upper left corner is a view from the direction oriented 32° from the α_4 axis and 90° from the α'_4 axis. The numbers in the square brackets are the relative ratios of scale. Each projection is a view from the positive direction of the axis not shown in the picture except for the one viewed from the $-\alpha_6$ axis. The dotted curve represents edges on the back (hidden) side of the orbit space.

F(4)

We choose the 26-dimensional representation for the basis. The stratum of each little group is represented as follows:

$\underline{SO_7 \times U_1}$:   (IV.1.68)

$26 = 1[0]+1[2]+1[-2]+7[0]+8[1]+8[-1]$

$\varphi = [2a, -2a, 8 \ a's, 8 \ (-a)'s, 8 \ 0's]$

$\alpha_6 = 1/96$,

$\alpha_8 = 11/6912$,

$\alpha_{12} = 19/442368$;

$\underline{Sp_6 \times U_1}$:   (IV.1.69)

$26 = 6[1] + 6[-1] + 14[0]$

$\varphi = [\ 6 \ a's, 6 \ (-a)'s, 14 \ 0's\ ]$

$\alpha_6 = 1/144$,

$\alpha_8 = 1/864$,

$\alpha_{12} = 1/124416$;

$\underline{SU_3 \times SU_2 \times U_1 \ (A)}$:   (IV.1.70)

$26 = (8,1)[0]+(3,2)[1]+(3,1)[-2]+(\overline{3},2)[-1]+(\overline{3},1)[2]$

$\varphi = [\ 6 \ a's, 6 \ (-a)'s, 3 \ (2a)'s, 3(-2a)'s, 8 \ 0's]$

$\alpha_6 = 11/1296$,

$$\alpha_8 = 43/46656 ,$$

$$\alpha_{12} = 683/60466176 ;$$

$\underline{SU_3 \times SU_2 \times U_1 (B)}$: $\qquad\qquad$ (IV.1.71)

$$26 = (1,1)[0]+(1,2)[3]+(1,2)[-3]+(1,3)[0]$$

$$+(3,1)[-2]+(3,2)[1]+(\bar{3},1)[2]+(\bar{3},2)[-1]$$

$$\varphi = [\ 2 \ (3a)\text{'s}, \ 2 \ (-3a)\text{'s}, \ 6 \ a\text{'s}, \ 6 \ (-a)\text{'s},$$

$$3 \ (2a)\text{'s}, \ 3(-2a)\text{'s}, \ 4 \ 0\text{'s}] ,$$

$$\alpha_6 = 23/2592 ,$$

$$\alpha_8 = 193/186624 ,$$

$$\alpha_{12} = 14933/967458816 ;$$

$\underline{SO_5 \times U_1 \times U_1}$: $\qquad\qquad$ (IV.1.72)

$$26 = 1[0,0]+1[2,0]+1[-2,0]+1[0,2]+1[0,-2]$$

$$+5[0,0]+4[1,1]+4[1,-1]+4[-1,1]+4[-1,-1] ,$$

$$\varphi = [2a,-2a,2b,-2b, \ 6 \ 0\text{'s},$$

$$4 \ (a+b)\text{'s}, \ 4 \ (a-b)\text{'s}, \ 4 \ (-a+b)\text{'s}, \ 4 \ (-a-b)\text{'s}] ,$$

$$\alpha_6 = \frac{2(2a)^6+2(2b)^6+8(a+b)^6+8(a-b)^6}{[2(2a)^2+2(2b)^2+8(a+b)^2+8(a-b)^2]^3} ,$$

$$\alpha_8 = \frac{2(2a)^8+2(2b)^8+8(a+b)^8+8(a-b)^8}{[2(2a)^2+2(2b)^2+8(a+b)^2+8(a-b)^2]^4} ,$$

$$\alpha_{12} = \frac{2(2a)^{12}+2(2b)^{12}+8(a+b)^{12}+8(a-b)^{12}}{[2(2a)^2+2(2b)^2+8(a+b)^2+8(a-b)^2]^6} ;$$

$\underline{SU_2 \times SU_2 \times U_1 \times U_1}$:
$\hspace{8cm}$ (IV.1.73)

$$26 = (1,1)[2,0]+(1,1)[0,0]+(1,1)[-2,0]+(1,3)[0,0]$$

$$+(2,1)[0,1]+(2,1)[0,-1]+(1,2)[1,1]+(1,2)[1,-1]$$

$$+(2,2)[1,0]+(1,2)[-1,1]+(1,2)[-1,-1]+(2,2)[-1,0] \ ,$$

$$\varphi = [2a,-2a,b,b,-b,-b,(a+b),(a+b),(a-b),(a-b),$$

$$(-a+b),(-a+b),(-a-b),(-a-b),\ 4\ a's,\ 4\ (-a)'s,\ 4\ 0's] \ ,$$

$$\alpha_6 = \frac{2(2a)^6+4b^6+4(a+b)^6+4(a-b)^6+8a^6}{[2(2a)^2+4b^2+4(a+b)^2+4(a-b)^2+8a^2]^3} \ ,$$

$$\alpha_8 = \frac{2(2a)^8+4b^8+4(a+b)^8+4(a-b)^8+8a^8}{[2(2a)^2+4b^2+4(a+b)^2+4(a-b)^2+8a^2]^4} \ ,$$

$$\alpha_{12} = \frac{2(2a)^{12}+4b^{12}+4(a+b)^{12}+4(a-b)^{12}+8a^{12}}{[2(2a)^2+4b^2+4(a+b)^2+4(a-b)^2+8a^2]^6} \ ;$$

$\underline{SU_3 \times U_1 \times U_1\ (A)}$:
$\hspace{8cm}$ (IV.1.74)

$$26 = 3[1,1]+\bar{3}[1,-1]+3[-1,1]+\bar{3}[-1,-1]$$

$$+3[0,-2]+\bar{3}[0,2]+8[0,0]$$

$$\varphi = [\ 3\ (a+b)'s,\ 3\ (a-b)'s,\ 3\ (-a+b)'s,\ 3\ (-a-b)'s,$$

$$3\ (2a)'s,\ 3(-2a)'s,\ 8\ 0's]$$

$$\alpha_6 = \frac{6(a+b)^6+6(a-b)^6+6(2a)^6}{[6(a+b)^2+6(a-b)^2+6(2a)^2]^3} \ ,$$

$$\alpha_8 = \frac{6(a+b)^8+6(a-b)^8+6(2a)^8}{[6(a+b)^2+6(a-b)^2+6(2a)^2]^4} \ ,$$

$$\alpha_{12} = \frac{6(a+b)^{12}+6(a-b)^{12}+6(2a)^{12}}{[6(a+b)^2+6(a-b)^2+6(2a)^2]^6} \ ;$$

$\underline{SU_3 \times U_1 \times U_1\ (B)}$: (IV.1.75)

$$26 = 1[2,0]+1[0,0]+1[-2,0]+1[0,0]+3[0,2]+\overline{3}[0,-2]$$

$$+1[1,3]+3[1,-1]+1[1,-3]+\overline{3}[1,1]$$

$$+1[-1,3]+3[-1,-1]+1[-1,-3]+\overline{3}[-1,1]\ ,$$

$$\varphi = [2a,0,-2a,0,\ 3\ (2b)'s,\ 3\ (-2b)'s,$$

$$(a+3b),\ 3\ (a-b)'s,(a-3b),\ 3\ (a+b)'s,$$

$$(-a+3b),\ 3\ (-a-b)'s,(-a-3b),\ 3\ (-a+b)'s\ ]\ ,$$

$$\alpha_6 = \frac{2(2a)^6+6(2b)^6+2(a+3b)^6+2(a-3b)^6+6(a+b)^6+6(a-b)^6}{[2(2a)^2+6(2b)^2+2(a+3b)^2+2(a-3b)^2+6(a+b)^2+6(a-b)^2]^3}\ ,$$

$$\alpha_8 = \frac{2(2a)^8+6(2b)^8+2(a+3b)^8+2(a-3b)^8+6(a+b)^8+6(a-b)^8}{[2(2a)^2+6(2b)^2+2(a+3b)^2+2(a-3b)^2+6(a+b)^2+6(a-b)^2]^4}\ ,$$

$$\alpha_{12} = \frac{2(2a)^{12}+6(2b)^{12}+2(a+3b)^{12}+2(a-3b)^{12}+6(a+b)^{12}+6(a-b)^{12}}{[2(2a)^2+6(2b)^2+2(a+3b)^2+2(a-3b)^2+6(a+b)^2+6(a-b)^2]^6}\ ;$$

$\underline{SU_2 \times U_1 \times U_1 \times U_1\ (A)}$: (IV.1.76)

$$26 = 1[2,0,0]+1[0,0,0]+1[-2,0,0]+3[0,0,0]+1[0,1,1]$$

$$+1[0,1,-1]+1[0,-1,1]+1[0,-1,-1]+2[1,1,0]+2[1,-1,0]$$

$$+2[1,0,1]+2[1,0,-1]+2[-1,1,0]+2[-1,-1,0]$$

$$+2[-1,0,1]+2[-1,0,-1]\ ,$$

$$\alpha_6 = \frac{2(2a)^6+2(b+c)^6+2(b-c)^6+4(a+b)^6+4(a-b)^6+4(a+c)^6+4(a-c)^6}{[2(2a)^2+2(b+c)^2+2(b-c)^2+4(a+b)^2+4(a-b)^2+4(a+c)^2+4(a-c)^2]^3}\ ,$$

$$\alpha_8 = \frac{2(2a)^8+2(b+c)^8+2(b-c)^8+4(a+b)^8+4(a-b)^8+4(a+c)^8+4(a-c)^8}{[2(2a)^2+2(b+c)^2+2(b-c)^2+4(a+b)^2+4(a-b)^2+4(a+c)^2+4(a-c)^2]^4}\ ,$$

$$\alpha_{12} = \frac{2(2a)^{12} + 2(b+c)^{12} + 2(b-c)^{12} + 4(a+b)^{12} + 4(a-b)^{12} + 4(a+c)^{12} + 4(a-c)^{12}}{[2(2a)^2 + 2(b+c)^2 + 2(b-c)^2 + 4(a+b)^2 + 4(a-b)^2 + 4(a+c)^2 + 4(a-c)^2]^6};$$

$\underline{SU_2 \times U_1 \times U_1 \times U_1 \ (B)}$: $\hspace{4cm}$ (IV.1.77)

$$26 = 1[2,0,0] + 1[0,0,0] + 1[-2,0,0] + 1[0,0,2] + 1[0,0,0]$$

$$+ 1[0,0,-2] + 2[0,1,0] + 2[0,-1,0] + 1[1,1,1] + 1[1,1,-1]$$

$$+ 1[1,-1,1] + 1[1,-1,-1] + 2[1,0,1] + 2[1,0,-1] + 1[-1,1,1]$$

$$+ 1[-1,1,-1] + 1[-1,-1,1] + 1[-1,-1,-1] + 2[-1,0,1] + 2[-1,0,-1]$$

$$\alpha_6 = \frac{\left[\begin{array}{c} 2(2a)^6 + 2(2c)^6 + 4b^6 + 4(a+c)^6 + 4(a-c)^6 \\ + 2(a+b+c)^6 + 2(a+b-c)^6 + 2(a-b+c)^6 + 2(-a+b+c)^6 \end{array}\right]}{\left[\begin{array}{c} 2(2a)^2 + 2(2c)^2 + 4b^2 + 4(a+c)^2 + 4(a-c)^2 \\ + 2(a+b+c)^2 + 2(a+b-c)^2 + 2(a-b+c)^2 + 2(-a+b+c)^2 \end{array}\right]^3},$$

$$\alpha_8 = \frac{\left[\begin{array}{c} 2(2a)^8 + 2(2c)^8 + 4b^8 + 4(a+c)^8 + 4(a-c)^8 \\ + 2(a+b+c)^8 + 2(a+b-c)^8 + 2(a-b+c)^8 + 2(-a+b+c)^8 \end{array}\right]}{\left[\begin{array}{c} 2(2a)^2 + 2(2c)^2 + 4b^2 + 4(a+c)^2 + 4(a-c)^2 \\ + 2(a+b+c)^2 + 2(a+b-c)^2 + 2(a-b+c)^2 + 2(-a+b+c)^2 \end{array}\right]^4},$$

$$\alpha_{12} = \frac{\left[\begin{array}{c} 2(2a)^{12} + 2(2c)^{12} + 4b^{12} + 4(a+c)^{12} + 4(a-c)^{12} \\ + 2(a+b+c)^{12} + 2(a+b-c)^{12} + 2(a-b+c)^{12} + 2(-a+b+c)^{12} \end{array}\right]}{\left[\begin{array}{c} 2(2a)^2 + 2(2c)^2 + 4b^2 + 4(a+c)^2 + 4(a-c)^2 \\ + 2(a+b+c)^2 + 2(a+b-c)^2 + 2(a-b+c)^2 + 2(-a+b+c)^2 \end{array}\right]^6},$$

$\underline{U_1 \times U_1 \times U_1 \times U_1}$: $\hspace{4cm}$ (IV.1.78)

$$\varphi = [2a, 0, -2a, 2c, 0, -2c, b+d, b-d, -b+d, -b-d,$$

$$a+b+c, a+b-c, a-b+c, -a+b+c, -a-b-c, -a-b+c,$$

$$-a+b-c, a-b-c, a+c+d, a+c-d, a-c+d, -a+c+d,$$

$$-a-c-d, -a-c+d, -a+c-d, a-c-d]$$

where we omitted the expressions for α_6, α_8, and α_{12}.

The orbit space is shown in Fig. IV.1.8. It is a very thin warped tetrahedron. Cusp **P1** of $[SO_7 \times U_1]$ and cusp **P2** of $[Sp_6 \times U_1]$ are connected by curve **C1** of $[SO_5 \times U_1 \times U_1]$. Cusp **P2** and cusp **P3** of $[SU_3 \times SU_2 \times U_1(A)]$ are connected by curve **C2** of $[SU_3 \times U_1 \times U_1(A)]$. **P1** and cusp **P4** of $[SU_3 \times SU_2 \times U_1(B)]$ are connected by curve **C3** of $[SU_3 \times U_1 \times U_1(B)]$. All the cusps are connected by curve **C4** of $[SU_2 \times SU_2 \times U_1 \times U_1]$. Surface **S1** (P1-P2-P3) and surface **S2** (P2-P3-P4) belong to the stratum of $[SU_2 \times U_1 \times U_1 \times U_1(A)]$. Surface **S3** (P1-P3-P4) and surface **S4** (P1-P2-P4) belong to the stratum of $[SU_2 \times U_1 \times U_1 \times U_1(B)]$. The interior is occupied by the generic stratum of $[U_1 \times U_1 \times U_1 \times U_1]$.

C2 and **C3** are convex plane-curves. **C1** and the portion of **C4** between **P3** and **P4** are concave space-curves. The other portions of **C4** are convex space-curves. Surface **P1** − **P3** − **P4** is totally concave. All the other surfaces are saddle-shaped.
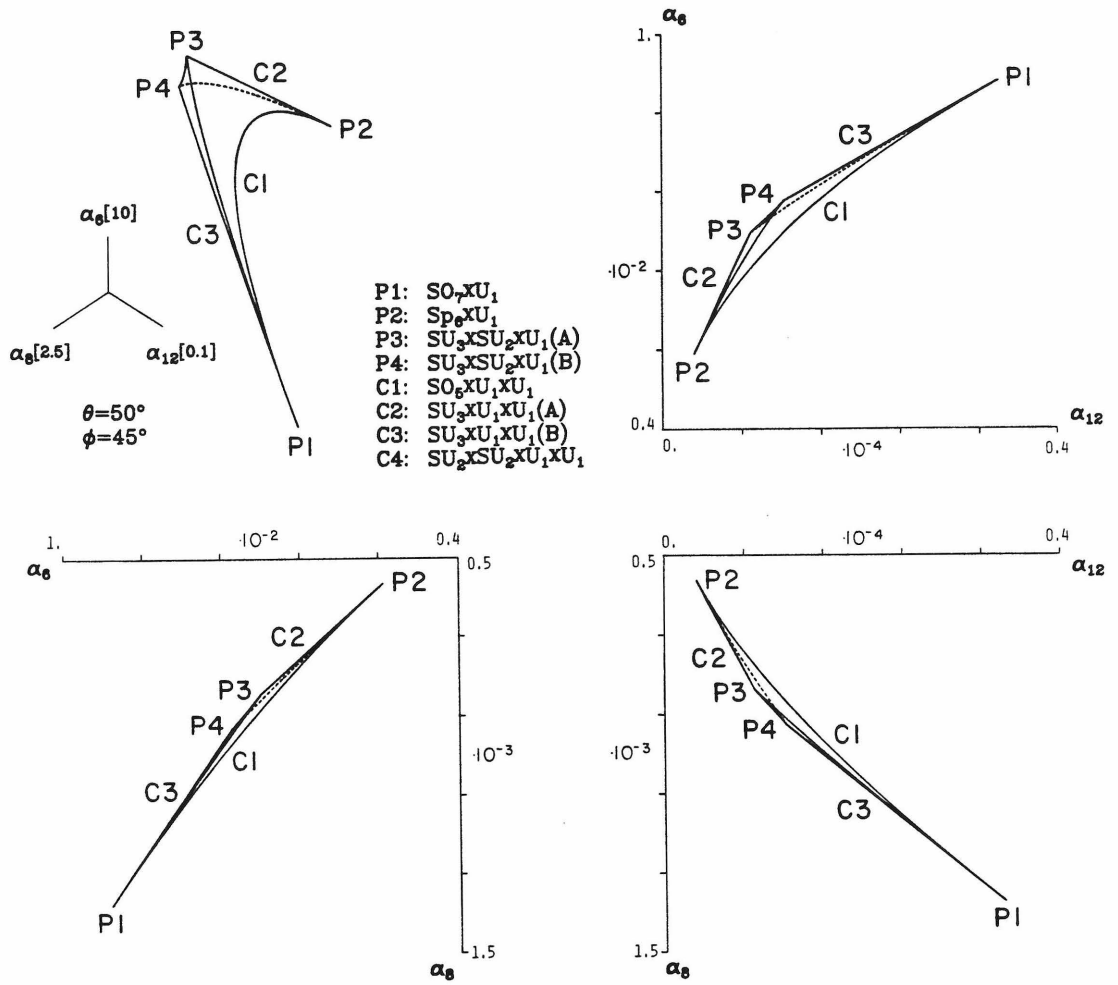
Fig. IV.1.8

The complete orbit space of the F_4 adjoint representation. Shown at the upper left corner is a view from the direction oriented 45° from the α_8 axis and 50° from the α_6 axis. The numbers in the square brackets are the relative ratios of scale. Each projection is a view from the positive direction of the axis not shown in the picture. The dotted curves represent edges on the back (hidden) side of the orbit space. The unlabeled curves are all portions of C4.

IV.1.4 COMMENTS

In the previous examples we have observed that the orbit spaces for the adjoint representations of SO_{2n+1} and Sp_{2n} have identical geometrical shapes. Another interesting observation is, as Michel [11] pointed out, that the orbit spaces of some representations of finite groups have also identical shapes to them. For example, the orbit space for the vector representation of the octahedral group O_h is identical to that of SO_7 adjoint. The basic set of invariants are $I_2=\varphi_1^2+\varphi_2^2+\varphi_3^2$, $I_4=\varphi_1^4+\varphi_2^4+\varphi_3^4$, $I_6=\varphi_1^6+\varphi_2^6+\varphi_3^6$. The orbit space is depicted in Fig. IV.1.9.

Fig. IV.1.9

Another interesting observation is that the orbit space for the adjoint representations of SU_N has the same geometrical shape as that of the symmetric tensor representations of SO_N. For example let us consider the traceless symmetric tensor of SO_5, φ_{ij}. The basic set of invariant polynomials consists of $Tr\,\varphi^2$, $Tr\,\varphi^3$, $Tr\,\varphi^4$, and $Tr\,\varphi^5$. Since φ_{ij} is a real symmetric matrix, it can be diagonalized [19] by an orthogonal transformation. Thus the orbit space is identical to the SU_5 adjoint. It is depicted in Fig. IV.1.10. Note that the little group of the generic stratum is the null group.

P I: $SU_2 \times SU_2$
P2: $SO_3 \times U_1$
C I: SO_3
C2: $U_1 \times U_1$
surface: U_1
interior: null

Fig. IV.1.10

The most interesting observation is that the orbit spaces for the adjoint representations of Lie groups of the same rank all have similar geometrical shapes, namely straight line for groups of rank two, triangle for groups of rank three, tetrahedron for groups of rank four, and so on. This implies that there is an interesting relationship between the degree of polynomial invariants and the shape of the orbit space. For example, SU_5 adjoint has only two maximal little groups but odd degree invariants such as I_3 and I_5 duplicate the number of cusps providing the third and fourth cusps needed to build a tetrahedron. But for the adjoint representations of all the other groups of rank four there are four maximal little groups and their invariants are of even degree yielding only four cusps, just enough to build a tetrahedron.

It will be both interesting and important to see if our last observation holds generally: Is it true that a three-dimensional orbit space of an irreducible representation is always a warped tetrahedron?

IV.2 TWO IRREDUCIBLE REPRESENTATIONS

The orbit spaces of two irreducible representations are normally high dimensional because after one of the representations is simplified only a small number of group parameters (which were called ϑ_L in CHI.2) are left for further simplification of the other representation. We have found two cases where the orbit space is three dimensional, SU_3 adjoint + vector and SO_5 adjoint + vector.

IV.2.1 SU(3) ADJOINT + VECTOR REPRESENTATIONS

Using the same notation as in CHIII.3, the orbit parameters are:

$$\alpha_3 = \frac{\sum \varphi_i^3}{(\sum \varphi_i^2)^{3/2}} \tag{IV.2.1}$$

$$\beta_1 = \frac{\sum \chi_i^* \varphi_i \chi_i}{(\sum \varphi_i^2)^{1/2}(\sum \chi_i \chi_i^*)}, \quad \beta_2 = \frac{\sum \chi_i^* \varphi_i^2 \chi_i}{(\sum \varphi_i^2)(\sum \chi_i \chi_i^*)} \tag{IV.2.2}$$

The stratum of each little group is represented as follows:

$\underline{SU_2}$: $8 = 1 + 2 + 2 + 3,$ $\tag{IV.2.3}$

$3 = 1 + 2,$

$\varphi = [a,a,-2a],$

$\chi = [0,0,c],$

$\alpha_3 = \pm 1/\sqrt{6},$

$\beta_1 = \pm 2/\sqrt{6},$

$\beta_2 = 2/3.$

$\underline{U_1}$: $\varphi = [a,b,-a-b],$ $\tag{IV.2.4}$

$$\chi = [0,0,c],$$

$$\alpha_3 = (a^3+b^3-(a+b)^3)/(a^2+b^2+(a+b)^2)^{3/2},$$

$$\beta_1 = -(a+b)/(a^2+b^2+(a+b)^2)^{1/2},$$

$$\beta_2 = (a+b)^2/(a^2+b^2+(a+b)^2).$$

The generic stratum is represented by eqs. (IV.2.1-2) and its little group is the null group. Can a curve confine a three-dimensional volume? The answer is no and thus the stratum of the null group must confine itself. The volume is extremized when either χ_1 or χ_2 is equal to zero with all the other components non-zero. The orbit space is shown in Fig. IV.2.1. The strata of SU_2, namely the cusps, are the most protrudent as we might guess from the fact that they satisfy the most singular boundary conditions. The stratum of U_1, namely the curve, is the next most singular. This may lead us to expect that such hierarchical relationship would be a prominent feature of the orbit space of two irreps. But as we shall see in the next example the strata of a lower level little group can be as singular as the higher level ones.
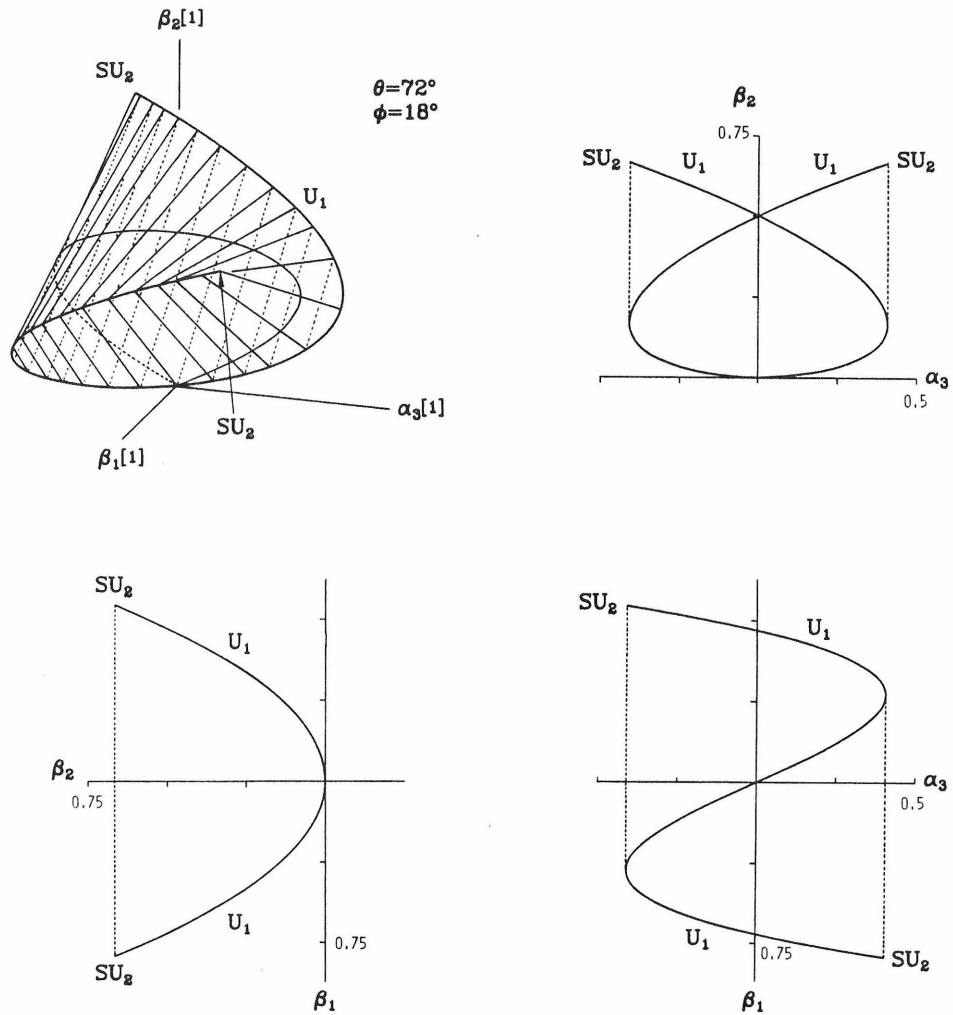
Fig. IV.2.1

The complete orbit space of the SU_3 adjoint + vector. Shown at the upper left corner is a view from the direction 18° from the β_1 axis and 72° from the β_2 axis. The dotted lines are hidden lines. The numbers in the square brackets are the relative ratios of scale. Each projection is a view from the positive direction of the axis not shown in the picture. Here the dotted lines are portions of the boundary belonging to the null group stratum. Thus the hidden curves are drawn solidly.

IV.2.2 SO(5) ADJOINT + VECTOR REPRESENTATIONS

Using the same notation as in CHIII.4, the orbit parameters are:

$$\alpha_4 = \frac{\sum \varphi_i^4}{2(\sum \varphi_i^2)^2} \qquad \qquad (\text{IV.2.5})$$

$$\beta_2 = \frac{\sum \chi_i \varphi_i^2 \chi_i}{(2\sum \varphi_i^2)(\sum \chi_i \chi_i + \chi_3 \chi_3)}, \qquad \beta_4 = \frac{\sum \chi_i \varphi_i^4 \chi_i}{(2\sum \varphi_i^2)^2(\sum \chi_i \chi_i + \chi_3 \chi_3)}, \qquad (\text{IV.2.6})$$

where i runs from 1 to 2. The stratum of each little group is represented as follows:

$\underline{SO_3}$: $10 = 1 + 3 + 3 + 3,$ $\qquad\qquad\qquad\qquad\qquad$ (IV.2.7)

$\qquad$ $5 = 1 + 1 + 3,$

$\qquad$ $\varphi = [a, 0],$

$\qquad$ $\chi = [c, 0, 0],$

$\qquad$ $\alpha_4 = 1/2,$

$\qquad$ $\beta_2 = 1/2,$

$\qquad$ $\beta_4 = 1/4.$

$\underline{SU_2 \times U_1}$: $\qquad\qquad\qquad\qquad\qquad\qquad\qquad\qquad$ (IV.2.8)

$\qquad$ $10 = 1(0)+1(2)+1(-2)+3(0)+2(1)+2(-1),$

$\qquad$ $5 = 1(0) + 2(1) + 2(-1),$

$\qquad$ $\varphi = [a, a],$

$\qquad$ $\chi = [0, 0, c],$

$$\alpha_4 = 1/4,$$

$$\beta_2 = 0,$$

$$\beta_4 = 0.$$

$\underline{U_1 \times U_1}$: (IV.2.9)

$$\varphi = [a,b]$$

$$\chi = [0,0,c]$$

$$\alpha_4 = (2a^4 + 2b^4)/(2a^2 + 2b^2)^2,$$

$$\beta_2 = 0,$$

$$\beta_4 = 0.$$

$\underline{U_1}$: (IV.2.10)

$$\varphi = [a,b]$$

$$\chi = [0,c,d]$$

$$\alpha_4 = (2a^4 + 2b^4)/(2a^2 + 2b^2)^2,$$

$$\beta_2 = (b^2c^2)/(2a^2 + 2b^2)(c^2 + d^2),$$

$$\beta_4 = (b^4c^2)/(2a^2 + 2b^2)^2(c^2 + d^2).$$

The generic stratum is represented by eqs. (IV.2.5-6) and its little group is the null group. The stratum of U_1 is two-dimensional and thus has a chance to enclose the whole volume. The U_1 stratum occupies the surfaces represented by dotted lines in Fig. IV.2.2, but the surface represented by solid lines is a part of the generic stratum. This is in contrast to the case of one irrep where there was

no mixture of this kind. That is, equally singular surfaces consist of both the stratum of a maxi-maximal little group and a lower level one. Though the portion of the surface belonging to the null group is more singular than the interior there is no way to distinguish them because there is no more subgroup left. The volume is extremized when either χ_2 is equal to zero (U_1) or χ_3 is zero (the null group) with all the other components non-zero.
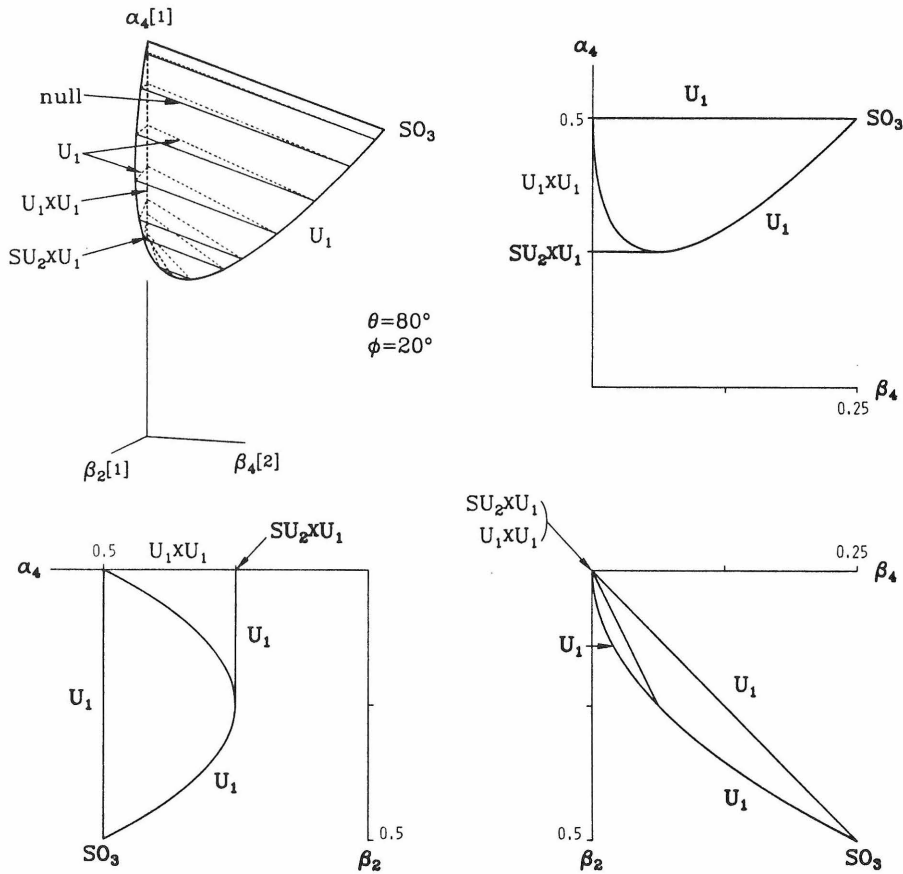
Fig. IV.2.2

The complete orbit space of the SO_5 adjoint + vector. Shown at the upper left corner is a view from the direction 20° from the β_2 axis and 80° from the α_4 axis. The dotted lines are hidden lines. The numbers in the square brackets are the relative ratios of scale. Each projection is a view from the positive direction of the axis not shown in the picture. Here the hidden curves and lines are drawn solidly.

IV.2.3 COMMENTS

Contrary to the case of one irrep where the strata of successively lower level little groups occupy successively higher dimensional and less singular (locally less protrudent) surfaces on the orbit space boundary, the orbit space boundary of two irreps is more complex and things are pretty much mixed. Whereas orbit parameters associated with each irrep tend to form warped concave boundary surfaces, orbit parameters associated with both irreps tend to destroy such behavior. With the field components of one irrep fixed (consequently orbit parameters associated with that irrep fixed), one can change the field components of the other irrep creating a volume traced by pencils.

Indeed we have already observed such mixing in the projected orbit spaces of the SU_N and SO_N adjoint + vector representations. The straight lines, namely vertical and horizontal lines, belong to either a maxi-maximal little group or a lower level little group. In the case of SU_3 adjoint + vector (Fig. IV.2.1) we find that the maxi-maximal little groups, SU_2 and U_1, occupy most protrudent portions of the boundary. But in the case of SO_5 adjoint + vector (Fig. IV.2.2) we find that the U_1 stratum occupies the boundary planes indicated by the dotted lines and the stratum of the null group occupies the boundary plane indicated by the solid lines. That is, there is no sharp distinction between the maxi-maximal little group, U_1, and the lower level little group, the null group, in terms of dimensionality and concavity. It may be that the mixing takes place only among the flat or concave portions of the boundary. But we do not have an argument to support this wild conjecture.

Another interesting point is that the little groups alone cannot distinguish the fine structure of the orbit space. In both of the above mentioned examples we see that the null group strata consist of two-dimensional surface <u>and</u> three-dimensional volume. In the SO_5 case the strata of U_1 consists of an edge curve

and two-dimensional surfaces. This indistinguishability comes from the fact that, whereas for a given group there are only a finite number of subgroups, there is no limit to the dimension, D, of a representation. The lower limit to the dimension of the corresponding orbit space is (D - the number of generators - 1) for one irrep and (D - the number of generators - 2) for two irreps. Thus the indistinguishability is observed in both cases. The difference between the two cases may be that, whereas in one irrep case there is no dimensional mixing between the strata of little groups of different levels, such dimensional mixing generally occurs in two irrep case.

CHAPTER V GENERALIZATION TO NON–LINEAR POTENTIAL

Because of the restriction that the classical Higgs potential must be made of at most fourth degree polynomial invariants, it contains only part of the complete set of orbit parameters (except in a few cases of low dimensional representations of small groups) and is linear with respect to them if they are independent. The potential can be readily minimized with respect to the partial list of orbit parameters, which is much less than the number of field components. Due to the linearity the absolute minimum is most likely to occur on the most protrudent portions of the orbit space boundary, where the boundary conditions reduce the number of independent parameters drastically. The boundaries, consisting of strata of higher little groups, extremize the complete orbit space and we see that the difficult extremization procedure employed in the conventional methods is transferred to the one of finding the boundary of the orbit space. The latter procedure is facilitated by some general mathematical results such as Michel's theorem [17] for one irreducible representation, which states that when $||\varphi||$ is held constant all invariants are stationary at a critical orbit corresponding to a maximal little group and thus implies that if we extremize one orbit parameter then we actually accomplish extremization of all the orbit parameters. If we carefully consider the necessary conditions for a boundary point, we further realize that in order to find a one-dimensional stratum all we need to do is to solve two equations of type eq. (II.3.2). In practice we do not attempt to solve such high degree algebraic equations but instead we simply look for singlets.

However if the orbit parameters appearing in the Higgs potential are not all independent then the potential is no longer linear with respect to basic orbit parameters. (For example this happens for two adjoint representations.) Therefore the danger arises that the absolute minimum may occur inside the

projected orbit space. In the examples we considered so far linearity was equivalent to monotonicity. But a non-linear function of a variable can still be monotonic with respect to the variable. What really counts in such extremum problems is *monotonicity* rather than linearity.

V.1 ONE IRREDUCIBLE REPRESENTATION

To see how monotonicity plays the major role in our problem let us reconsider the case of SU_5 adjoint representation alone. Let us examine the following hypothetical potential:

$$V = Mr^2 + B\beta r^3 + (A + A_1\alpha)\, r^4 + D\beta^2 r^6 \qquad (V.1.1)$$

where $r \equiv ||\varphi||^{1/2}$, $\beta \equiv Tr\,\varphi^3/\,||\varphi||^{3/2}$, and $\alpha \equiv Tr\,\varphi^4/\,||\varphi||^2$. We impose the positivity condition:

$$D > 0 \ , \ A + A_1\alpha > 0 \qquad (V.1.2)$$

to ensure that $V \to +\infty$ for all (α,β) as $||\varphi|| \to \infty$. Partial derivatives of the potential with respect to r, α, and β are:

$$\frac{\partial V}{\partial r} = 2Mr + 3B\beta r^2 + 4(A+A_1\alpha)r^3 + 6D\beta^2 r^5 \ , \qquad (V.1.3)$$

$$\frac{\partial V}{\partial \alpha} = A_1 r^4 \ , \qquad (V.1.4)$$

$$\frac{\partial V}{\partial \beta} = r^3(B + 2D\beta r^3) \ . \qquad (V.1.5)$$

The potential is monotonic with respect to α because eq. (V.1.4) has a definite sign. Let us proceed to find extrema neglecting for the moment subtleties concerning β. Setting eq. (V.1.5) equal to zero we obtain

$$\beta_o = -B/2Dr_o^3 \ . \qquad (V.1.6)$$

Substituting eq. (V.1.6) into eq. (V.1.3) we obtain

$$r_o^2 = -M/2(A+A_1\alpha) \ .$$ (V.1.7)

We choose $M < 0$ to guarantee that eq. (V.1.7) is positive. From eqs. (V.1.6) and (V.1.7) we obtain

$$\beta_o = -\frac{B}{2D}\left[\frac{2(A+A_1\alpha)}{-M}\right]^{3/2} \ .$$ (V.1.8)

We can choose $B > 0$ without loss of generality. Then eq. (V.1.8) represents a curve which, if it traverses the orbit space at all, passes through the lower left corner of the orbit space for $A_1 > 0$ or the upper left corner of the orbit space for $A_1 < 0$ without crossing $\beta = 0$ (Fig. V.1.1).
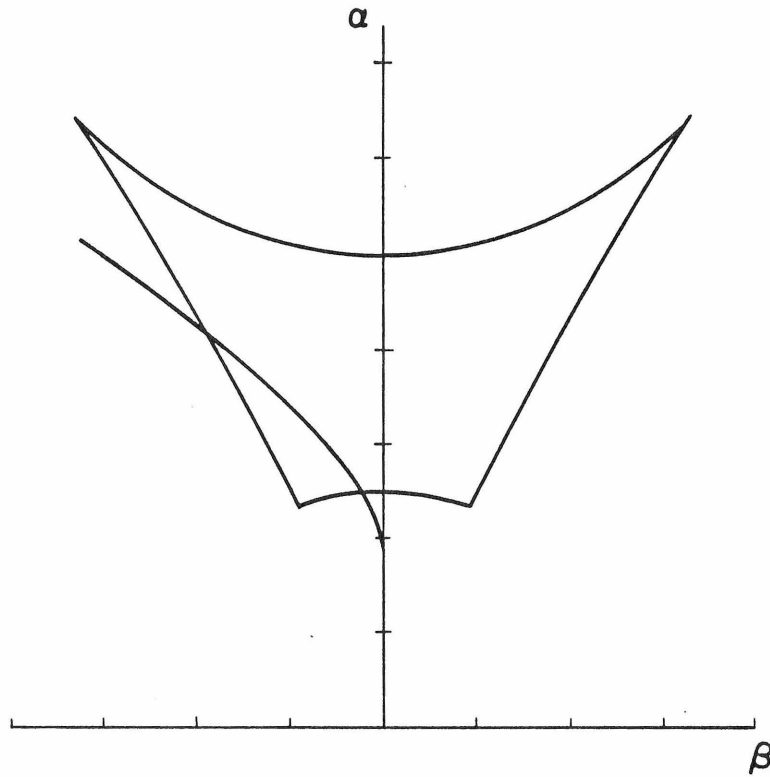

Fig. V.1.1

If the curve does not pass through the orbit space, then there is no "physical" value of β that satisfies eq. (V.1.6) and thus the potential is monotonic with respect to β despite the non-linearity. The absolute minimum will occur somewhere on the boundary curve, most likely at the cusps because they are most protrudent.

If the curve passes through the orbit space (Fig. V.1.1), then extrema occur on the portion of the curve immersed in the orbit space. Substituting eqs. (V.1.6) and (V.1.7) into eq. (V.1.1) we obtain the extremum value of the potential,

$$V_o = -\frac{M^2}{4(A+A_1\alpha)} - \frac{B^2}{4D} \; . \tag{V.1.9}$$

As we can expect from the monotonicity of the potential with respect to α the absolute extremum along the curve occurs at a point where the curve and the orbit space boundary meet. We have confirmed that for fixed α our solutions, eqs. (V.1.6) and (V.1.7), satisfy the inequalities for a local minimum among the partial derivatives of the potential with respect to r and β:

$$\frac{\partial^2 V}{\partial r^2} > 0, \quad \frac{\partial^2 V}{\partial \beta^2} > 0, \quad \frac{\partial^2 V}{\partial r^2}\frac{\partial^2 V}{\partial \beta^2} > \left[\frac{\partial^2 V}{\partial r\,\partial \beta}\right]^2 \quad . \tag{V.1.10}$$

Therefore the absolute extremum obtained above is indeed the absolute minimum.

Suppose we make a 3-dimensional map of the directional minimum $V(r_o)$ on the orbit space (Fig. V.1.1). Then we can imagine that the A_1 term tends to make a north-south-wise slope, the B term tends to make a east-west-wise slope, and the D term tends to make a valley along the $\beta = 0$ line. Our slopes are not rugged at all but very monotonic. Look! There is a canyon descending from northwest to southeast marked eq. (V.1.8) and it is lower than the central line which fails to become a valley. The above map refers to a case where $A_1 > 0$,

$B > 0$, and $D > 0$. The last point comes from the fact that the directional minimum on the $\beta = 0$ line, equal to $-M^2/4(A+A_1\alpha)$, is always higher than V_0 of eq. (V.1.9). The absolute minimum occurs at the end of the canyon, i.e., where the curve and the orbit space boundary meet and the little group is semi-maximal. This example shows that when the directional minimum of the potential is monotonic in all but one orbit parameter the lowest possible little group of the absolute minimum is one level lower than the maximal little groups. We believe that the level can be lowered at most by one each time we have a constraint like eq. (V.1.8).

Let us consider the general situation on a more solid ground. The procedure employed in the previous example does not always yield the absolute minimum and sometimes leads to a trivial solution. Thus we are not guaranteed that we would get all the local minima and only the minima in this way. Conceptually, the best way to find the extremum is to solve first $\partial V/\partial r = 0$ for $r_0(\alpha,\beta)$ and then compute $\partial V/\partial\alpha|_{r=r_0}$ and $\partial V/\partial\beta|_{r=r_0}$. Physical extrema can occur only on the $r_0(\alpha,\beta) > 0$ side of the orbit space. The curves defined by

$$\partial V/\partial\alpha|_{r=r_0} = 0 \ , \tag{V.1.11}$$

$$\partial V/\partial\beta|_{r=r_0} = 0 \tag{V.1.12}$$

divide the orbit space into regions. In each of them the partial derivatives have definite signs. In each region we repeat the same procedure as we did for a monotonic case. The absolute extremum of the region will occur on the regional boundary, which consists of portions of the orbit space boundary and the portions of the curves, $\partial V/\partial\alpha = 0$ and $\partial V/\partial\beta = 0$ passing through the orbit space. If the potential is a smooth function of its variables the potential extremizing k-contour will be a smooth curve and the first contact with the regional boundary is most likely to occur at cusps including new ones, though there is a possibility

that it may occur on concave curves corresponding to semi-maximal little groups. When the directional extremum is monotonic with respect to one of the orbit parameters (say, α) the absolute extremum may still occur at the cusps corresponding to maximal little groups. But a new possibility arises that it may occur at the new cusps, where the concave boundary curves and the curve $\partial V/\partial\beta = 0$ meet. It will never occur at those points on the curve $\partial V/\partial\beta = 0$ which lie inside the orbit space because the directional extremum is still monotonic with respect to α and the absolute extremum is carried to end points, namely the new cusps.

A necessary condition for an interior point to be the absolute extremum is that both eqs. (V.1.11) and (V.1.12) should be satisfied in the orbit space. This situation is undesirable because the interior points of our projected orbit space correspond to a set of little groups, $\{SU_2\times U_1\times U_1\times U_1,\ U_1\times U_1\times U_1\times U_1\}$, and we cannot exclude either of them in favor of the other because the boundary condition is not applicable to an interior point. (However the interior points of the complete orbit space do correspond to a unique little group, $U_1\times U_1\times U_1\times U_1$.)

V.2 TWO IRREDUCIBLE REPRESENTATIONS

A similar result is obtained for a simple but non-linear potential for two irreps. For example let us consider the following potential:

$$V = -\frac{M^2}{2}r^2 + \frac{A'}{4}r^4 - \frac{m^2}{2}s^2 + \frac{C'}{4}s^4 - Brs\vartheta + \frac{D}{2}r^2s^2\vartheta^2 \qquad (V.2.1)$$

where $r \geq 0$, $s \geq 0$, and $-1 \leq \vartheta \leq 1$. Eq. (V.2.1) can be considered as a simplified potential for any two identical real irreps, e.g., two adjoints or vectors. In general A' and C' contain orbit parameters. In order to ensure that $V \to +\infty$ as $r \to \infty$ and $s \to \infty$ we impose

$$A' > 0, \ C' > 0, \ D\vartheta^2 > -\sqrt{A'C'} \tag{V.2.2}$$

Partial derivatives of the potential with respect to r, s, and ϑ are:

$$\frac{\partial V}{\partial r} = -M^2 r + A'r^3 - Bs\vartheta + Drs^2\vartheta^2 , \tag{V.2.3a}$$

$$\frac{\partial V}{\partial s} = -m^2 s + C's^3 - Br\vartheta + Dsr^2\vartheta^2 , \tag{V.2.3b}$$

$$\frac{\partial V}{\partial \vartheta} = -Brs + Dr^2s^2\vartheta . \tag{V.2.3c}$$

Disregarding the uninteresting solutions where r and/or s vanishes, and solving eq. (V.2.3c) for ϑ_0 we obtain

$$\vartheta_0 = B/Drs . \tag{V.2.4}$$

Substituting eq. (V.2.4) into eqs. (V.2.3a), (V.2.3b) we obtain

$$r_0^2 = M^2/A' , \ \ s_0^2 = m^2/C' . \tag{V.2.5}$$

This makes it necessary to impose $M^2 > 0$ and $m^2 > 0$. Substituting eq. (V.2.5) back into eq. (V.2.4) we obtain

$$\vartheta_0 = \frac{B\sqrt{A'C'}}{DMm}. \tag{V.2.6}$$

To be more specific let us choose $D > 0$, $B > 0$ and consider a case where $A' \equiv A + A_1\alpha$ and $C' \equiv C + C_1\gamma$. Then eq. (V.2.6) represents a quadrant of a cone (Fig. V.2.1). Its vertex is located at $(\alpha = -A/A_1, \ \gamma = -C/C_1, \ \vartheta = 0)$ and its axis lies in the $\alpha-\gamma$ plane midway between the α and γ axes. Note that the two lines, $\alpha = -A/A_1$ and $\gamma = -C/C_1$, are always on the cone.

For acceptable potentials with $V \to +\infty$ as r or $s \to \infty$, the planes $\alpha = -A/A_1$ and $\gamma = -C/C_1$, lie outside the orbit space, which is in any case centered about

$\vartheta = 0$ (Fig. V.2.1). If the cone is too wide in the ϑ direction to intersect the orbit space, then there is no "physical" value of ϑ that satisfies eqs. (V.2.4), (V.2.5) and the potential is monotonic with respect to ϑ. In this case the apparent non-linearity gives way to monotonicity of the directional minimum and the absolute minimum occurs on the orbit space boundary, most likely on the strata of the maxi-maximal little groups.
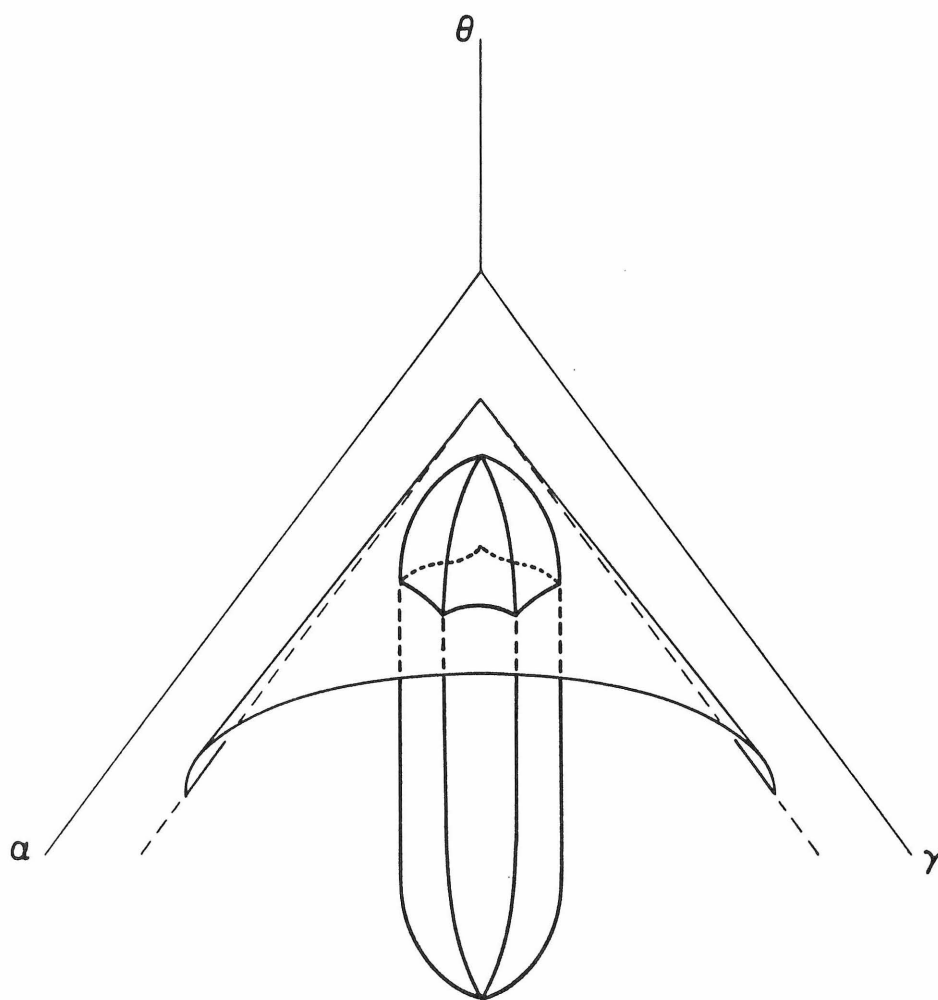

Fig. V.2.1

If the cone is narrow enough to pass through the orbit space (Fig. V.2.1), then extrema occur on the portion of the cone immersed in the orbit space. Substituting eqs. (V.2.5) and (V.2.6) into eq. (V.2.1) we obtain

$$V_0 = -\frac{M^4}{4A'} - \frac{m^4}{4C'} - \frac{B^2}{2D} \cdot \qquad (V.2.7)$$

Since we chose $D > 0$ we are assured at least that V_0 of eq. (V.2.7) is lower than the directional minimum at $\vartheta = 0$. We have confirmed that for fixed α and γ our solutions, eqs. (V.2.4) and (V.2.5), satisfy the inequalities for a local minimum among the partial derivatives of the potential with respect to r, s, and ϑ, including a 3×3 determinant. Therefore the absolute minimum occurs at a boundary point of the intersection of the orbit space cut by the cone.

In the "wide" case where eqs. (V.2.4) and (V.2.5) are not satisfied in the orbit space, a two-dimensional k-surface moves to meet the three-dimensional orbit space and the most protrudent portions of the boundary get the first contact. But in the "narrow" case where these equations are satisfied in the orbit space, eq. (V.2.4) introduces a constraint among the orbit parameters and thus reduces the dimension of the whole space effectively. On the cone the situation becomes similar to a monotonic case. A potential-minimizing k-contour moves to meet the boundary of a two-dimensional intersection. What was a curve is now a cusp and what was a three-dimensional volume is now a two-dimensional surface (Fig. V.2.1). Thus some portions of the boundary which were less protrudent can now be utilized. Since the maxi-maximal little groups occupy first few low-dimensional boundary surfaces (though mixed with lower level ones) they can still be utilized but there is a new possibility that lower level little groups can also be utilized.

There are two formidable difficulties in analyzing a realistic potential. First a general fourth degree Higgs potential for two irreps is of the form:

$$V = -\frac{M^2}{2}||\varphi|| + \frac{B'}{3}||\varphi||^{3/2} + \frac{A'}{4}||\varphi||^2 \qquad (V.2.8)$$

$$-\frac{m^2}{2}||\chi|| + \frac{D'}{3}||\chi||^{3/2} + \frac{C'}{4}||\chi||^2$$

$$+ S'||\varphi||^{1/2}||\chi||^{1/2} + T'||\varphi||||\chi|| + p'||\varphi||^{1/2}||\chi||$$

$$+ q'||\varphi||^{1/2}||\chi||^{3/2} + P'||\chi||^{1/2}||\varphi|| + Q'||\chi||^{1/2}||\varphi||^{3/2}$$

where primed quantities normally contain orbit parameters. T' contains S'^2 and thus makes the potential non-linear with respect to the orbit parameters that are in S'. The S' term is present only when the two fields belong to the same real representation. It can be removed by redefining φ and χ but non-linearity still shows up in higher degree terms, e.g., A' and C' terms. Secondly the orbit space of two irreps is very complicated and of very high dimension.

Whether the Gell-Mann-Slansky conjecture, which states that the absolute minimum of a fourth degree Higgs potential for two irreps preserves a maxi-maximal little group, holds or not depends on the structure of the orbit space boundary. A good test-case is provided by two adjoints [30,42] of SU_4. The most general Higgs potential [42] is of the form eq. (V.2.8) with each primed quantity containing one orbit parameter except for the T' term which contains three including S'^2. Diagonalizing φ and counting the number of singlets, we can make the following rough sketch of the orbit space: the most salient and low dimensional portions of the boundary consist of the strata of the maxi-maximal little groups. However the stratum of the smallest maxi-maximal little group, $U_1 \times U_1$, is at most 6-dimensional and cannot cover the whole boundary surface of the 11-dimensional projected orbit space. Less salient portions of the boundary surface correspond to the semi-maxi-maximal little group, U_1, whose stratum is at most 10-dimensional. The least salient portions of the boundary surface

correspond to the null group. A detailed analysis will take a tremendous amount of algebra. At this stage we suppose that the lowest possible little group will be U_1*, considering that it corresponds to the second most protrudent portions of the boundary surface. Therefore it is likely that the Gell-Mann-Slansky conjecture does not hold in this case.

If we impose separate reflection symmetries on each scalar field then the S term disappears along with other terms. We believe that this additional symmetry removes all the non-linearity, whether it comes explicitly as explained above or implicitly from a constraint among apparently independent orbit parameters. Another advantage of even degree Higgs potentials is that the potential minimizing k-surface for this case is known in general to be the cone of CHIII.1. (When there are more than three orbit parameters the k-cone represents a cone in a hyper-space.) Consequently the most protrudent portions of the orbit space boundary, which we conjectured correspond to the maxi-maximal little groups, will get the first contact. We believe that the Gell-Mann-Slansky conjecture for two irreps holds at least for an even degree Higgs potential.

The main source of non-linearity, namely S', is absent when the two fields belong to different representations. It will be a challenging problem to find the potential minimizing k-surface for a non-even degree potential without S' term and check whether or not the Gell-Mann-Slansky conjecture holds in such cases.

However non-monotonicity does not always yield violation of the conjecture. Even when the directional minimum is non-monotonic with respect to some orbit parameters, there are instances where the conjecture still holds because of the

* Wu [42] stated without proof that the absolute minimum of a Higgs potential for two adjoint representations of SU_N could diminish the little group to nothing. His statement can be true when several orbit parameters are non-monotonic so that non-salient portions of the orbit space boundary, which may correspond to the null group, are utilized. But in his problem there is only one non-monotonic orbit parameter.

orbit space geometry. In the case of two vectors the whole orbit space corresponds to the maxi-maximal little groups.

Finally we would like to point out that though classification of little groups of two irreps in the way explained in CHIII.2 is relatively effective to the first level, it becomes much less effective because the second level little groups cover almost all the subgroups left and the mixing occurs both ways. But we cannot think of a better classification scheme.

REFERENCES

[1] R. Brout and F. Englert, Phys. Rev. Lett 13 (1964), 321;

 P. Higgs, Phys. Lett. 12 (1964), 132;

 G. Guralnik, C. Hagen, and T. Kibble, Phys. Rev. Lett. 13 (1964), 585;

 P. Higgs, Phys. Rev. 145 (1966), 1156;

 T. Kibble, Phys. Rev. 155 (1967), 1554.

[2] G. 't Hooft, Nucl. Phys. B35 (1971), 167;

 B.W. Lee and J. Zinn-Justin, Phys. Rev. D5 (1972), 3121, 3137, 3155;

 S. Coleman, Secret Symmetry, Ettore Majorana Lecture Notes (1973).

[3] R. Jackiw and K. Johnson, Phys. Rev. D8 (1973), 2386;

 J.M. Cornwall and R.E. Norton, Phys. Rev. D8 (1973), 3338;

 J.M. Cornwall, Phys. Rev. D10 (1974), 500;

 E. Eichten and F. Feinberg, Phys. Rev. D10 (1974), 3254.

[4] L. Susskind, Phys. Rev. D20 (1979), 2619;

 S. Dimopoulos and L. Susskind, Nucl. Phys. B155 (1979), 237;

 E. Eichten and K.D. Lane, Phys. Lett. 90B (1980), 125;

 E. Fahri and L. Susskind, Phys. Rep. 74 (1981), 279.

[5] S. Weinberg, Phys. Rev. Lett. 19 (1967), 1264;

 A. Salam, Elementary Particle Theory, ed. N. Svartholm (Almquist and Wiksell, Stockholm, 1968), p. 367.

[6] J.C. Pati and A. Salam, Phys. Rev. D8 (1973), 1240;

H. Georgi and S.L. Glashow, Phys. Rev. Letters 32 (1974), 438;

H. Fritzsch and P. Minkowski, Ann. of Phys. 93 (1975), 193.

[7] H. Georgi, H.R. Quinn, and S. Weinberg, Phys. Rev. Letters 33 (1974), 451;

E. Gildner, Phys. Rev. D14 (1976), 1667;

S. Weinberg, Phys. Lett. 82B (1979), 387.

J. Ellis, M.K. Gaillard, A. Petermann, and C. Sachrajda, Nucl. Phys. B164 (1980), 253.

[8] L.D. Landau, Phys. Z. Soviet 11 (1937), 26;

L.D. Landau and E.M. Lifschitz, Statistical Physics (Pergamon, London, 1958).

[9] P.W. Anderson, Concepts in Solids (Benjamin, N.Y., 1963);

P. Kadanoff et al., Rev. Mod. Phys. 39 (1967), 395;

A.G. McLellan, The Classical Thermodynamics of Deformable Materials (Cambridge Univ. Press, Cambridge, 1980).

[10] W. Cochran, Advances in Physics 10 (1961), 401;

R.M. White and T.H. Geballe, Long Range Order in Solids (Academic Press, N.Y., 1979).

[11] L. O'Raifeartaigh, Rep. Prog. Phys. 42 (1979), 159;

L. Michel, CERN TH 2716 (1979); Rev. Mod. Phys. 52 (1980), 617;

See also ref. [22].

[12] S. Aronhold, J.f.d. reine und angew. Math., Bd. 62 (1863), 281.

[13] D. Hilbert, Math. Ann. 36 (1890), 473; *ibid.* 42 (1893), 313.

[14] H. Weyl, Classical Groups, 2nd Ed. (Princeton Univ. Press, 1946).

[15] G.E. Bredon, Introduction to Compact Transformation Groups (Academic Press, N.Y.,1972);

D. Mumford, Geometric Invariant Theory, Erg. der Math. 34 (1965);

W.C. Hsiang and W.Y. Hsiang, Ann. Math. 92 (1970), 189;

G.W. Schwarz, Inv. Math. 49 (1978), 167;

See also ref. [23].

[16] R. Brout, Nuovo Cim. 47A (1967), 932.

[17] L. Michel, C.R. Acad. Sc. Paris 272 (1971), 433;

[18] L. Michel and L.A. Radicati, Ann. Phys. 66 (1971), 758.

[19] L.-F. Li, Phys. Rev. D9 (1974), 1723.

[20] F. Buccella, H. Ruegg and C.A. Savoy, Nucl. Phys. B169 (1980), 68;

H. Ruegg, Phys. Rev. D22 (1980), 2040.

[21] F. Buccella, H. Ruegg and C.A. Savoy, Phys. Lett. 94B (1980), 491.

[22] M. Gell-Mann, private communication (1980);

R. Slansky, Phys. Rep. 79c (1981), 1.

[23] M. Abud and G. Sartori, Phys. Lett. 104B (1981), 147.

[24] J.S. Kim, Nucl. Phys. B196 (1982), 285.

[25] S. Frautschi and J.S. Kim, Nucl. Phys. B196 (1982), 301.

[26] J.S. Kim, Nucl. Phys. B197 (1982), 174.

[27] J.S. Kim, SO(N) Higgs Problem with Adjoint + Vector Representations, Cal-Tech preprint 68-877 (Jan 1982).

[28] M. Gell-Mann and J.S. Kim, work in progress.

[29] M.D. Sturge, Solid State Physics 20 (1967), 91;

M.V. Jarić, private communication (1982); He pointed out that Gufan [Yu. M. Gufan, Soviet Physics - Solid State 13 (1971), 175] devised "angular variables" similar to ours [25]. He also pointed out that Jarić [Lecture Notes in Physics 135 (1980), 12] realized that it is economical to work with invariant polynomials directly. A similar point was noticed and utilized by Ruegg et al. [20,21] simultaneously.

See also W. Cochran in ref. [10].

[30] P. Mitra, J. Math. Phys. 22 (1981), 2069;

L. O'Raifeartaigh, S.Y. Park, and K.C. Wali, Symmetries in Science, ed. Gruber (Plenum, N.Y., 1980);

See also ref. [20].

[31] W. McKay and J. Patera, Tables of Dimensions, Second and Fourth Indices and Branching Rules of Simple Algebras (Dekker, N.Y., 1980).

[32] M. Magg and Q. Shafi, Z. Phys. C4 (1980), 63;

See also ref. [20].

[33] M.S. Chanowitz, J. Ellis, and M.K. Gaillard, Nucl. Phys. B128 (1977), 506;

F. Gürsey, P. Ramond, and P. Sikivie, Phys. Lett. 60B (1976), 177;

Y. Achiman and B. Stech, Phys. Lett. 77B (1978), 389.

[34] B.C. Georgalas, F.T. Hadjioannou, and A.E. Kappela-Economou, Phys. Lett. 96B (1980), 297.

[35] S. Coleman and E. Weinberg, Phys. Rev. D7 (1973), 1888;

R. Jackiw, Phys. Rev. D9 (1974), 1686,

See also Weinberg and Ellis et al. in ref [7].

[36] J.S. Kim, work in progress.

[37] M. Gell-Mann and F.E. Low, Phys. Rev. 95 (1954), 1300;

T.P. Cheng, E. Eichten, and L.-F. Li, Phys. Rev. D9 (1974), 2259;

See also J. Ellis et al. in ref. [7].

[38] B. Kostant, Am. J. Math. 85 (1963), 327;

M. Couture and R.T. Sharp, J. Phys. A13 (1980), 1925;

J. Patera, C. Rousseau, and D. Schlomiuk, J. Math. Phys. (1982).

[39] G. Racah, Ergeb. Exakt. Naturwiss. 37 (1965), 28.

[40] B. Wybourne, Classical Groups for Physicists (Wiley, N.Y., 1974);

J.E. Humphreys, Introduction to Lie Algebras and Representation Theory
(Springer, N.Y., 1972);

R. Gilmore, Lie Groups, Lie Algebras, and Some of Their Applications (Wiley,
N.Y., 1974).

[41] B. Gruber and L. O'Raifeartaigh, J. Math. Phys. 5 (1964), 1796.

[42] D.-d. Wu, The Symmetry Breaking Pattern of Scalars in Low Dimension
Representations, Harvard Univ. preprint (Jan, 1981).